Quantifying the downstream impacts of dams with hydrologic signatures and a large-scale hydrologic model

by

Yiran Liu
B. Eng., Memorial University of Newfoundland, 2020

A Thesis Submitted in Partial Fulfillment of the Requirements for the Degree of

MASTER OF APPLIED SCIENCE

in the Department of Civil Engineering

University of Victoria

Supervisory Committee

Quantifying the downstream impacts of dams with hydrologic signatures and a large-scale hydrologic model

by

Yiran Liu
B. Eng., Memorial University of Newfoundland, 2020

Supervisory Committee

Dr. Tara J. Troy (Department of Civil Engineering)
Supervisor

Dr. Tom Gleeson (Department of Civil Engineering)
Departmental Member

Abstract

Rivers are regulated worldwide and are segmented by dams, primarily built in the last century. The impact of dams on flow immediately downstream has been studied for decades. However, the downstream propagation of the hydrologic impacts in a river network still needs to be better quantified, particularly in humid regions. This study aims to test a method of investigating the impacts of large reservoirs by using different hydraulic signatures, determining how the signatures propagate downstream of the dams, and exploring the potential to utilize a hydrologic model to determine dam impacts. By solely analyzing streamflow observations in the Delaware River Basin, hydrologic signatures can detect the dams' impacts immediately downstream of the New York City reservoirs and are able to show the length scale at which hydrologic signatures return to unimpacted values within the Delaware River basin. Results show that the streamflow downstream was influenced by the large reservoirs but with a propagation distance of approximately 35 kilometers, after which the signatures are likely to be consistent with gauges upstream of the reservoirs. Unlike the western U.S., the streamflow below large dams shows the potential to recover via streamflow contributions from the tributaries in a humid watershed, resulting in a less vulnerable river regime; however, the flashier streamflow and the change in timing locally downstream of the dams may result in ecological degradation. This method developed for the Delaware basin to compare hydrologic signatures in time and space is transferable to other river basins.

Another potential approach is to use a hydrologic model to simulate unregulated streamflow which can serve as a proxy for naturalized hydrologic signatures. The Variable Infiltration Capacity (VIC) model was selected to explore the possibility of expanding the observation-based method. Due to the poor streamflow performance in an initial simulation, especially for the baseflow, the second chapter of this thesis focuses on better understanding the

VIC baseflow generation and its sensitivity to model parameters. To do this, seven calibration parameters with three different values each are selected for a sensitivity analysis. The results suggest that the infiltration parameter (*infil*), the exponent in the equation for hydraulic conductivity (*exp*), and the parameter that specifies the maximum baseflow (*dsmax*) play important roles in determining the baseflow simulation and also influence the baseflow sensitivity of other parameters. This emphasizes the importance of precipitation partitioning and the vertical drainage process in baseflow simulation, in addition to the actual baseflow curve for the bottom soil layer. Based on the results of the sensitivity analysis, VIC is expected to be able to correctly simulate baseflow and total streamflow after calibration but this modeling exercise revealed significant challenges and limitations. Typical calibration methods that rely on monthly streamflow need to be improved, while calibrating to daily streamflow is important because of the need to capture the hydrograph characteristics, like the correct recession curve. Spatial heterogeneity needs to be considered, and the calibration parameters may not be transferable between gauges, even at a relatively small distance. If VIC can represent the naturalized streamflow regime, there is a potential to do a similar tracing downstream as in Chapter 2. Both methods could then be applied to other basins.

Table of Contents

List of Figures

List of Tables

Acknowledgments

First and most, thank my supervisor Tara J. Troy for mentoring and inspiring me during the research, and also my life at UVic. This thesis would not have been possible without her support.

I would also like to thank Dr. Tom Gleeson for mentoring me as my committee member, and an extended thank you to his Groundwater Science and Sustainability Group for an enjoyable time every week, and for friendship.

Lastly, special thanks to my family and friends for providing support, encouragement, and care throughout this degree.

Chapter 1: Introduction

1.1 Background and motivation

Dams play a significant role in regulating rivers and have become ubiquitous in many parts of the world. Over 50,000 large dams higher than 15 meters were recorded worldwide by 2006 (Berga et al., 2006). The impoundment of surface water by dams benefits water supply, hydropower production, flood control, irrigation, recreation, and other activities. Hydropower contributes more than 70% of renewable electricity generation globally (*Tracking SDG 7*, 2021), and 55% of large rivers in the U.S. have over a 25% decrease in the median annual floods due to dams (FitzHugh & Vogel, 2011). For water supply, reservoirs provide 30% of residential water use throughout the world (Berga et al., 2006). For example, Hoover Dam, located on the Colorado River in the U.S., supplies 25 million people in Nevada, Arizona, and California (Hoover Dam, 2015). The Delaware River basin in the northeastern US supplies water for approximately 8.3 million people in the basin and 5 million people outside of the basin (DRBC, 2022).

However, dams also have negative impacts. They segment rivers and are one of the major anthropogenic forces on the global water system as identified by Vörösmarty et al. (2004). Dams can cause problems downstream such as with channel morphology (Chong et al., 2021; Graf, 2006; Petts, 1979), water quantity (Graf, 2006; Magilligan & Nislow, 2005a; Marcinkowski & Grygoruk, 2017; Singer, 2007), water quality (Daniels & Danner, 2020; Kükrer & Mutlu, 2019), and biodiversity (Diehl et al., 2020; Galat & Lipkin, 2000; Vörösmarty et al., 2004). Ecological integrity can be largely degraded by the flow regime change (Bunn & Arthington, 2002; Galat & Lipkin, 2000; Poff et al., 1997a; Poff & Zimmerman, 2010). The flow regime of rivers can be altered by increasing water residence time, shifting the timing of flow, and changing the magnitude and frequency of the flows (Poff et al., 1997a). The downstream flow alteration in streamflow and sediment harms aquatic animals and changes the biochemical cycles (Poff & Hart, 2002). In addition, stream

temperature changes by reservoirs may also lead to species change or decline and the fragmented rivers challenge biotic migration (Poff & Hart, 2002).

Past hydrologic studies focused on the impact of impoundment immediately downstream (Batalla et al., 2004; Graf, 2006; Magilligan & Nislow, 2005b; Singer, 2007); however, the downstream propagation of hydrologic alteration through the river network is still poorly understood. For example, the streamflow may continue to be altered significantly downstream of reservoirs with no streamflow recovery. Alternatively, unregulated tributaries may restore the flow regime and mitigate the impact on habitats (Sabo et al., 2012). There is a range of possibilities for downstream impact propagation due to large dams, and quantifying the propagation can contribute to a better understanding of river regime change in the basin. Specifically, unregulated tributaries may play a role in protecting food-web structure alteration by large dams, and the protection of tributaries can be important for hydropower management (Sabo et al., 2018). Therefore, flow alteration propagation analysis may not only support dam and river management, and the detection of the vulnerable area downstream, but also identify tributaries' roles in mediating the negative influence (Ruhi et al., 2022).

There have been numerous studies on dams' impact both immediately downstream and within a river system in the western U.S. (Galat & Lipkin, 2000; Sabo et al., 2018; Singer, 2007; Stewart et al., 2005; Zhou et al., 2018). This is in contrast to the eastern US, where there are very few studies, possibly because water scarcity is less of an issue. Recently, river basins in the western U.S., such as the Colorado River Basin and Missouri Rivers Basin (Harrell et al., 2022; Ruhi et al., 2022; Skalak et al., 2013), have detailed studies on dam impact propagation along with biodiversity, and they have noted that the near-historical return of ecological integrity is not viable in drought regions such as the western U.S. (Dettinger et al., 2015; Ruhi et al., 2022; Zhou et al., 2018). In turn, there is a paucity of studies on flow alteration both directly below dams and the propagation downstream in humid regions like the eastern US. As a result, Delaware River Basin is selected to be

my study basin, where the propagation of downstream impact due to dams remains poorly quantified.

This thesis uses hydrological signatures for assessing hydrologic alteration downstream. Hydrologic signatures are widely used in evaluating streamflow response in time and spatial (Ferrazzi & Botter, 2019a; Kibler & Alipour, 2017; K. Sawicz et al., 2011) and can be used to detect the modification of hydrologic behavior between the observed and naturalized flows (Addor et al., 2018; Euser et al., 2013; H. K. McMillan, 2021; K. Sawicz et al., 2011; Yadav et al., 2007). Different hydrologic signatures can focus on different aspects of the flow regime, including flow magnitude (Olden & Poff, 2003; Stuefer et al., 2011; Yarnell et al., 2020), timing (Addor et al., 2018), and variability (Euser et al., 2013; Shamir, Imam, Gupta, et al., 2005). Based on these studies, they should be able to demonstrate the flow alteration due to the dams, since the change in hydrologic signatures describes the impacts on a regulated river.

Methods for quantifying downstream impacts should be developed that can be applied to the available data and that are transferable to another location so that further comparison between basins might be able to be performed. The historical approach relying on historical streamflow observations focuses on the differences before and after the construction of dams. Many studies use this approach, such as the degree of regulation (DOR) method (Ferrazzi & Botter, 2019a; Magilligan & Nislow, 2005a; Pegg et al., 2003; B. D. Richter et al., 1996a; Singer, 2007; Skalak et al., 2013). However, the historical, observation-based method is not always appropriate to use due to limited streamflow data availability, particularly for the pre-dam period.

Another possible approach would compare streamflow observations in the post-dam period with the modeled streamflow which considered no regulations and can be a proxy for naturalized flow. This approach does not require long data records prior to dam construction and can distinguish the impact from the dam regulation alone, whereas the result in the historical approach could include climate change effects. However, using a model requires careful calibration to

simulate the natural flow regime; otherwise, the framework of reference from a model would not work.

One possible model for this approach would be the Variable Infiltration Capacity (VIC) model, a macroscale land surface hydrological model that can simulate components of the water and energy balance (Liang et al., 1994). The VIC model is widely used across a range of hydrometeorological applications, including streamflow simulation (Bai et al., 2016; DeChant & Moradkhani, 2014; Kumari et al., 2021; Su et al., 2005), snow modeling (Andreadis & Lettenmaier, 2006; Pan et al., 2003; Sheffield et al., 2003), and flood monitoring (Khan et al., 2011; Schumann et al., 2013; Wu et al., 2014). Therefore, the VIC model has the potential to be a proxy for naturalized flow in the post-dam period for analyzing dam impact propagation.

The study area for this thesis, the Delaware River Basin, is located in the eastern U.S., and the Delaware River is the longest un-dammed river east of the Mississippi. The Upper Delaware Basin is home to the eastern brook trout, inland wintering habitat for the bald eagle, and includes large protected areas with biodiversity conservation strategies (Allen et al., 2011; DRBC, 2022). In addition, surface water from the Delaware River is a critical source that supplies water to two major U.S. cities, Philadelphia and New York City. For its relatively small drainage area compared to other rivers in the continental US, it supplies water to a significant population: over 13.3 million people, nearly 4% of the U.S. population. In addition, the Delaware River has the possibility of recovery from the dams' impacts because of its humid climate and the upper large dams have a relatively short residence time. Most of the studies in the Delaware River Basin have focused on water quality, floods, and problems driven by the estuary tidal area (Botter et al., 2007; Cottrell et al., 2005; Groot, 1966; Leck, 2003; Sheldon & Hites, 1978; Smith et al., 2010; Weisberg et al., 1996). Some of them related to flow magnitude have focused on a portion of the watershed, particularly the lower basin (Hammond & Fleming, 2021; Shoemaker et al., 2019; Smith et al., 2010). However, no study has focused on the propagation of the dam's impacts downstream.

1.2 Research questions and thesis objectives

Overall, this thesis is aiming to answer the question: How can downstream propagation of the dams' impacts be quantified using observations and/or models? To address this overall question, the two specific research questions addressed in this thesis are:

Q1. How do NYC reservoirs impact hydrologic signatures immediately downstream of the dams, and at what length scale do hydrologic signatures return to their state consistent with upstream of dams in the Delaware River Basin?

Q2. What is the ability of the VIC model to simulate the hydrologic signatures needed to provide estimates of the naturalized hydrologic regime? If it is poor, is it possible to improve the performance through parameter calibration and identifying important parameters to correctly simulate streamflow and baseflow characteristics?

This thesis originally aimed to propose a model-based method of dam impact propagation analysis by evaluating the difference in hydrologic signatures between the naturalized and observed streamflow in the post-dam period. To do this, the VIC model would be used to estimate naturalized streamflow, but initial model runs showed that the model skill was insufficient in its current set-up. As a result, only historical observations for the Delaware River Basin are used in Chapter 2, which studied the local and further downstream impact and narrow down to the length scale of propagation to provide an answer to Q2. After that, Chapter 3 investigates whether using VIC for naturalized estimates would be possible in future work by answering Q3. If it is, then it would allow further confirmation of Chapter 2's results with a model-based approach.

1.3 Author Contributions

Yiran Liu: Conceptualization, Methodology, Formal analysis, Investigation, Visualization, Writing- Original draft. **Tara J. Troy**: Conceptualization, Methodology, Resources, Writing- Review & Editing, and Supervision.

Chapter 2: Hydrological signature alteration in the Delaware River Basin

2.1 Introduction

Dams are constructed throughout the contiguous United States, and their downstream impacts have been ongoing in many regions due to decades of large impoundments (Graf, 1999). Reservoirs can increase residence time and alter biophysical processes such as the basin's water balance, flow regime, reoxygenation, and sediment transport (Dingman, 2015). The impact directly below dams has been studied with various focuses. For example, for channel morphology, dams can cause riverbed degradation, such as coarser material, problems with sediment transport, and changes in riverbed geometry (Chong et al., 2021; Grant et al., 2013; Magilligan & Nislow, 2005b; Sabo et al., 2012). The water quantity changes by dams may include the change in magnitude, frequency and time, and the common ability to reduce peak flow and increase low flow. Water quality impacts from dams can include changes in dissolved oxygen levels, turbidity, pH, electrical conductivity, hardness, and water temperature (Benedini & Tsakiris, 2013; Daniels & Danner, 2020; Kükrer & Mutlu, 2019). The flow regime is the foundation of ecological features, and changes in flow regime may reduce habitat availability and quality. For instance, species and community composition change after the dam because more seeds can be transported via streamflow in the growing season without the dam (Merritt & Wohl, 2006). Because of the relationship between streamflow quantity and quality with biota, managing flows to sustain ecosystems is critical. This includes managing the spatial and temporal variability in streamflow, including flooding, all of which can be essential for the river ecosystem (Gillespie et al., 2015). The streamflow alteration caused by dams can be considered a primary impact, as other variables are impacted directly or indirectly by hydrology, such as channel morphology and water temperature. This primary impact on streamflow will be the focus of this chapter.

Streamflow impacts immediately downstream of the dam have been studied, particularly annual mean and maximum flow (Batalla et al., 2004; Graf, 2006; Magilligan & Nislow, 2005b; Singer, 2007). Given the impact of dams on streamflow, the impact and quantification of hydrologic change have been the focus of many studies in recent decades. For example, the concept of natural flow regime was introduced by Poff et al. (1997), and the regime was summarized in terms of magnitude, frequency, duration, timing, and rate of change to describe the change in river flow and further affect the biodiversity, production, and sustainability of river ecosystems. A similar framework was proposed by Richter et al. (1997; 1996b) with the concept of the Index of Hydrologic Alteration, which provided suggestions for river ecosystem management. Hydrological alteration studies often focus on one or more components of these signatures at local gauges, and extreme flows such as flood magnitude have been widely studied (Galat & Lipkin, 2000; Graf, 2006; Kingsford, 2000; Magilligan & Nislow, 2005b; Mei et al., 2017; Pegg et al., 2003; Singer, 2007). Reductions in the magnitude and duration of mean and peak flow are common impacts of the regulated rivers in different regions (Batalla et al., 2004; Galat & Lipkin, 2000; Graf, 2006; Magilligan & Nislow, 2005b; Skalak et al., 2013). These impacts can also have direct effects on the ecosystem. Due to the reduction of flooding by dams, over 50% of floodplain wetlands in Australia have been altered with a reduction in biodiversity and biota becoming different to the habitat (Kingsford, 2000). Low flows can also be increased by reservoir management (Magilligan et al., 2003), and the number of pulses can increase (Archer & Newson, 2002; Magilligan & Nislow, 2005b). Magilligan & Nislow (2005) also indicated that the river regimes change throughout the U.S. from the suspension of flow during construction and the filling of the reservoir for both large and small streams. The largest hydrologic alteration is in the low and peak flows over periods (Magilligan & Nislow, 2005b). In addition, flood control dams can decrease flexibility and heterogeneity, while water supply dams can increase both (Ferrazzi & Botter, 2019a). Spatial

variability in the dams' impact on maximum flows may be more related to changes in latitude rather than longitude (Mei et al., 2017).

The downstream impacts of large dams are not limited to immediately below the dams and can propagate downstream, affecting entire watersheds. Recently, hydrologic alteration in the Colorado Basin has been studied spatially within the river network in terms of biodiversity (Ruhi et al., 2022). The dam effects downstream are likely to be driven by network characteristics, such as the locations of regulation, rather than individual dam's properties of impoundment, emphasizing the spatial link for flow alteration and ecosystem restoration (Ruhi et al., 2022). In addition, naturalized flows may be difficult to restore downstream of large dams in the western United States, where water scarcity is an issue due to increasing water use and climate change; however, significant ecological features can be protected by understanding the dam propagation in a spatial network and managing flows regarding the potential impacts (Dettinger et al., 2015; Ruhi et al., 2022). However, the full extent of hydrologic alteration caused by large dams and their downstream impacts is not yet fully understood, which can pose challenges to effective watershed management and conservation efforts. These include whether dams have a similar downstream impact in humid areas as they do in arid regions, whether reservoirs induce a flashier response in streamflow, and how far the impact dissipates or continues.

To understand the downstream response, a propagation tracing with the distance from the endpoint of outflow is developed to show the change along rivers. The evaluation of the dams' impacts on streamflow uses hydrologic signatures. Hydrologic signatures are quantitative metrics that can describe flow response statistically or dynamically (Ferrazzi & Botter, 2019a). They have been widely applied to model prediction and calibration, hypotheses testing of catchment response, detection of hydrologic change and spatial flow networks, and ecological habitat assessment. (Archer & Newson, 2002; Clark et al., 2011; Leach et al., 2015; Olden & Poff, 2003; K. Sawicz et al., 2011; Wagener et al., 2007). Hydrologic signatures are not only useful when comparing large

watersheds (Wagener et al., 2007), but can also help to extract hydrologic change in a specific area (Batalla et al., 2004; Ferrazzi & Botter, 2019b; Livneh et al., 2013). McMillan (2021) states that hydrologic signatures are not straightforward to select with the related processes, since one flow response signature can be induced by multiple processes. Signatures are usually used in a small context after identifying the "potential causative processes" to mitigate the complexity (Ali et al., 2013). Not all indices may be affected by impoundment at a specific gauge or across the region.

This chapter investigates the propagation of dam impacts downstream in the Delaware River Basin by using hydrologic signatures, extending beyond the immediate areas below the dams. The research questions below will be addressed:

Q1. How can downstream propagation of the dams' impacts be quantified using observations?

Q2. How do NYC reservoirs impact hydrologic signatures immediately downstream of the dams, and at what length scale do hydrologic signatures return to their natural state in the Delaware River Basin?

By analyzing the propagation of dam impacts, we can develop a better understanding of the downstream effects of large dams involving flow magnitude, variability, and time. This study takes a historical, observation-based approach, focusing on the differences before and after the construction of dams, and compares the post-dam change along the Delaware River with upstream gauges. Flood and low-flow modeling are also gaining importance, but hydrologic analysis of variability and downstream change is relatively limited. Therefore, this chapter focuses on the local changes that propagate or dissipate through the Delaware River due to the New York City reservoirs. This study may provide valuable insights for dam management and regulation of dams in other river basins and for the management of water quantity in the Delaware River, but the approach is also likely to be applicable in other regions.

2.2 Study region and data

The Delaware River Basin is a densely populated region in the northeastern United States (Figure 1), draining an area of 34,965 square kilometers area through the states of New York, New Jersey, Pennsylvania, and Delaware and discharging into the Atlantic Ocean. The Upper Delaware River Basin is primarily covered by forest, while the lower regions are characterized by a mix of agriculture, urban areas, forests, and wetlands (DRBC, 2016). The northernmost tributaries of the Delaware River begin in the Catskill Mountains at elevations above 1200 m, and the east and west branches merge at Hancock, NY, with an elevation drop of approximately 240 meters down to the estuary (State of the Delaware River Basin, 2019). Recent research on the Delaware River has focused on quality monitoring and prediction for the headwaters and estuary (Hoang et al., 2019; Meyer et al., 2020).

To share planning, development, and regulation in the Delaware Basin, the Delaware River Basin Commission (DRBC) was established in 1964. Power generation, public water supply, and industry dominate the water use in the region with 95% of water use coming from surface water rather than groundwater (State of the Delaware River Basin, 2019). The changes in consumptive water use in the Delaware River Basin have been relatively small over the past decades, except for out-of-basin transfers (Thompson & Pindar, 2021). One of the major out-of-basin transfers is the water supply to New York City, which serves 13.3 million people and was authorized by a U.S. Supreme Court decree in 1954 (Thompson & Pindar, 2021; U.S. Supreme Court, 1954). Figure 1 illustrates the location of the Delaware River Basin, the streamflow gauges used in this study, and the mean annual streamflow at each gauge normalized by basin area [mm/year]. The highest streamflow occurs in the northernmost tributaries in the Catskill Mountains, with relatively little spatial variability in streamflow throughout the lower basin. This study focuses on the Delaware River basin upstream of Trenton, NJ, excluding the Schuylkill River, a major tributary that joins the lower bay area at Philadelphia, as this section of Delaware is influenced by tides.

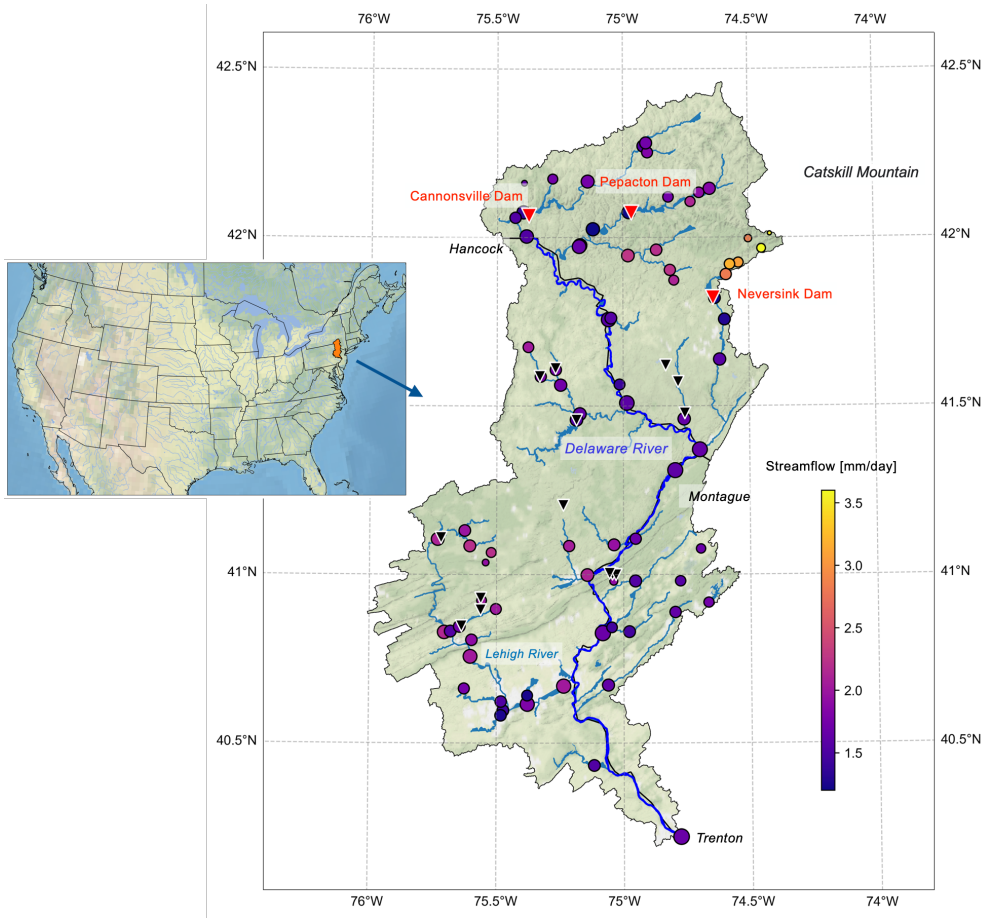

Figure 1: Location of the Delaware River basin in the US in orange (inset). The larger map to the right shows the Delaware River Basin. The main stem and tributaries are plotted in blue, and dots indicate the location of the USGS gauges used in this study. The dot size indicates the drainage area, and the color bar shows the mean annual streamflow [mm/day]. Red triangles indicate the location of the NYC reservoirs in the upper basin, and the smaller black triangles indicate other dams in this region. Background colored by Stamen Terrain.

The main stem of the Delaware River, which officially begins at Hancock, NY (Figure 1), is one of the major rivers in the eastern U.S. that has not been dammed. While there are no reservoirs on the main stem of the Delaware River, there are several dams on its tributaries, such as the New York City (NYC) reservoirs in the upper basin. The NYC reservoirs are Cannonsville, Pepacton, and Neversink and they play a critical role of the New York City water supply system, providing around 50% of New York City's drinking water (Adams & Aggarwala, 2021). The NYC Department of Environmental Protection monitors reservoir releases and storage levels, and the U.S. Supreme Court allows a maximum withdrawal of up to 800 million gallons per day from NYC reservoirs.

According to the National Inventory of Dams (NID) database (USACE, 2020), the reservoirs have a maximum storage capacity of approximately 85% of the annual volumetric streamflow at Cannonsville, 165% at Pepacton, and 100% at Neversink. Table 1 summarizes the reservoir and dam characteristics.

Table 1: Summary of New York City dam and reservoir characteristics

Dam Name	Closest Gauge ID	Completed Filling Year	Max Storage [km^3]	Normal Storage [km^3]	Dam height [m]	Primary Purpose(s)
Cannonsville	Downstream 01425000 Upstream 01423000	1964	0.536	0.370 (69%)	53.3	Hydroelectric Water Supply
Pepacton/ Downsville	Downstream 01417000 Upstream 01413500	1955	0.752	0.518 (69%)	62.2	Water Supply
Neversink	Downstream 01436000 Upstream 01435000	1954	0.175	0.134 (77%)	57.9	Water Supply

The DRBC has developed a drought management program to address salinity control and estuary management, which includes the establishment of the Trenton Flow Objective. The objective of this flow management system is to ensure that the releases from the NYC reservoirs maintain a minimum streamflow of 3000 cfs in Trenton, NJ as determined by the DRBC, to protect water supply downstream of Philadelphia from saltwater intrusion. The management principle is to store water during high flow periods and release it during low flow periods to meet downstream demands. The Trenton minimum flow objective is compatible with the primarily storage to the NYC water supply system, where it provides a reliable and consistent water supply for New York City while minimizing the impacts of water withdrawals on downstream communities and ecosystems. It should be noted that the NYC reservoirs are not systematically operated for flood control.

Historical daily streamflow data are obtained from the U.S. Geological Survey (USGS) database for 78 stations in the Delaware River Basin. Gauges were selected to have sufficiently long records, with the shortest being 29 years. Of these gauges, 58 includes records prior to the construction of the NYC reservoirs, and 10 have records ending before the year 2000. The upstream

Neversink (Gauge 01435000) has a missing period from June 1949 to July 1951. The pre-dam period of record for the reservoir gauges is between 9 and 13 years, and the period of construction and dam filling is excluded from the analysis. The drainage area varies from 2 km^2 to 17,560 km^2. Precipitation data were collected from a gridded daily meteorological dataset with a 1/16° spatial resolution covering the period from 1915 to 2011 (Livneh et al., 2013).

The average annual streamflow, as a depth per unit area, at Trenton is 612 mm from 1913 to 2020. This is divided into approximately 64% base flow and 36% surface runoff according to a standard hydrograph separation (Arnold & Allen, 1999; Pradhanang et al., 2013). The average annual precipitation in the Delaware River Basin is 1164 mm. Streamflow is typically highest in April and lowest in August, while precipitation is higher in summer and lower in winter at most of the gauges. The spatial variation in mean annual streamflow, converted to an average runoff depth, is shown in Figure 1. The highest streamflow is observed in the upper Neversink and other high-elevation areas in the northern parts of the basin.

2.3 Methods

The study seeks to evaluate the effects of hydrologic changes on the Delaware River by analyzing various hydrologic signatures between gauges. The selected signatures are analyzed for a set of stream gauges located along the Delaware River and its tributaries. The changes in hydrologic signatures of paired stations upstream and downstream at NYC reservoirs are first examined in a long-term time series. The upstream gauge is considered a control gauge with limited human impact, while the downstream gauge shows the direct impact of the dam. The analysis is then expanded and focused to trace the hydrologic signatures through the river network to quantify the downstream propagation along the Delaware River. The distance of each gauge to the Trenton gauges is calculated and the hydrologic signatures can be detected by comparing the gauges. Additionally, the relationship between streamflow and drainage area provides a separate line of

evidence for the change as does the rate of change between pre- and post-dam periods, which would reinforce the hydrologic propagation change.

2.3.1 Selected hydrologic signatures

As a useful metric to detect changes in downstream hydrological behavior, hydrologic signatures are selected based on previous applications of the hydrologic change detection (Addor et al., 2018; Euser et al., 2013; H. K. McMillan, 2021; K. Sawicz et al., 2011; Yadav et al., 2007), which have been shown to be effective in describing the basin's hydrology. The selected ones would describe specific hydrological processes and can be calculated using the daily streamflow data. Our selected hydrologic signatures are designed to capture changes in the flow magnitude (Olden & Poff, 2003; Stuefer et al., 2011; Yarnell et al., 2020), timing (Addor et al., 2018), and variability (Euser et al., 2013; Shamir, Imam, Gupta, et al., 2005). As a result, annual mean flow, annual maximum flow, annual low flow, annual runoff ratio, rising limb density, baseflow index, flow duration curve slope, annual half flow date, and streamflow elasticity are selected as hydrologic signatures, all of which were computed using daily discharge and precipitation time series. Some of the signatures are used only in either the local or basin-wide comparison depending on their properties.

Basic Flow Statistics

The average, high, and low flows describe the flow regime, which is the bedrock of a riverine ecosystem (Poff et al., 1997b). To summarize the basic flow, the annual mean, maximum, and 7-day low streamflow are selected as hydrologic signatures. Streamflow is converted to a depth of flow per unit area for comparison across different drainage areas.

Annual Runoff Ratio

The long-term average annual runoff ratio indicates the fraction of the precipitation that results in streamflow, $\frac{Q}{P}$ where Q is mean annual streamflow and P is mean annual precipitation. Broadly, streamflow dominates in areas with higher runoff ratios, while evapotranspiration dominates in areas with lower runoff ratios. Higher runoff ratios are typically associated with higher impervious surface and steep slope areas. Runoff generation in the Delaware River is dominated by saturation excess (Pradhanang et al., 2013).

Rising Limb Density

Rising limb density (RLD) is a measure of the flashiness of a basin, also known as how quickly the basin responds to a precipitation input. The rate of change in streamflow ($\frac{\partial Q}{\partial t}$) can indicate a rapid or gradual rate of the rising limb ($\frac{\partial Q}{\partial t} > 0$) or recession ($\frac{\partial Q}{\partial t} < 0$) (Fleischmann et al., 2016). RLD is calculated by quantifying the rate of change in streamflow during the rising limb of a hydrograph, and it is independent of the flow magnitude (Mathai & Mujumdar, 2021; K. A. Sawicz et al., 2014). Specifically, the annual RLD can be expressed as the number of peaks over the duration of risings (Shamir, Imam, Morin, et al., 2005),

$$RLD = \frac{No.\ of\ total\ rising\ limbs}{No.\ of\ days\ in\ rising\ period} \qquad \textit{[Eq. 2-1]}$$

with a frequency unit [T^{-1}]. Larger values indicate a flashier response. All rising limbs are included in this analysis, regardless of magnitude. This method is not intended to detect the source of the water, such as surface runoff vs. baseflow.

Baseflow Index

The baseflow index (BFI) is a useful metric for estimating the baseflow proportion, and also helpful in assessing subsurface storage residence time (Bulygina et al., 2009). BFI is the proportion

of long-term baseflow to total streamflow, where a higher BFI indicates a longer residence time (Bastola et al., 2018; H. McMillan, 2020; K. Sawicz et al., 2011). To calculate BFI in this study, the recursive digital filter method proposed by Eckhardt (Eckhardt 2005, 2008), which has been found as the best performance through different filter method (Xie et al., 2020), was used and expressed as,

$$B_i = \frac{(1-BFI_{max})\times a\times B_{i-1}+(1-a)\times BFI_{max}\times Q_i}{1-a\times BFI_{max}} \quad \textit{[Eq. 2-2]}$$

where B_i baseflow, the subscript i is the time step; Q_i is the total streamflow at time step i; a is the filter parameter; BFI_{max} is the maximum baseflow index. The filter parameter, a, relates to the recession constant and can be selected by linear recession analysis (Eckhardt, 2008). Different filter parameter values influence the smoothness of the filtered baseflow time series. An a of 0.96 is selected by observation of the recession period in the upper Delaware River Basin. BFI_{max} is assumed to be a reflection of geology in the basin. It is calculated based on the backwards filter method (Collischonn & Fan, 2013), and 0.6 has been selected in this study.

Flow Duration Curve Slope

The flow duration curve is a cumulative frequency curve that represents the percentile for the specified discharge value that was equaled or exceeded during a time. The flow duration curve slope is the index of the streamflow probability distribution of a flow in a specific range (Yilmaz et al., 2008). The slope of the middle part of the FDC curve is selected associate with daily runoff variance. A steeper slope may indicate surface runoff with flashier hydrographs in response to rainfall. Due to the shortage of surface and subsurface storage, a higher slope may also indicate a watershed's reduced ability to sustain low flows during dry period (Leach et al., 2015). The average flow duration curve slope equation for the middle portion can be written as,

$$FDC\ Slope = \frac{log\ (Q_{33})-log\ (Q_{66})}{0.66-0.33} \quad \textit{[Eq. 2-3]}$$

where FDC slope is the flow duration curve slope for average conditions, Q_{33} is the streamflow at the 33rd percentile and Q_{66} is the streamflow at the 66th percentile. High-FDC and low-FDC slopes are represented from Q_{80} to Q_{95} and $Q_{0.5}$ to Q_{20}, respectively.

Mean Half Flow Date

The mean half flow date is the day of the year during which half of the accumulated annual discharge occurs (Addor et al., 2018). The timing of flows and the annual maximum and minimum flows are altered by dams, sometimes by as much as six months (Fleischmann et al., 2016). The date of the half flow may also indicate the time concentration of snowmelt.

Streamflow Elasticity

Streamflow elasticity is defined as the percent change in streamflow resulting from a 1% change in precipitation. It is usually used to test the sensitivity of streamflow with respect to precipitation over a long term. Sankarasubramanian et al. (2001) modified the elasticity concept of Schaake (Schaake, 1990) into a median format as,

$$\varepsilon_{P,Q} = Median\left(\frac{dQ}{dP}\ \frac{P}{Q}\right) \qquad \textit{[Eq. 2-4]}$$

where $\varepsilon_{P,Q}$ is the streamflow elasticity to precipitation; $\frac{dQ}{dP}$ is the ratio between the annual difference of streamflow and precipitation compared to last year. $\frac{P}{Q}$ is the ratio between annual mean precipitation and streamflow this year. The median is a nonparametric estimator that has a low bias and is more robust in identifying streamflow sensitivity with climate (Sankarasubramanian et al., 2001). They found that the streamflow elasticity to precipitation through the United States often ranges from 1.0 to 2.5.

2.4 Results

The impacts of the NYC reservoirs are quantified using the selected hydrologic signatures. The results are divided into two sections: the first evaluates the immediate downstream changes in

signatures at the NYC reservoirs, and the second section tracks signatures along the Delaware River through the NYC reservoirs to the downstream gauges. All available time periods are used in the first section, and the post-dam period is used for propagation tracking.

2.4.1 Local impact of the dam

The time series comparison between the paired gauges immediately upstream and downstream of the NYC reservoirs shows the direct impact of the three dams (Figure 2), reflecting the reservoir operations. For this analysis, three signatures are not included. The baseflow index is omitted, as it lacks physical meaning immediately downstream of the dam where most of the streamflow is released from the reservoir. The annual runoff ratio is omitted because the denominator, annual precipitation, is essentially the same for the paired gauges, thereby repeating the differences shown in annual mean streamflow. The streamflow elasticity is a long-term average signature and is not shown in Figure 2.

The paired gauges are strongly correlated in the pre-dam period, with a correlation coefficient of over 0.95 for Cannonsville and Pepacton, both of which have more than 10 years of pre-dam observations. Mean annual streamflow in the pre- and post-dam periods at the upstream gauges are similar, with a small increase (<5%) in the latter period at Cannonsville and Pepacton due to climate. After the construction of NYC dams, annual flows at the downstream gauges at Cannonsville, Pepacton, and Neversink were 25.9%, 66.5%, and 71.6% (168 mm/year, 453 mm/year, 735 mm/year) lower than at the upstream gauges, respectively. The correlation between the paired gauges decreased with correlation coefficients of 0.80, 0.70, and 0.48 for Cannonsville, Pepacton, and Neversink, respectively. During both the pre- and post-dam periods, the coefficient of variation for downstream gauges is significantly higher than for upstream gauges. Cannonsville has a relatively small coefficient of variation for downstream mean annual flow (0.4) whereas Neversink has a much larger value, implying a larger variability compared to the mean (0.84). The strong positive relationship in the pre-dam period between upstream and downstream gauges

indicates that the NYC reservoirs play a significant role in the downstream hydrologic regime change.

Figure 2: Time series of upstream (blue line) and downstream (orange) hydrologic signatures, where the orange shading indicates the pre-dam period for each reservoir (columns). The top row plots the annual mean streamflow [mm/year]; the second is the annual maximum daily streamflow [mm/day]; the third is the annual 7-day minimum streamflow [mm/day]; the fourth is the annual rising limb density, an indicator for flashiness; the fifth row is the slope of the flow duration curve (FDC); and the bottom row plots the mean half flow date as the number of days from October 1st, the start of the water year.

The annual maximum daily flow (AMF) and 7-day minimum flow showed similar results to the annual mean flows between pre- and post-dam periods. The AMF declined after the NYC reservoirs were completed due to their storage capacity during high flow events. However, there is not always sufficient reservoir capacity during flood events to mitigate flooding downstream. Peak

discharge in the three NYC reservoirs occurred on June 28, 2006, while storms and flooding occurred in central New York and northeastern Pennsylvania. During this time, Cannonsville and Pepacton reservoirs exceeded their capacity and were spilling, with similar peak flows across paired gauges (DRBC, 2006). Therefore, the downstream peak flows during this flood were not attenuated by the reservoirs and resulted in an equivalent flow rate as at the upstream gauges.

The 7-day minimum flow decreased significantly at Pepacton after the reservoirs were filled. Neversink has the highest minimum flow per unit area and also the largest reduction in the post-dam period, where the flow in the downstream gauge is 49% lower than upstream. Cannonsville and Pepacton decreased by 20% and 44%, respectively. Inadequate environmental flow protection led to the establishment of the Flexible Flow Management Program (FFMP) in 2007 and subsequent revisions. As a result, Delaware's release policies after the FFMP implementation increased the low flow below the reservoirs. Cannonsville's 7-day minimum flow increased from an average of 0.071 mm/day to 0.264 mm/day before and after 2007; Pepacton increased from 0.068 mm/day to 0.181 mm/day; Neversink increased from 0.153 mm/day to 0.506 mm/day. As a result of this policy, the downstream 7-day minimum exceeded the upstream values in some years, allowing the dams to reduce the impact of drought downstream. For example, the downstream, 7-day minimum flows at Cannonsville after 2007 are 44% higher than the upstream gauge. After 2007, the correlation coefficients decreased and Pepacton has a negative correlation, which highlights the change due to human management. Because of the regulation, the immediate downstream of NYC reservoirs have the lowest 7-day minimum flow in October and November throughout the year.

In the post-dam period, the rising limb density (RLD) has larger interannual variability downstream of all the dams, and there is essentially no correlation between the paired gauges as compared to the pre-dam period when there was a positive correlation. Both Neversink and Pepacton have a slight increase in the mean RLD post-dam, but Cannonsville has an 11% decrease

downstream compared to pre-dam. The RLD was anomalously low in 2006 for all three reservoirs, likely due to the June 2006 floods that resulted in full reservoirs with a slow steady release thereafter. Like the RLD, the slope of flow duration curve (FDC) provides a measure of flashier hydrograph responses. The paired gauges' FDC slope is positively correlated pre-dam but have little correlation post-dam; this is consistent with the RLD. Post-dam, the FDC slope became steeper downstream of Cannonsville, indicating a more variable flow regime. The same is seen downstream of Pepacton and Neversink but only for a period of time after the reservoir was filled and then it returned to mild values. The variance at Pepacton is the largest, with a coefficient of variance of 0.86, due to the unusually high post-dam slope. In addition, the low-FDC slope at Cannonsville remains consistent and mild, and this flow regime may be related to the environmental flow regulation, while Pepacton has the steepest slope and higher interannual variability. The high-FDC slope at Pepacton and Neversink indicates an intermittent flow due to reservoir filling.

Lastly, the mean half flow date at the downstream gauge indicates the reservoir regulation and release time within a year. The overall mean half flow date at the downstream gauges is delayed with much higher interannual variability, especially at Pepacton. The daily cumulative streamflow, of which the half flow date is one statistic, shows a relatively uniform temporal distribution in the downstream gauges. In contrast, the upstream gauges show seasonality, with a pattern of high cumulative flow in the spring and lower in the summer. To quantify this, the seasonal cycle of the streamflow statistics for the paired gauges is plotted in Figure 3.

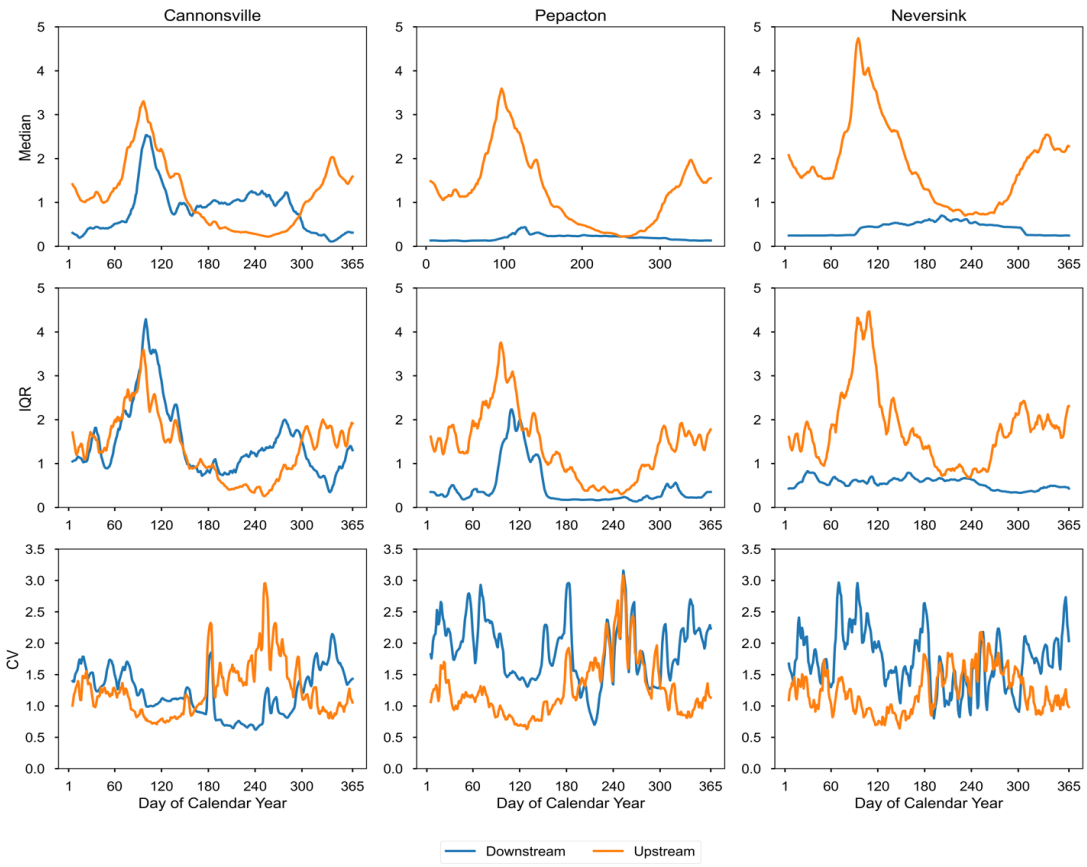

Figure 3: Median, interquartile range (IQR), and coefficient of variation (CV) of streamflow by day of year a date of a year for NYC reservoirs.

The upstream gauges show a consistent seasonal cycle, with streamflow peaking in April. While downstream of Cannonsville shows a similar seasonal cycle to upstream, Pepacton and Neversink's streamflow releases show little seasonality. Pepacton's downstream gauge has a significantly smaller, delayed peak flow; Neversink's releases are bimodal, with low, constant streamflow releases in winter and higher releases in summer. The interquartile range (IQR) follows the seasonality of the median flow, with the upstream high flow period having a larger IQR. This is also true for the IQR of the Cannonsville downstream gauge. Summer has a higher coefficient of variation at the upstream gauges, while there is no clear seasonal pattern at the downstream gauges. The high coefficient of variation compared to the IQR is due to the lower mean flow in

summer (with values less than 1). It is also worth noting that the mean flow has a higher values during peak flow season than the median, resulting in a lower coefficient of variation in spring.

2.4.2 Downstream propagation of hydrologic alteration

After quantifying the local hydrologic alteration immediately downstream of the dam, the propagation downstream of the reservoir impacts can be evaluated through the gauges along Delaware River and its tributaries. The three headwater tributaries of the NYC reservoirs join downstream (Figure 3a), and all distances are calculated moving upstream from the gauge at Trenton. The Cannonsville reservoir lies on the west branch of the Upper Delaware, while Pepacton reservoir lies on the east branch. The west and east branches join at Hancock, but the nearest gauge is at Callicoon, where the nearest gauge is 252 km upstream from Trenton. Later, the Neversink River joins the Delaware river at Point Jervis, where the nearest gauge is 160 km upstream from Trenton. The Lehigh River joins the Delaware River 86 km upstream of Trenton, contributing an average of 25% of the streamflow at Trenton.

2.4.2.1 Propagation downstream of annual flow statistics

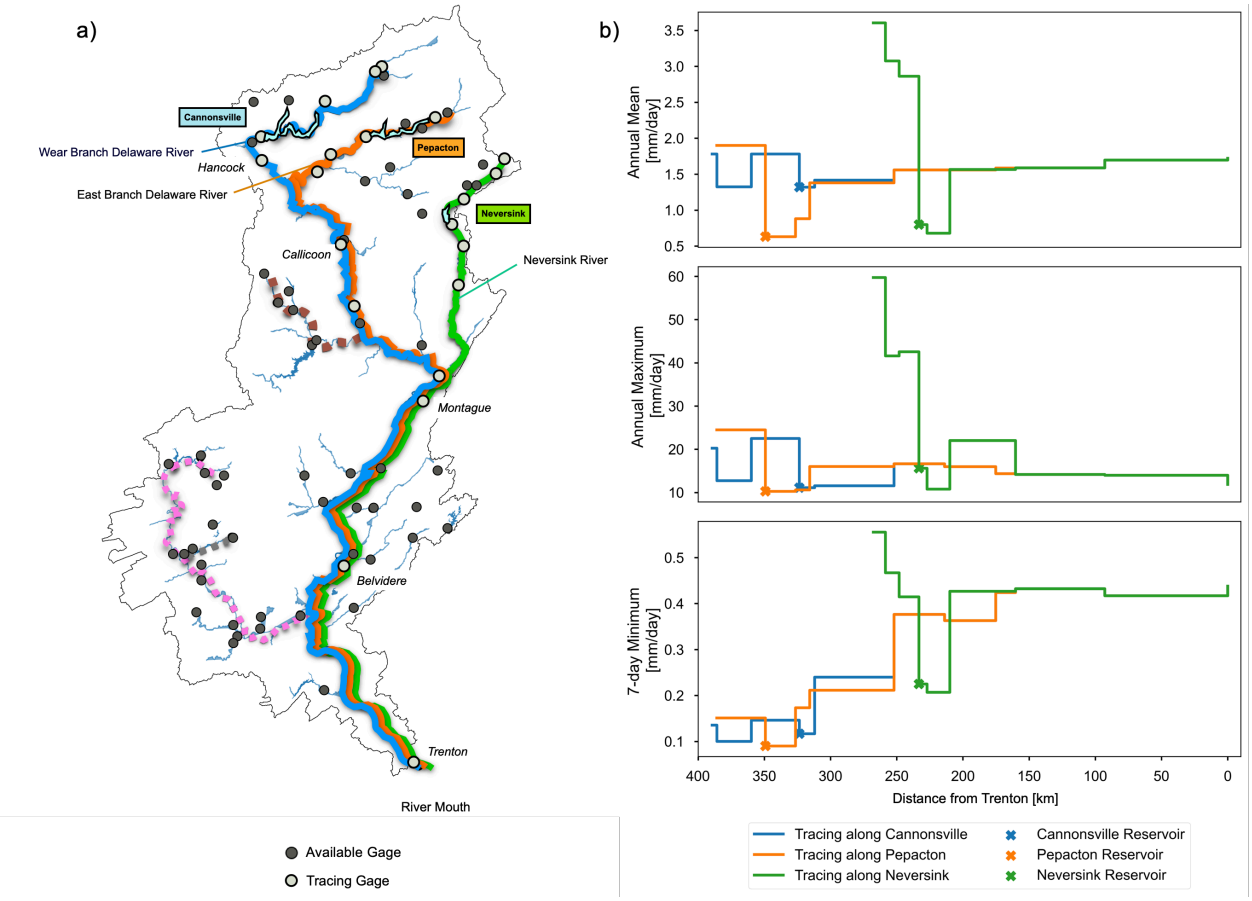

Figure 4a): Tracing streams of available gauges passed Cannonsville (blue), Pepacton (orange), and Neversink (Green). The Lackawaxen River (brown) and Lehigh River (pink) tributaries are also shown in the figure. A dark gray dot indicates the location of USGS gauges not on the mainstem evaluated and light gray indicates the location of tracing gauges used. The light blue shapes show the location of NYC reservoirs. Figure 4b) The trace along the river of the average annual mean flow, average annual maximum flow, and average 7-day minimum flow from the estuary station (0 km) to the upstream headwater station. The colors correspond to Figure 4a; the NYC reservoir locations are represented by an asterisk.

Figure 4 plots the annual flow statistics as a function of distance upstream of Trenton, NJ for the post-dam period. Mean annual flow in the post-dam period declined immediately downstream of the NYC reservoirs as shown in Figure 2, but Figure 4 shows that flow increases to similar levels upstream within 35 km (Figure 4b). This quick recovery could be due to inflowing tributaries or lateral flow from surface runoff and groundwater. Of the three dammed headwaters, the average flow in the upper Neversink River drops the most significantly after passing through the reservoir, and it returns to the natural values after a tributary, the Sheldrake River, joins the lower Neversink

River. In addition, the Neversink River contributes 5% of the total volumetric flow to the Delaware River to the streamflow at Montague. As for the other dams, the east branch, which passes through the Pepacton reservoir, has a larger decrease than the west branch (Cannonsville), and the east branch also contributes more discharge to the Delaware River.

The contribution of the Neversink River is less in the post-dam period, with less than 5%. In the upper Delaware region, the contribution of the west branch to the streamflow at Callicoon, increases from 63% in the pre-dam period to 83% in the post-dam period, which would also indicate a smaller influence of outflow through the Cannonsville outflow compared to Pepacton. In addition, the west branch contributes 66% in April (the wettest month), and 97% in August (the driest month) to the Delaware River, reflecting the retention of environmental flows at Cannonsville but not at Pepacton. Along the Delaware River, the volumetric flow at Montague, the first gauge downstream of all three NYC reservoirs, has an 11% decrease in the post-dam period. Further downstream, volumetric flow at Belvidere remains almost the same in the pre- and post-dam periods, and volumetric flow at Trenton has a slight increase due to the increase in flow in the Lehigh River. To summarize, Neversink has less impact on the lower Delaware River, and the Pepacton is of more importance, especially in the dry season. The drainage area increases downstream and could be a reason for the rapid dissipation. The increase of mean streamflow per unit area in Figure 4b illustrates that the water replenishment comes primarily from tributary confluences instead of lateral flow, as river outflow is close to the sum of the inflow in main stem gauges.

The downstream propagation of the annual maximum flow impacts is similar to the annual mean flow but with slightly reduced peak flows downstream of the dams. Although the primary purpose of the NYC reservoirs is not flood control, the annual peak flow is attenuated due to the impoundment. The highest peak flow in the upper Neversink reflects snowmelt on the high slopes of Catskill Mountain, and the NYC reservoirs have the ability to lower the peak flow.

The 7-day minimum flow also follows a similar pattern, with a drop immediately after the reservoirs and a quick return to the natural levels. The minimum flow increases along the main stem to around 0.4 mm/day at Trenton. The localized decrease in the 7-day minimum below the dams increases to the next gauges downstream and back to the upstream levels 24 km downstream and continues to increase to Belvidere. Along the Neversink River, the 7-day minimum flow has a large increase downstream of the dam due to the Sheldrake River.

To investigate whether there is a similar or unique behavior of different reservoirs along tributaries, trajectories along the Lehigh River and Lackawaxen River are plotted using the same process as Figure 4. Both rivers contain reservoirs that are used for water supply and flood control. From the results, the Lehigh River basin, especially the Pohopoco Creek tributary, shows a similar pattern to the main Delaware River, but tracking along the Lackawaxen River did not show any visible impact of the upstream dam in either spatial or temporal. Therefore, different dams may have great variability in the response along the reach.

2.4.2.2 Relationship with drainage area

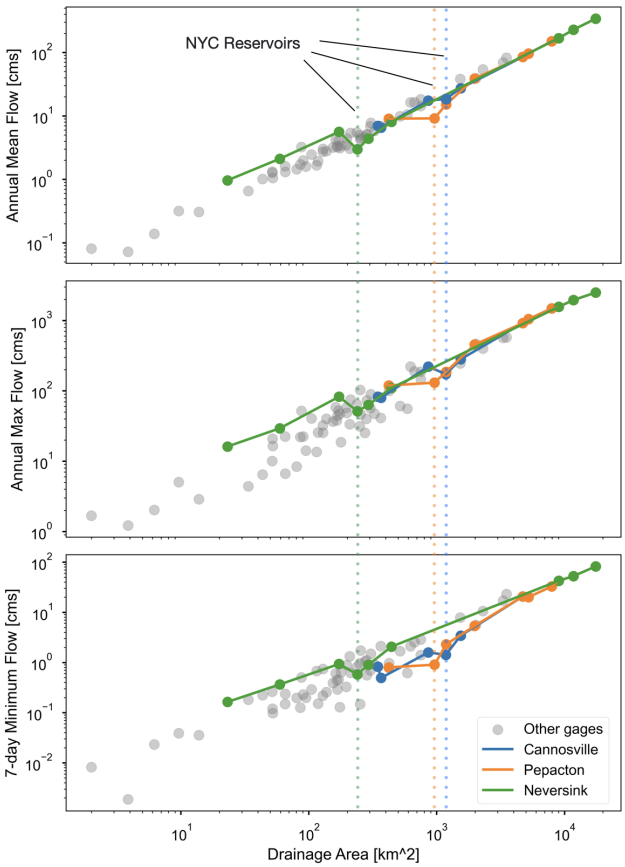

Figure 5: Scaling relationship between discharge and drainage area. The colored lines and dots are the tracing gauges passing NYC reservoirs. The gray dots are all available gauges in Delaware River Basin. The vertical dotted color lines indicate the location of the downstream gauge below the NYC reservoirs.

To further investigate the relationship between streamflow and drainage area, the power law relationship between annual streamflow statistics and drainage area is plotted in Figure 5. Mean annual discharge for the 78 gauges in the Delaware basin shows a strong relationship with drainage area in logarithmic space, with an R^2 of 0.981. The annual maximum flow and the 7-day minimum flow have R^2 of 0.932 and 0.910, respectively. The three branches are indicated by the colored lines, showing the reduction in mean annual flow downstream of the dam, particularly for Neversink and Pepacton. Streamflow in the upper Neversink is higher than in other gauges of similar drainage size. It is likely due to the Neversink drains the highest peaks of the Catskill Mountains. The minimum flow here has a smaller exponent in the scaling relationship, where the

minimum flow of the Neversink River is higher than expected compared to the same drainage area in the Delaware River Basin. On the other hand, Pepacton has a similar result to Cannonsville, but a larger impact on annual mean flow. Compared to the pre-dam period, the exponent is slightly lower, and the coefficient is increased in the post-dam period, which also reveals a slightly smaller discharge in a large drainage area and a larger one in a small drainage area. The coefficient of determination becomes slightly lower in the post-dam period, which would also indicate the variations, and the relationship between discharge and drainage area becomes more complex. Seasonality also alters the coefficient of drainage area, but the exponent is approximately constant, with more water tending to drain in April and May.

Other signatures have ambiguous relationships with drainage area (see Appendix A). The flow duration curve slope, mean half flow date, and streamflow elasticity do not show a relationship with drainage area. The BFI and RLD are likely to show a negative relationship, especially along the reservoir trace. This may be due to the gradual increase in streamflow and a slower response time in larger downstream drainage areas. However, this relationship did not show a strong relationship between all gauges, and hydrologic signatures may be highly dependent on other factors such as climate, topography, and land cover change.

2.4.2.3 Propagation of individual flood events

To further analyze the impact on the annual maximum flow, three large flood events are selected: September 2004, April 2005, and June 2006 (Figure 6). With the exception of the Neversink in 2004 and 2006, the dams did little to attenuate the peak flows during these events, as shown by both through the plot of the left column's plotting as a function of distance and the linearity of the scaling relationship with no decreases at the dams, as was seen in for the mean annual maximum flows in Figures 4 and 5. This highlights the limitations of the dams' ability to reduce downstream flows. First, the reduction is quickly attenuated as other tributaries join the

river. Second, the reservoirs have a limited flood control capacity, so when there is insufficient storage, outflows match inflows.

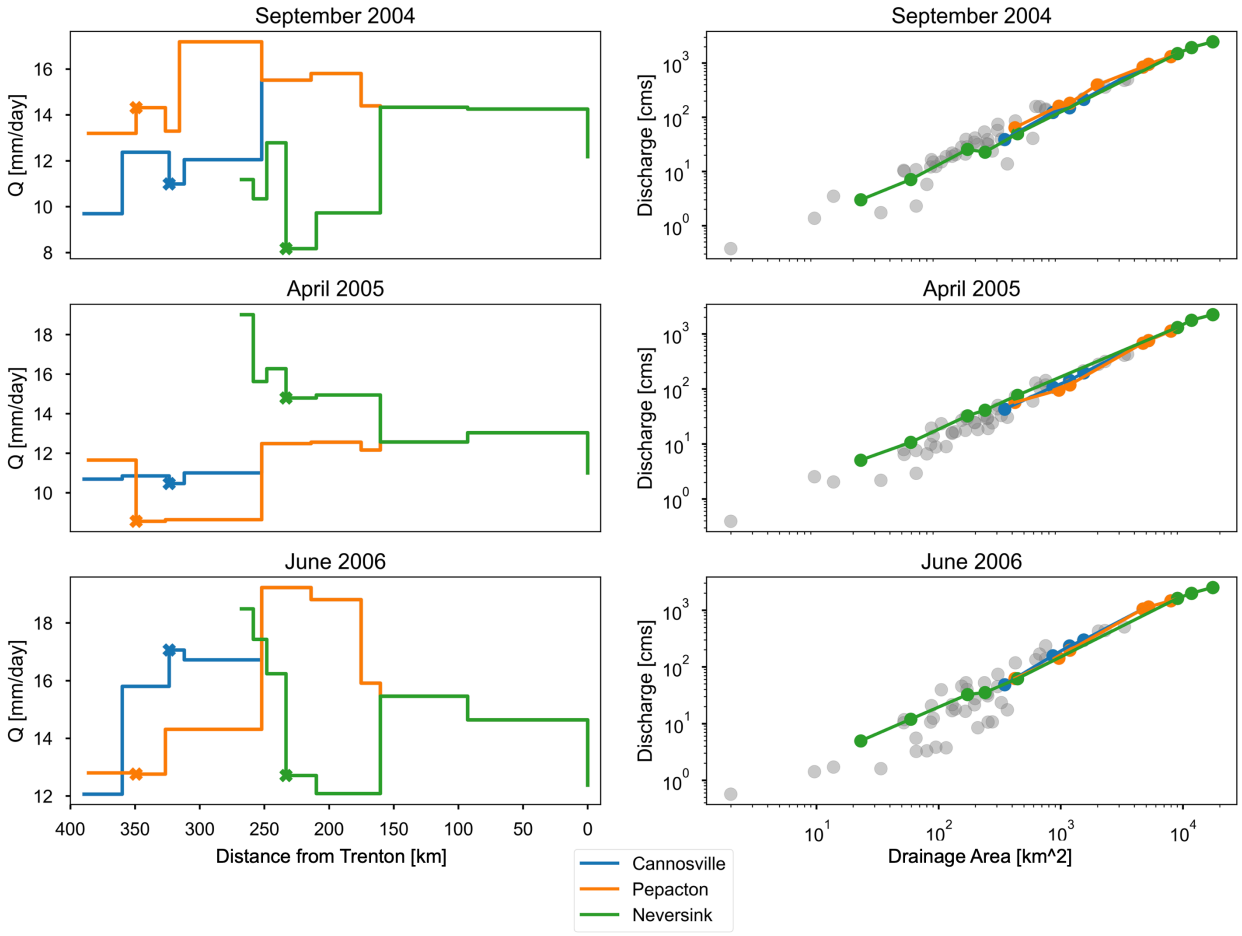

Figure 6: Tracing peak flows downstream for three flood events in the upper Delaware.

During the 2004 floods, the Pepacton area, particularly at Beaver Kill which is a subbasin near the Pepacton reservoir, had the largest streamflow anomaly. Dams did not play a role, as the increase in streamflow began downstream of the dam, and a large decrease occurred when the river joined the west branch of upper Delaware. Similarly, the Neversink area was most affected by the 2005 event, and both the west and east brunches were the focus of the 2006 event. The high flow decreased where the Neversink joins the Delaware River. During flood periods, the storage capacity of the NYC reservoir system is full and flows over the spillways according to the record of Water Resources Data New York Water Year 2005. From the right-hand subplot, the discharge of

the flood region lay in the upper range among the same drainage area. The extreme flood event can wash out the dam and affect the relationship between discharge and drainage area. There is no significant outlier in the flood region compared to Figure 5, where the reservoirs are reduced by the annual maximum flow.

2.4.2.4 Propagation of flow variability signatures

The other selected signatures reflect the temporal variability of the streamflow response in the Delaware; their downstream propagation is plotted in Figure 7. The runoff ratio shows the proportion of precipitation that becomes streamflow. Because precipitation does not have much spatial variation, it mimics what was seen in the mean annual flow plot (Figure 4). All three dams have significantly lower runoff ratios immediately downstream. This includes the Neversink, which has notably high runoff ratios in its headwaters, possibly reflecting the different hydrological conditions in the mountain peaks, including snowpacks. The baseflow index (BFI) decreases as one moves downstream. At all three dams, there is a significant drop in the baseflow index, which reflects the dam operations and the baseflow filter rather than the actual contribution of baseflow at the downstream gauges. What is notable is how quickly it recovers to its natural values.

Rising limb density decreases as the drainage area increases downstream. The effect of reservoirs on RLD varies, with a large increase at Neversink, and a small decrease at Cannonsville and Pepacton. The increase in RLD at Neversink dissipates at the next stream gauge located 25 km downstream. Similar to RLD, the FDC slope provides a measure of variability. The FDC slope generally becomes milder downstream. The abrupt slope around Cannonsville reservoir followed the local result in the previous reach, while Pepacton showed no anomaly at the reservoir. FDC at Neversink has a slightly steeper slope, but then the slope becomes small after a few kilometers. In addition, the variation of the low-FDC slope at Pepacton is larger than at Cannonsville, and the high-

FDC slope at Pepacton is higher than the other two. Fluctuations in flow became more frequent but dissipated quickly in nearby downstream gauges.

The tracing pattern for the mean half flow date is consistent: all reservoirs postpone the timing, and the date returns to the natural values within 50 km. Neversink has the largest impact on the half flow date, although the interannual variation of Pepacton is the largest. The flow in the first half of the water year is usually high compared to the second half, and storage can be increased in this period and then released in the dry requiring period. Streamflow elasticity varies widely along the Delaware River, increasing at Neversink, decreasing at Cannonsville, and remaining relatively unchanged at Pepacton. After merging the east and west branches, the streamflow elasticity becomes lower at Callicoon (250 km from Trenton), with a 1.3% change in streamflow caused by a 1% change in precipitation. However, the streamflow becomes less sensitive to precipitation after Callicoon. Streamflow elasticity changes largely in the lower Neversink River.

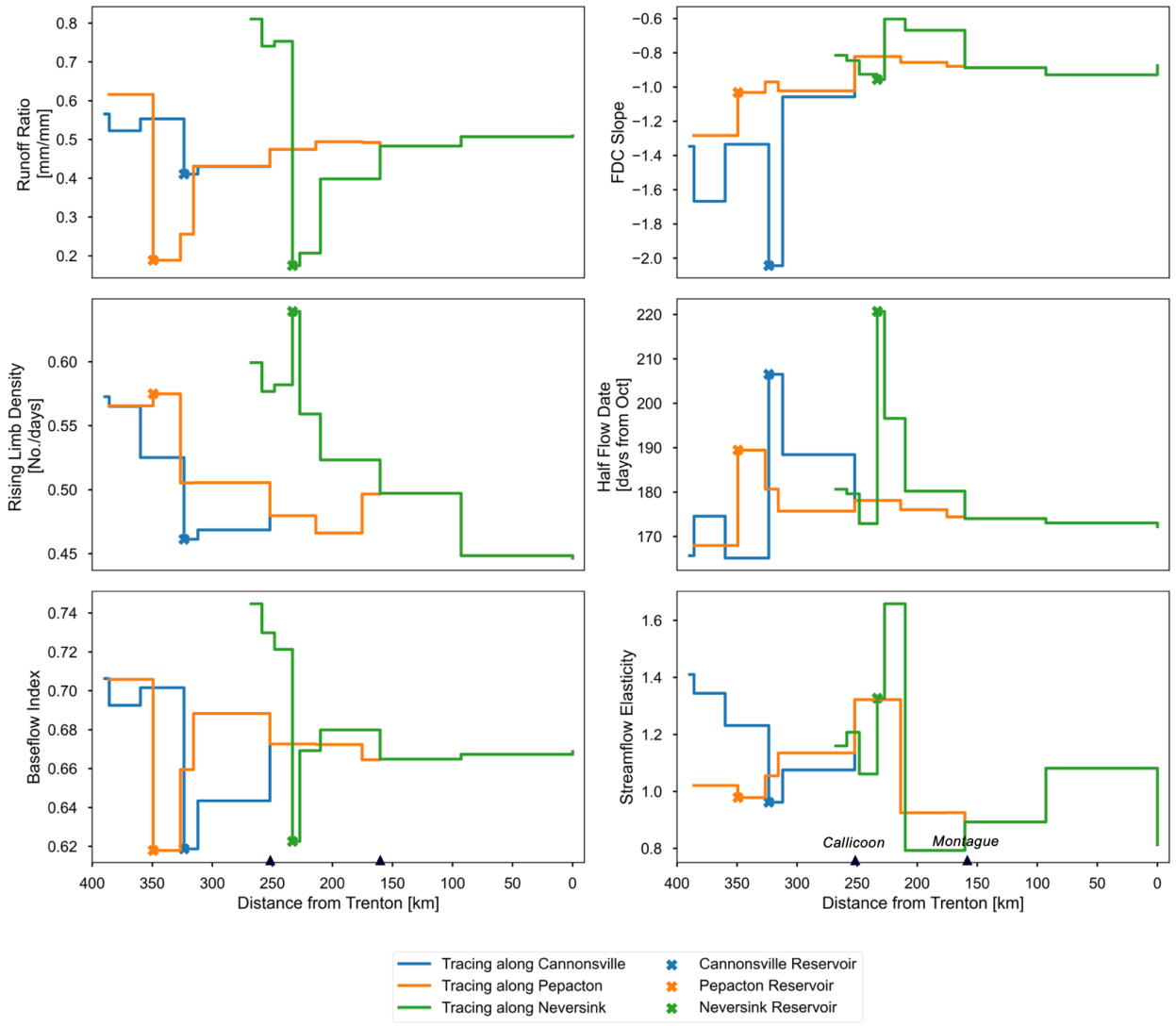

Figure 7: Similar to Figure 4b with signatures of runoff ratio, rising limb density, baseflow index, FDC slope, mean half flow date, and streamflow elasticity.

In summary, the flow magnitude pattern includes annual mean, annual maximum, 7-day minimum flow, runoff ratio, and baseflow index indicating that: NYC reservoirs decrease the flow magnitude; Pepacton can have the largest decrease downstream; and the rapid return in magnitude is mainly due to the tributaries' contributions. The mean half date shows that NYC reservoirs can largely change the time by the management of flow release. The flow variability involves RLD, FDC slope, and streamflow elasticity response differences along different reservoirs. Cannonsville could have a gradual release with smaller variations compared to Pepacton.

2.4.2.5 Pre- and post-dam period comparison downstream

The previous analysis relied on the post-dam period with the assumption that the headwaters were the "natural" state to which the streamflow signatures returned, which may or may not be true. Another way to analyze the data is to look at the difference between the post- and pre-dam periods. Any difference in the headwaters above the dam would be due to climate. Differences downstream would be primarily due to the dams, and these differences can be compared against the headwaters to understand climate. Figure 8 plots the relative difference in signatures as,

$$\frac{X_{post}-X_{pre}}{X_{pre}} \qquad \textit{[Eq. 2-5]}$$

where X is a signature, such as the RLD. It is worth noting that the pre-dam record lengths are shorter than the post-dam records, particularly upstream of the dams. Dam construction and reservoir filling were ongoing for 12 years for three NYC reservoirs between the two periods. Three gauges are missing for the Neversink River compared with Figures 4 and 7, two from upstream of the dam and one from downstream due to the lack of observations in the pre-dam period. The same is true for Cannonsville. The gauge before Hancock, which is the last gauge of the west branch before joining to the upper Delaware, is also missing in the pre-dam period. However, the gauges on the main stem of the Delaware River all have observations since 1942. Therefore, although some gauges are missing in Figure 8, the difference between the pre- and post-dam periods can still be observed in the trace. Changes in upstream gauges are solely due to climate forcing, but the result is not robust due to the shortage of data availability.

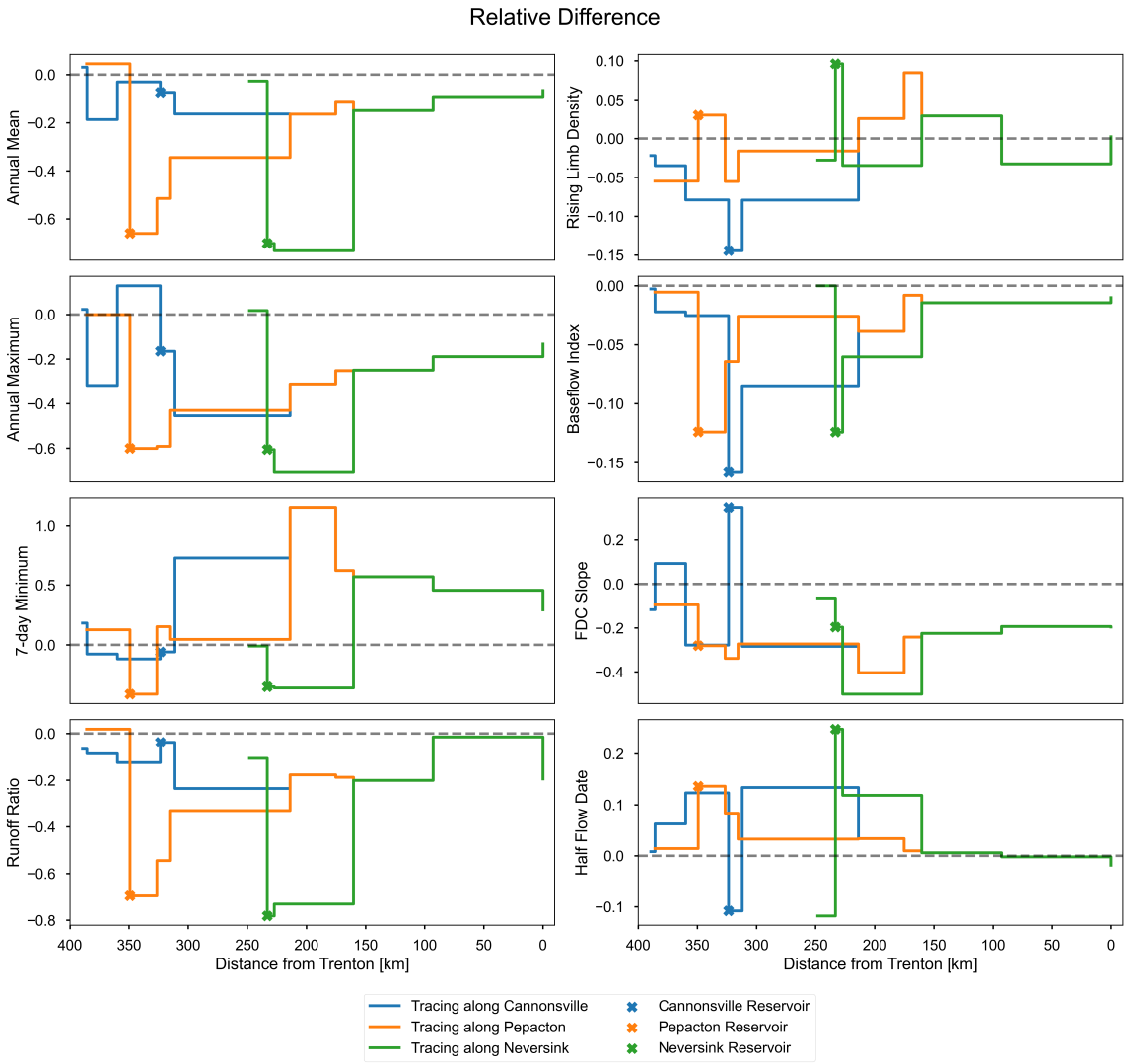

Figure 8: Relative difference between pre- and post-dam periods, calculated as the difference between post- and pre-dam normalized by the pre-dam values. The gray dotted line indicates zero change.

The change in almost all hydrologic signatures due to dams is consistent in Figures 4 and 7. The half flow date is the only signature with a significant difference in dam impact from the previous figures, with an earlier date at Cannonsville in the post-dam instead of the delayed one. Some signatures have a similar pattern across dams but with varying degrees, such as RLD at downstream Pepacton and FDC slope at downstream Neversink. Flow variability has decreased at Cannonsville, releasing the most consistent flow through the NYC reservoir system. This is

evidenced by the lower rising limb density at Cannonsville, as shown in Figure 8, while there is a vague decrease in Figure 7. Smooth release may be applied at Cannonsville.

The FDC slope in the downstream Neversink River shows a large decrease, and the FDC slope at Trenton decreased by 20% in the post-dam period. The mean half flow date increased as expected, but there is a large decrease in the Neversink above the dam, which could be caused by climate change, including changes in snowpack. The flow time is highly dependent on the flow release management of flow releases to downstream flow targets, especially in the dry period.

2.4.2.6 Spatial patterns of seasonality

Signatures of streamflow mean, maximum flow, 7-day minimum flow, rising limb density and baseflow index on the seasonal time scale can show the variability of intra-annual flows. Figure 9 shows the same tracing gauges as Figures 4 and 7 on a map of the Delaware River Basin. In general, the upper Neversink watershed has larger flow and variability in all seasons in the Delaware River Basin. The seasonal flow tracing along the Delaware River downstream has a similar change along the river length (see Appendix A), but the magnitude shifts up and down with the season. The Neversink reservoir's RLD is smaller in spring and higher in summer. In addition, RLD in winter has a large increase at NYC reservoirs compared to the other seasons. For BFI, a higher index occurs in summer and spring, while fall has the lowest BFI among the seasons. BFI downstream of NYC reservoirs is low. The biggest range of BFI occurs in summer.

Figure 9: Seasonal variation of the signatures in the post-dam period. Rows are selected signatures, and columns are Spring (March, April, May), Summer (June, July, Aug), Fall (Sep, Oct, Nov), and Winter (Dec, Jan, Feb).

2.5 Discussion and conclusions

The flow regime immediately downstream of the NYC reservoirs has been largely changed in both magnitude and variability; however, these impacts dissipate quickly downstream in most cases. Most of the hydrologic signatures have a large local decrease and then recover within 35 km, showing good resilience. The recovery is mainly due to the streamflow contribution of tributaries, and baseflow can comprise a significant portion of the tributaries' streamflow especially in dry periods. Considering not only the streamflow but also the baseflow contribution can provide an understanding of how the downstream streamflow should be maintained during dry periods.

The increasing drainage area can be an essential element in interpreting the fading of downstream effects of reservoirs (Batalla et al., 2004). The downstream reaches with larger drainage areas are less sensitive to runoff and all reservoirs shift the timing. These results also reflect the ability of hydrologic signatures to identify which and where the hydrologic alteration is sustained by dams in wet areas. From the scaling relationship between discharge and drainage area, the dams' impact immediately downstream can be identified as an outlier in the basin, but this impact is not present in extreme flood events. The consistent scaling relationship, except for the gauges immediately downstream of the dams, implies that the NYC dams only impact the local streamflow downstream in the long-term average.

Among the NYC reservoirs, Cannonsville has a smaller impact locally. The larger capacity reservoirs may reduce the connection between climate and streamflow (Vicente-Serrano et al., 2017), where the dams' regulation and tributary contribution play more important roles in determining downstream streamflow. The flow regime in the upper Neversink River may be different from the main stem due to changes in the hydroclimatology, with a higher drop in the mean flow per area, as well as a high runoff ratio and flashiness. Interaction with groundwater may be a key factor in this area. Snowmelt was not a focus of this study, but it can be observed in the seasonality, where peak flow is often reached in the spring. Winter-spring streamflow increased at

over 50% of the gauges from 1948 to 1988. The snowmelt becomes earlier in North America, which increases annual streamflow in spring (Stewart et al., 2005). The spatial pattern is relatively constant across seasons. Some observations can be seen, such as the low flow is more critical in the upper western basin and streamflow elasticity is low in the upper eastern basin.

The result is similar to the Sacramento River Basin, where the dam-influenced hydrograph characteristics rapidly vanish with distance downstream and tributaries' confluence (Singer, 2007; Singer & Dunne, 2004). A similar recovery trajectory can be found in most of the signatures, where the Delaware River downstream is minimally altered by the NYC reservoirs in both magnitude and variability. If this method was implemented in other river basin, the tracing variation in streamflow signatures may demonstrate different results by different dams with different dam purposes, and various heterogeneity with respect to regional climate. The flood control dams retain climate signatures in flow regimes, but decrease the downstream hydrographs of regional heterogeneity (Ferrazzi et al., 2021). In contrast, water supply reservoirs increase the independence of climate signatures and even break the connection between climate and flow regime with a higher spatial diversity in hydrology (Ferrazzi et al., 2021). The difference between NYC reservoirs and the Prompton Dam along the Lackawaxen River may reflect the difference in releases by purpose. Uncertainties in the streamflow and precipitation measurements may have more impact on “high-frequency response” values, but less impact on spatial or temporal averages (Westerberg & McMillan, 2015).

Some major ecosystem changes have been reported, such as thermal fish kills, a shift from a coldwater community to a warmwater, loss of native and long-living brook trout loss due to heavy angling, stocking of domesticated brook trout and exotic species (Ravindranath et al., 2016). Depth and distance from the dam can strongly influence the response of the fish community (Prchalová et al., 2009). Although the decrease in mean streamflow impacts the extent of the ecosystem and reduces the diversity of aquatic life, there is no evidence of incursive species growing downstream

of water supply reservoirs (Ferrazzi & Botter, 2019a). The mean half flow date at large reservoirs could affect fish or animals that require water in a particular season. Additionally, stream temperature can be direct evidence of aquatic change. The temperature at the upstream gauge is higher than downstream at NYC reservoirs, especially in summer, while the downstream temperature can be slightly warmer in winter (October to February). The large flow reductions and fluctuations in NYC reservoirs can lead to thermal changes in the stream temperature (Daniels & Danner, 2020), result in a biodiversity loss.

This study is based on observed data, and the method is straightforward with few assumptions. The likely limitation for the extension to other basins or a larger scale is the availability of headwater gauges, pre-dam streamflow data, and the distance between gauges. In our study, the length of data available in the pre-dam period is a shortcoming, where each year in the pre-dam period has a greater weight on the statistics than any given year in the post-dam period. Climate signatures are not specifically included in the tracing other than precipitation, but they can play a significant role in seasonality. Modeled streamflow can help to address these concerns. In addition, the uncertainty of the hydrologic signatures can be important to consider, and the subjective selection in this qualitative method may lead to different results, such as BFI in different methods. To apply the method to another basin, dense gauges are required, and they must start early enough to detect the pre-dam streamflow. Climate change may not be ignored if the dam is constructed after the late 90s.

For future studies, using a hydrologic model, such as the Variable Infiltration Capacity (VIC) model, can be used to simulate the naturalized streamflow and further be used to compare with the observed tracing. This can address the problem of the short pre-dam period data. The VIC model will be discussed in the next Chapter. The impact of reservoirs is required in combination with a river fragmentation and connectivity metric (Jumani et al., 2020). The impact of climate change on a regulated river in local and long-term variation might also be critical to study, and a more

comprehensive view can be combined with climate change on these hydrological signatures through the VIC model, which will be able to simulate any climate impacts. In addition, a detailed influence on biodiversity can help to better monitor and plan for ecosystem affluence. The Ecological Limits of Hydrologic Alteration (ELOHA) framework (Arthington, 2016) can be a useful tool for integrating the hydrologic response into an ecological metric, and there is an ongoing project related to the Delaware River Basin.

Chapter 3: Evaluation of the VIC model's ability to simulate baseflow

3.1 Introduction

In the first chapter, two possible methods for analyzing hydrological alteration in a regulated river basin are proposed: using historical observations and a model-based approach. Chapter 2 used the historical approach in the Delaware River Basin, demonstrating how far downstream dam impacts propagated through the river network. Whether it is feasible to implement the model-based approach remains in question. Such a model needs to have the ability to correctly simulate the hydrologic signatures. However, hydrologic models are typically evaluated based on mean streamflow rather than specific hydrologic signatures. A preliminary evaluation is required to ensure the model's ability to simulate certain hydrologic processes and signatures, such as baseflow and the baseflow index, to determine the feasibility of this approach. This chapter presents an exploratory analysis to determine whether using the Variable Infiltration Capacity (VIC) model for naturalized estimates of hydrologic signatures would be possible in future work.

Hydrologic models, such as the Variable Infiltration Capacity (VIC) model (Anghileri et al., 2016; Harrell et al., 2022) and Soil and Water Assessment Tool (SWAT) (Jha et al., 2004; Oo et al., 2020; Rahman et al., 2013), have been successfully used for simulating streamflow response. Although model uncertainty cannot be avoided, the results are valuable for isolating human interventions and being able to estimate naturalized streamflow (Botter et al., 2010). The VIC model is a large-scale, physics-based model that has been widely used through a range of hydro-meteorological conditions, including streamflow simulation (Bai et al., 2016; DeChant & Moradkhani, 2014; Kumari et al., 2021; Su et al., 2005), snow modeling (Andreadis & Lettenmaier, 2006; Pan et al., 2003; Sheffield et al., 2003), and flood monitoring (Khan et al., 2011; Schumann et al., 2013; Wu et al., 2014). VIC has been shown to perform well in many river systems throughout

the world (Maurer et al., 2002; Nijssen et al., 1997), such that it is likely to simulate the processes needed for naturalized estimates of streamflow. It has specifically been shown to be able to simulate mean naturalized streamflow in the Delaware River Basin (Liang et al., 1994; Troy et al., 2008).

Like many hydrologic models, VIC requires calibration, and most studies have focused on monthly discharge (Elsner et al., 2014; Maurer et al., 2002; Troy et al., 2008; Zhao et al., 2019). Calibrating is the process of adjusting the parameters for output results to match observations, and validating means verifying that the calibrated result is satisfactory to use, usually by testing in other time periods and locations. Although calibrating and validating against observed streamflow has been widely done at the monthly scale, there is a gap in both with respect to hydrologic signatures from the VIC model. The concept of "signature-domain" calibration has been presented to accommodate different hydrologic features (Fenicia et al., 2018). In this approach, there is a streamflow calibration function that includes annual streamflow, baseflow index, high flow, and low flow, which was recently generated for the VIC model (Yang et al., 2019) and involves three possible sensitive soil parameters (Demaria et al., 2007). Despite the lack of flashiness, which may affect the possibility of an information loss (Fenicia et al., 2018), and the small amount of calibration parameters, this calibration method has largely improved streamflow prediction in the eastern United States. However, there is also no substantial proof that the streamflow predicted by the VIC model can be used to calculate correct hydrologic signatures, particularly the proportion of streamflow that comes from baseflow. Since the VIC model more typically matches mean streamflow (Troy et al., 2008), this may mean the model simulates monthly streamflow well but for the wrong reasons, such as the relative contributions of baseflow and runoff to streamflow. Therefore, there is a gap in understanding the model's ability to accurately represent baseflow, which is a key component in the characterization of hydrologic signatures. Further research is necessary to close this gap and improve the accuracy of the VIC model in simulating baseflow to

reach the original goal of evaluating the hydrological alteration in a regulated river. The separation of baseflow from streamflow and VIC's ability to simulate the baseflow will be the focus of this Chapter to gain a better understanding of slow flow response in the VIC model.

Sensitivity analyses have been applied to hydrologic models to identify and prioritize the parameters most influential to the system, and to understand interactions between parameters (Razavi & Gupta, 2015; Ruano et al., 2012). The soil parameters affect the water and energy budgets more than the vegetation properties in the land-surface model parameterizations (Liang & Guo, 2003). Sensitivity analysis of the VIC model's soil parameters has been performed for streamflow. A sensitivity analysis of soil parameters by Demaria et al. using the Monte Carlo method identified that the dominant parameters for simulating streamflow are *infil*, *exp*, and *depth2* (Demaria et al., 2007). Melsen et al. (2016) used Distributed Evaluation of Local Sensitivity Analysis and found that *infil*, *ds*, *exp*, and *dsmax* are the most sensitive parameters of four catchments in Switzerland.

Although there are an increasing number of studies on VIC's calibration, the parameter estimation and sensitivity analysis for the VIC model is thus far insufficient for simulating most hydrologic signatures capable of detecting human alteration along river networks, and no studies have focused on baseflow. There are still gaps in understanding the role of VIC parameters in baseflow and streamflow simulation and how they may interact with each other. Accordingly, a sensitivity test of soil parameters with a focus on baseflow simulation is performed in this chapter to investigate whether it is possible to correctly simulate baseflow characteristics. This chapter answers research question 3:

> *What is the ability of the VIC model to simulate the hydrologic signatures to provide estimates of the naturalized hydrologic regime? If it is poor, is it possible to improve the performance through parameter calibration and identifying important parameters to correctly simulate streamflow and baseflow characteristics?*

First, the initial model set-up with a previous soil parameter calibration is assessed. Then, a subset of sensitivity runs is performed where soil parameter values are varied to detect their impact on the baseflow generation. Runoff is also included in the analysis to supplement the baseflow results. The preliminary sensitivity analysis would help understand the subsurface response to the soil parameters and identify the most and least influential calibration parameters for baseflow.

3.2 Model-based method

The model-based method proposes to use the difference between the model, as a proxy for naturalized flow without dams, and the observations in the post-dam period to quantify the dams' downstream impact in a river network. The difference between the modeled and the observed hydrologic signatures would be used as a metric to detect the downstream impacts in the same way as the historical observations in Chapter 2.

Figure 10 demonstrates the model-based approach by tracking the annual mean flow from upstream of the Pepacton Dam down to Trenton, NJ. Theoretically, the observed and modeled results would be expected to be the same if there were no dams throughout the entire trace. For the post-dam period, a decrease in the observed streamflow at the reservoirs is expected due to the impoundment and out-of-basin transfer to NYC, and relatively constant streamflow is expected from the modeled streamflow normalized by area. The example of the Pepacton reservoirs and the downstream river network (Figure 10) shows the expected result for VIC with relatively constant mean streamflow normalized by area. At the reservoir, the observed flow significantly decreases, as expected given the water supply diversions. This difference between observed and modeled streamflow, along with the distance downstream, can be quantified as the alteration due to regulation, with the dam's effects dissipating within 100km downstream. Ideally, this approach could be applied with all the hydrologic signatures used in the previous chapter, thereby providing a robust result of the impact propagation on the streamflow magnitude and variability. In other

words, the modeled streamflow must be shown to be a reliable proxy for the calculation of naturalized hydrologic signatures, especially those related to baseflow.

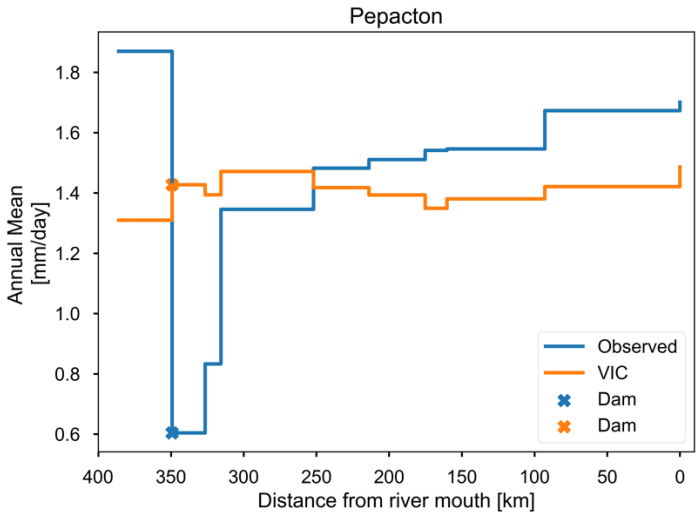

Figure 10: Tracing the average annual mean flow for available gauges along the Pepacton reservoir's branch from observation (blue) and the VIC model (orange). The x dot shows the gauge immediately downstream of the reservoir.

3.3 VIC Model

The Variable Infiltration Capacity (VIC) model is a land surface hydrological model that simulates the components of the water and energy budgets (Liang et al., 1994, 1996). The processes are calculated for spatially distributed grid cells (>>1km), and the grid cells are independent of each other, neglecting horizontal flow between grid cells except in the river channel. The land-atmosphere fluxes and the water and energy balances can be run at daily or sub-daily time steps. Figure 11 illustrates the basic concept of the soil layers in the VIC model and the two principal relationships for infiltration and baseflow that will be explored in this chapter.

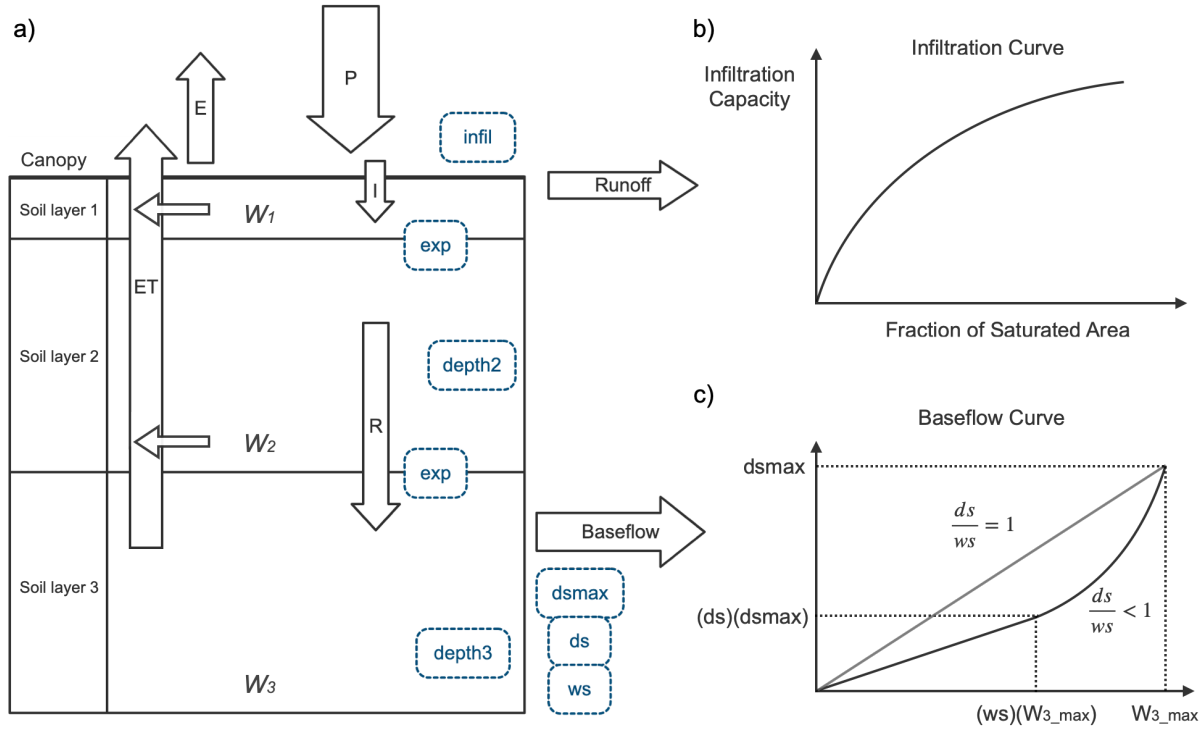

Figure 11a): Schematic of VIC model recreated from Liang et al. (1994, 1996). W_1, W_2, W_3 are the time-varying soil moisture storage in each layer; E is evaporation; ET is evapotranspiration; P is precipitation; Runoff is the surface runoff; I is the infiltration; R is the drainage recharge between the two lower vertical layers. Model parameters are in the dotted boxes and summarized in Table 1. Figure 11b): Infiltration curve as a function of storage in soil layer 1. Figure 11c): Baseflow curve in soil layer 3. W_{3_max} is the maximum soil moisture in layer 3; ws is the fraction of soil moisture at the beginning of the non-linear curve; ds is the fraction of dsmax where non-linear baseflow begins; dsmax is the maximum rate of baseflow.

The subsurface is represented by three vertical layers as shown in Figure 11a, where the upper layer affects the dynamic response between soil moisture and infiltration. The thickness of soil layer 1 is usually 10 cm (Liang et al., 1996). The variable infiltration curve partitioning process is plotted in Figure 11b, incorporating both saturation and infiltration excess runoff generation mechanisms. The direct runoff is calculated for the upper layer, and it allows for subgrid soil heterogeneity. The infiltration capacity can be expressed as,

$$i = i_m \left[1 - (1 - A)^{\frac{1}{infil}}\right] \qquad \textit{[Eq. 3-1]}$$

where i is the infiltration capacity; i_m is the maximum infiltration capacity; A is the fractional area of the saturated grid cell; and *infil* is the infiltration shape parameter.

Soil layers 2 and 3 are used to capture the slower change in soil moisture that is characteristic of subsurface dynamics. Baseflow (slow flow runoff) can only be generated in soil layer 3. Figure 11c illustrates the baseflow generation curve in the bottom layer. The form of this equation assumes the baseflow response is linear when soil moisture is below a threshold and is nonlinear above this threshold. *ds* must be smaller or equal to *ws*, and when *ds* equals *ws*, the whole process becomes linear. The equation describing the baseflow curve can be expressed as,

$$B = \begin{cases} \frac{(ds)(dsmax)}{(w_s)(W_{3\_max})} W_3, \ 0 \le W_3 \le (w_s)(W_{3\_max}) \\ \frac{(ds)(dsmax)}{(w_s)(W_{3\_max})} W_3 + (dsmax - \frac{(ds)(dsmax)}{ws}) (\frac{W_3 - (w_s)(W_{3\_max})}{W_{3\_max} - (w_s)(W_{3\_max})}), \ (w_s)(W_{3\_max}) \le W_3 \le W_{3\_max} \end{cases} \quad \textit{[Eq. 3-2]}$$

where *B* is the baseflow (subsurface runoff); W_{3_max} is the maximum soil moisture in layer 3; *ws* is the fraction of soil moisture where the non-linear part starts; *ds* is the fraction of *dsmax* where non-linear baseflow begins; *dsmax* is the maximum velocity of baseflow; W_3 is the time-varying soil moisture in the bottom layer.

The drainage process between each layer is designed through gravity drainage by the Brooks-Corey relationship. The vertical drainage between three soil layers is expressed as

$$Q_{i,\ i+1} = K_{s_i} (\frac{W_i - \theta_i}{W_{i\_max} - \theta_i})^{exp}, \ i = \{1, 2\} \quad \textit{[Eq. 3-3]}$$

where $Q_{i,\ i+1}$ is the drainage from the upper layer (*i*)to lower layer (*i*+1); K_{s_i} is the saturated hydraulic conductivity in layer *i*; W_i is the soil moisture content of layer *i* ; W_{i_max} is the maximum soil moisture content of layer *i* ; θ_i is the residual moisture content of layer *i* ; *exp* is the exponent which equals to $(\frac{2}{p} + 3)$, where *p* is the pore size distribution index.

Water can also be extracted upwards through evapotranspiration in all three layers. Evapotranspiration is calculated by the Penman-Monteith equation, where ET is a function of net radiation, vapour pressure deficit, soil moisture, and aerodynamic resistance. The total ET consists of the canopy evaporation, transpiration from vegetation, and evaporation from the bare soil, with each flux weighted by the land cover fractions within the grid cell. The detailed VIC model structure and equations can be found in the literature (Liang et al., 1994, 1996).

3.4 Methods and data

3.4.1 Sensitivity analysis

The sensitivity analysis of baseflow and runoff simulations to soil parameters from the VIC model will not only help to identify the parameters influencing the baseflow, but also to detect the interactions between each parameter. Seven parameters are selected to investigate in this analysis, summarized in Table 2. These parameters are called calibration parameters because they are used for calibration and cannot be physically measured or have ambiguous values at the model's spatial scale. Three different values are run for each parameter, resulting in a total of 2187 unique parameter sets for each grid cell. The selected values are based on the feasible range of the parameters (Troy, personal communication).

Table 2: Parameters varied in the sensitivity analysis

Parameter	Meaning	Unit	Selected Values
infil	Infiltration curve parameter	-	0.01, 0.3, 0.7
ds	Fraction of *dsmax* where non-linear baseflow begins	-	0.1, 0.4, 0.7
dsmax	Maximum baseflow that can occur from soil layer 3.	mm/day	5, 10, 30
ws	Fraction of maximum soil moisture where non-linear baseflow occurs	-	See context ws_{sub} *in* 0.1, 0.4, 0.7
depth2	Thickness of the second soil moisture layer	m	1, 2.5, 4
depth3	Thickness of the third soil moisture layer	m	1, 2.5, 4
exp	Exponent for unsaturated hydraulic conductivity (Brooks–Corey relationship)	-	5, 15, 30

The *infil* is the infiltration curve shape parameter, where a higher *infil* value would lead to larger infiltration for a given precipitation value and soil moisture state. The *infil* parameter is non-observable and determines the exponent in the infiltration curve (Eq.3-1). The d*smax* parameter will change the maximum baseflow contribution, and higher *dsmax* will represent a higher peak of

baseflow. *ds* is the fraction of *dsmax* above which baseflow becomes nonlinear, and it has a relationship with *ws*, where if *ds* is close to *ws*, the hydrograph recession curve becomes steeper.

According to the baseflow curve, *ds* cannot exceed *ws*. For computational ease, a different variable, ws_{sub}, was varied in the sensitivity runs that is a fraction of *ds.* The equation to calculate *ws* from the ws_{sub} parameter is,

$$ws = ds + (1 - ds) \times ws_{sub} \qquad \textit{[Eq. 3-4]}$$

where *ws* is the value of the fraction of maximum soil moisture where non-linear baseflow occurs and ws_{sub} is the variable in the VIC run and values of 0.1, 0.4, 0.7 were run.

The *depth2* and *depth3* are the thickness of the lower soil layers, where the *depth2* will impact the vertical drainage process and evapotranspiration, and *depth3* will directly change baseflow generation due to the soil moisture capacity. A higher *depth3* will enlarge W_{3_max}, and result in a smaller peak in baseflow simulation. The *exp* is the exponent of the drainage equation, and a larger *exp* will represent slower drainage, which ends up with a lower baseflow. The *exp* parameter is the exponent in the vertical drainage equation (Eq.3-3).

Each simulation is run in full energy balance mode at 1/8° spatial resolution from Jan 1979 to Dec 1989 at an hourly time step. The first four years are used for spin-up, and 1983 to 1989 are used for sensitivity analysis. The three study sites are located at upper Cannonsville (Gauge 01435000), upper Pepacton (Gauge 01413500), and upper Lehigh River (Gauge 01449360), all of which are above the reservoirs and therefore have minimal human influence. The streamflow observation data are from the U.S. Geological Survey (USGS), and they are used for model validation and baseflow estimation using the method described below. The meteorological and radiative forcing data are from the North American Land Data Assimilation System project (NLDAS), version 2 (Xia et al., 2012). Forcings include air temperature, precipitation, downward shortwave, and longwave radiation, wind speed, surface pressure, and specific humidity (Cosgrove et al., 2003). The vegetation library is from SECHIBA, a parameter set of hydrologic exchange between soil-

vegetable, and atmosphere (Ducoudré et al., 1993). This study uses the version of VIC 4.1.2; more information can be found in the UW GitHub repository (https://github.com/UW-Hydro/VIC).

3.4.2 Baseflow separation and comparison

The Eckhardt filtered method (Eckhardt, 2005, 2008) is used to separate baseflow from the observed streamflow, and it was found as the best performing among different filter methods in the continental U.S. (Xie et al., 2020). The Eckhardt filter, which was also used for the baseflow index in Chapter 2, is expressed as,

$$B_i = \frac{(1-BFI_{max})\times a\times b_{i-1}+(1-a)\times BFI_{max}\times q_i}{1-a\times BFI_{max}} \quad \textit{[Eq. 3-5]}$$

where B_i is baseflow at time step i; b_{i-1} is baseflow at time step *i-1*; q_i is streamflow at time step i; a: filter parameter; BFI_{max} is the maximum baseflow index (ratio of baseflow to the total streamflow). The filter parameter is set at 0.96 and BFI_{max} is 0.6, replicating the previous setup in Chapter 2. The recession constant and backward filter method (Collischonn & Fan, 2013) were used to determine the value. Figure 12 shows the filtered baseflow at the upper Cannonsville gauge from May to October 1986. Although baseflow cannot be measured, the Eckhart filtered baseflow time series is reasonable compared to the observed streamflow and can be used as the proxy of the "observed" baseflow.

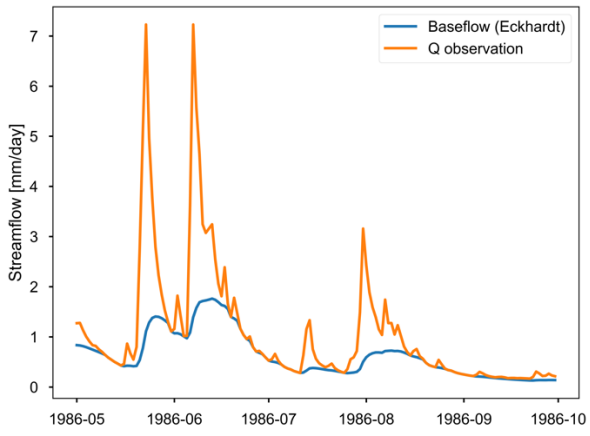

Figure 12: A demonstration of baseflow separation for USGS gage 01423000. The USGS streamflow is orange, and the Eckhardt-filtered baseflow is blue.

The root mean square error (RMSE) is applied as a metric for evaluating the VIC simulation by comparing the Eckhardt method filtered baseflow with all VIC runs. Optimal parameter sets are identified in the sensitivity runs by using RMSE. The RMSE equation is expressed as,

$$RMSE = \sqrt{\frac{\sum_i^N (B_{Eck} - B_{VIC})^2}{N}} \quad \textit{[Eq. 3-6]}$$

where N is the number of days; B_{Eck} is the filtered baseflow from the Eckhardt method; B_{VIC} is the baseflow simulation by VIC for each parameter set. RMSE is widely used as a basic function of evaluating the performance of a model.

3.4.3 Local sensitivity analysis

The local sensitivity analysis is used to identify parameters with the highest sensitivity and to understand the interaction between parameters. The equation upon the gradient of the performance index ψ (Rakovec et al., 2014) is expressed as,

$$\left.\frac{\partial \psi}{\partial \theta_j}\right|_l \quad \textit{[Eq. 3-7]}$$

where ψ is the selected performance index; θ_j is the j^{th} value of parameter θ; l represents the set of parameter values other than θ. The ψ can be any metric defining the baseflow simulation in that parameter set. In this study, mean value and standard deviation are used for the representation of model sensitivity. For example, for a given performance index and no secondary parameter varies, the gradient equation between median and high value for a parameter θ can be expressed as,

$$\left.\frac{\partial \psi}{\partial \theta_j}\right|_l = \frac{\psi(\theta_{high}) - \psi(\theta_{median})}{\theta_{high} - \theta_{median}} \quad \textit{[Eq. 3-8]}$$

where ψ is the performance index (e.g. the average baseflow); θ_{high} is the high value of parameter θ; l is the rest of the parameter set and l is held in the median when not considering the additional parameter's impact at θ. The second parameter in l can be varied to reveal the interaction between parameters and evaluate which parameter has a large influence on other parameters. To normalize different categories of θ, a percentage change from the lower value (e.g. median to high) is used for

a comparison between parameters. The new denominator represents a gradient change per change in θ_{median} and calculated as,

$$\frac{\psi(\theta_{high})-\psi(\theta_{median})}{\frac{(\theta_{high}-\theta_{median})}{\theta_{median}}} \quad \textit{[Eq. 3-9]}$$

The percentage change from the low to the median value of parameters is also calculated based on Eq. 3-8. The difference between these two ranges in the performance index shows that the model sensitivity depends on the range of values selected. The *infil* and *exp* parameters have a disproportionate impact due to the changing the exponent in the applicable equations, which can result in a large impact on runoff and baseflow.

3.5 Results

Section 3.5.1 evaluates the ability of the VIC model to simulate streamflow and baseflow using an existing model configuration (Troy et al., 2008). The following subsection presents the results of the sensitivity run and the possibility of simulating baseflow correctly. The goal of this section is to evaluate if the VIC model can accurately simulate baseflow, and therefore baseflow-related hydrologic signatures, by varying the calibration parameters. Later, the parameter sensitivity analysis of the baseflow identifies the parameters with the largest and smallest impacts on the simulated baseflow. Finally, the impact of parameters on surface runoff is evaluated to better understand the potential for VIC to simulate streamflow accurately.

3.5.1 Initial VIC simulation

VIC simulates the runoff and baseflow from the land surface, and a routing model is used to simulate streamflow. For this analysis, monthly streamflow in small basins is analyzed so streamflow is calculated using a lumped routing approach. Figure 13 evaluates the model's simulation of the seasonal cycle, annual mean, and monthly mean streamflow for the three selected gauges from 1980 to 2010.

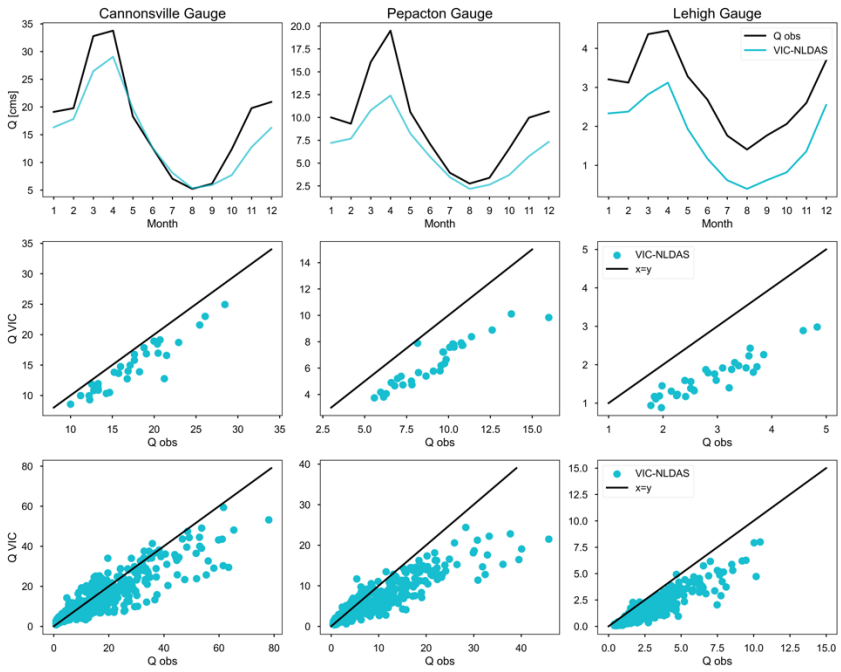

Figure 13: Initial VIC streamflow simulation validation. The top row is the mean seasonal cycle of streamflow, where the black line is the observed USGS streamflow and the cyan is the VIC streamflow. The second row compares the annual mean streamflow between the observed (x-axis) and VIC (y-axis), with each dot representing a single year. The bottom row is the same as the second row but for monthly streamflow, with each dot representing a single month.

Although the seasonal average, annual mean streamflow, and monthly mean streamflow tend to be underestimated in most years, the initial VIC result is reasonable for the mean streamflow, and it could likely be improved by adjusting model parameters. The seasonal cycle and annual mean streamflow for all gauges have a correlation coefficient above 0.93, and the monthly mean streamflow above 0.88, indicating a strong positive correlation. There is a large difference among gauges, and Cannonsville has a lower bias in all three categories among the three gauges. In fact, the mean absolute percentage error (MAPE) for annual mean streamflow is 14%, 30%, and 42% at Cannonsville, Pepacton, and Lehigh gauges, respectively. The results reveal the heterogeneity in the region. For example, this initial VIC model set-up has less bias at the Cannonsville gauge compared to Pepacton, despite the two gauges being physically close, about 45 km apart.

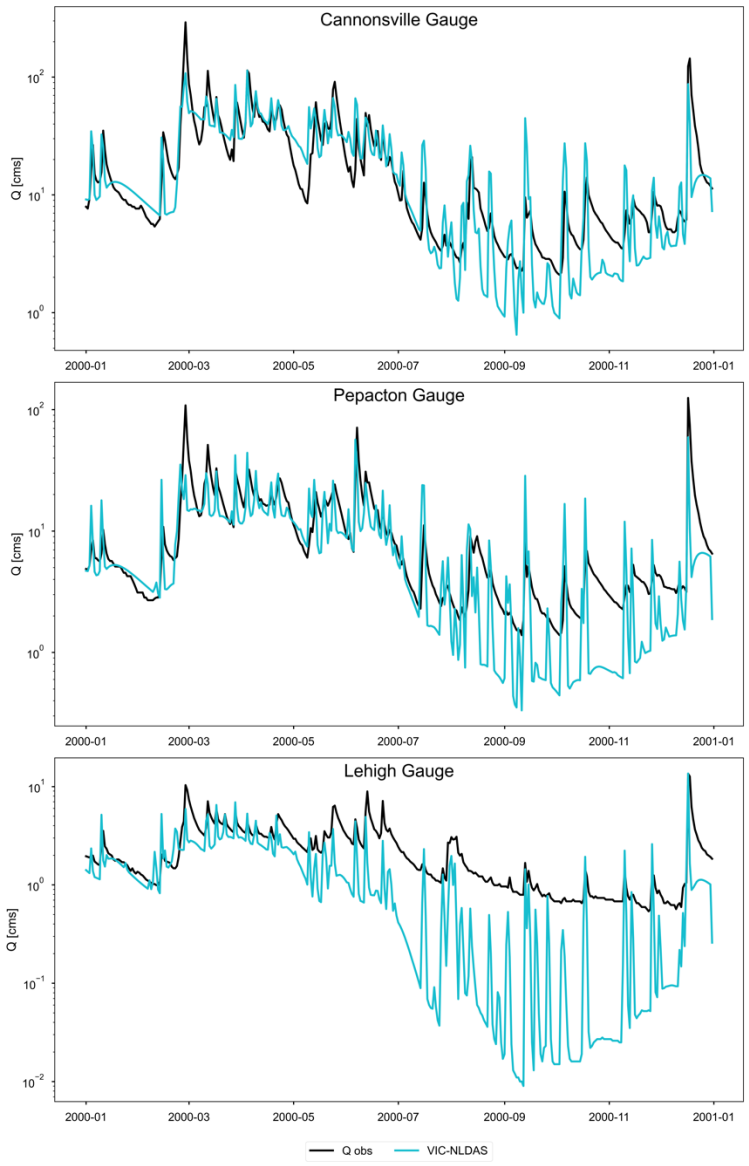

Figure 14: Streamflow time series for the observed and initial VIC streamflow in the year 2000. The y-axis is plotted in log scale to highlight the lower flow periods.

After evaluating the average streamflow, Figure 14 shows the daily streamflow time series for a randomly selected year. Unlike the mean streamflow in Figure 13, the daily streamflow shows that the peaks are often overestimated and the baseflow-dominated dry periods are underestimated. The poorly simulated hydrograph recessions indicate that the runoff and baseflow are both incorrect: the high runoff may be compensating for the low baseflow to achieve the correct mean streamflow. Therefore, VIC may be partitioning too much precipitation into runoff and underestimating infiltration. In addition, the baseflow generation is inaccurate, possibly due the

underestimation of infiltration leading to low soil moisture or due to poor parameter values controlling the baseflow curve. With this concern, the initial VIC setup will likely be unable to simulate some hydrologic signatures, indicating that using monthly streamflow for calibration is insufficient for our study. For example, the baseflow-related signatures, such as baseflow index and 7-day minimum flow, show a poorer fit to observations compared with others in this initial setup.

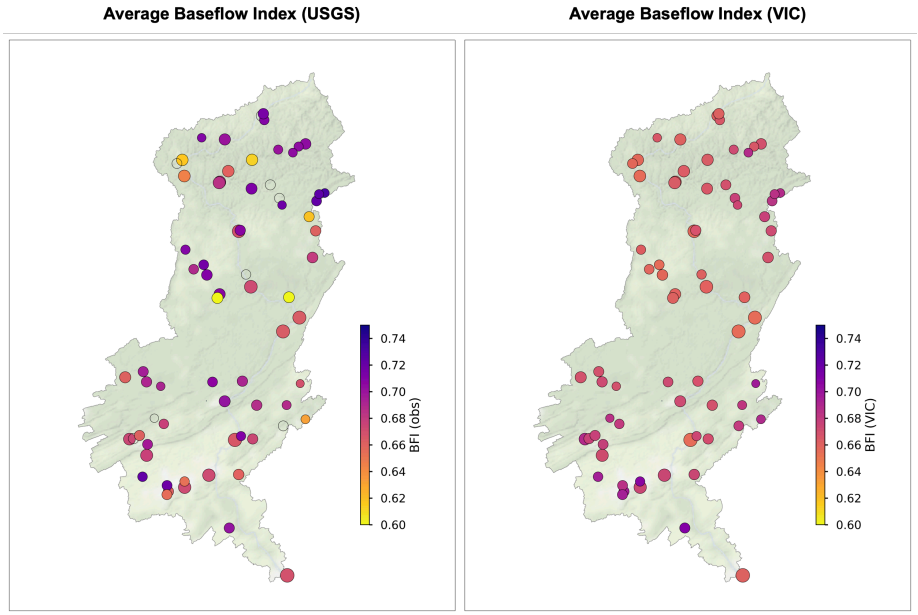

Figure 15: The average baseflow index from the Eckhardt-filtered observations (left) and from the initial VIC baseflow result (right) from 1981 to 2010.

To verify if VIC simulates the baseflow index accurately, Figure 15 maps the mean baseflow index (BFI) calculated by the Eckhardt procedure from the observed flow (left) and the VIC baseflow (right). BFI is the baseflow divided by the total streamflow. The results show that BFI is typically underestimated in the initial VIC simulation, especially in the Upper Delaware River Basin, whose dams were the focus of Chapter 2. Besides the long-term average, the time series of annual BFI is also consistently underestimated, as well as the 7-day minimum flow. The baseflow recession curve has the most problematic result in the initial VIC simulation, and the hydrologic signatures that depend on it cannot be used in the current VIC set-up. Therefore, baseflow will be the focus of the following section and determine whether it can be approved by varying soil parameters.

3.5.2 Potential to improve VIC baseflow simulation through parameter calibration

Due to VIC's poor performance in simulating the baseflow index, the question becomes whether it is possible to improve the simulations through parameter calibration to simulate the correct baseflow and total streamflow. A sensitivity analysis is performed to explore the possible results. Furthermore, this allows for the identification of the parameters important to achieve a better simulation to baseflow to better inform future calibration work.

3.5.2.1 Baseflow performance in time series

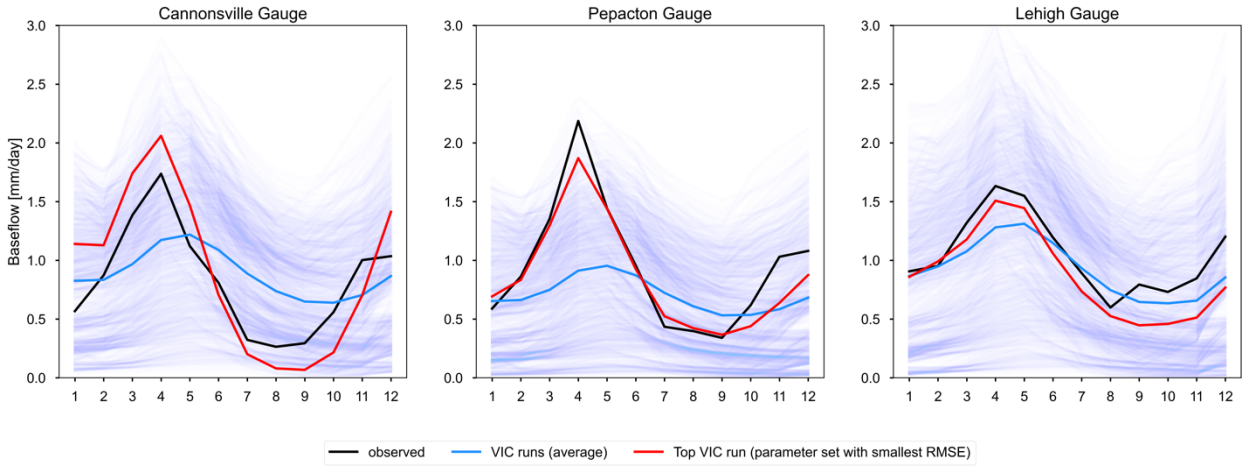

Figure 16: Seasonal cycle of the filtered observations and the VIC simulations. The black line is the Eckhardt-filtered baseflow from observed streamflow. The blue line is the VIC ensemble average, and the multiple lavender lines are the individual simulations. The red line is the VIC simulation with the lowest RMSE for each site.

Figure 16 plots the seasonal cycle from 1984 to 1989 for all the VIC runs with varying parameters (see Section 3.4). Although there is no formal calibration, the optimal parameter sets can be selected from the smallest RMSE, indicated by the red line. The result shows that the top VIC run can simulate the seasonal cycle of baseflow at all three gauges. Across the three gauges, parameter runs at the Pepacton gauge have a lower ability to simulate the spring peak, while baseflow at the Lehigh gauge is likely to achieve better performance due to the large range of simulated behaviour and a high probability of obtaining both peaks and troughs from different

parameter sets (individual runs). The number of runs that have a higher value compared to the one observed in April at Pepacton is only 16 of the 2187 total runs, while Lehigh and Cannonsville have 743 and 411 runs, respectively, indicating a lower probability of the correct peak at Pepacton. In addition, the average percentage of error in April is 58% at the Pepacton gauge and 22% at the Lehigh gauge.

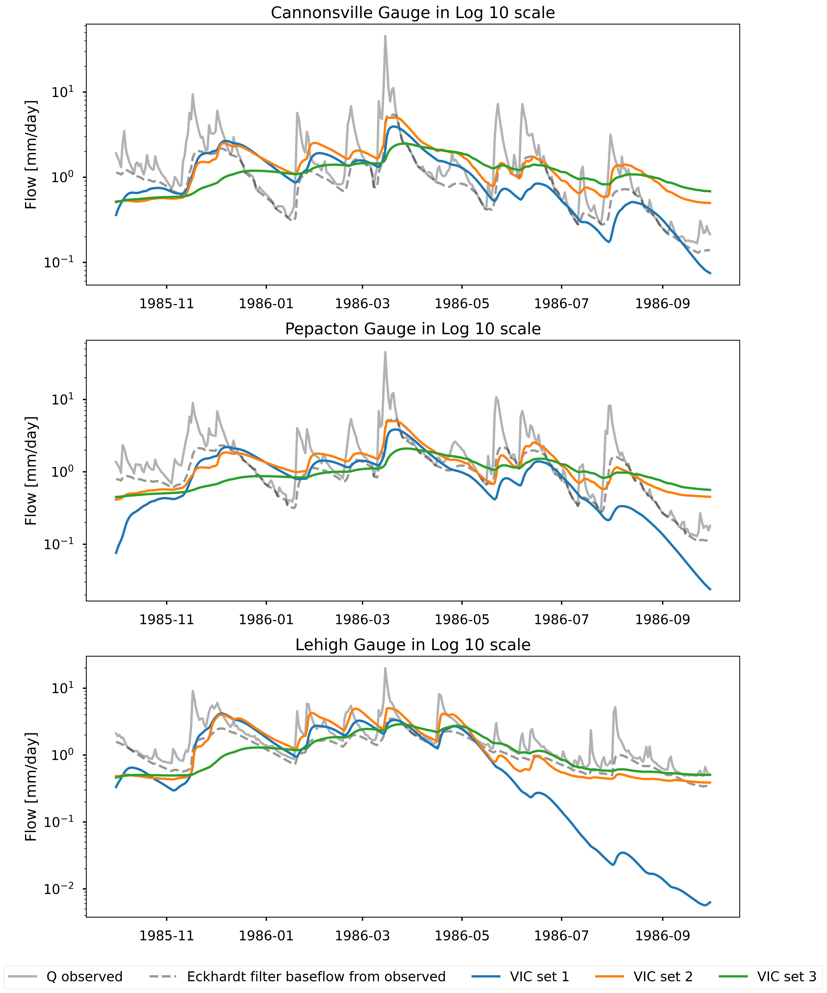

Figure 17: Selected baseflow simulations for the 1989 water year; note the y-axis is in log scale. The observed is in black and the blue, orange, and green lines are the best-performing simulations for Cannonsville, Pepacton, and Lehigh grid cells, respectively.

After evaluating the ability to simulate the seasonal average, Figure 17 plots the optimal parameter sets, one from each gauge (red lines in Figure 16), that is then used to simulate streamflow for all three to detect the ability to transfer optimal parameter sets across different locations. Although the magnitude is overestimated, two VIC sets (optimal from Cannonsville and

Pepacton gauges, respectively) can simulate most of the shape of baseflow. The VIC set 1 underestimates the magnitude in low flow periods, such as the summer at the Lehigh gauge, and similar results are found during other years. The VIC set 2 has a slightly higher baseflow compared to VIC set 1 most of the time, and VIC set 3 does not simulate the peak as well as the other two sets. This result shows that VIC can possibly simulate the correct baseflow recession as the recession decay rate is reasonable, such that calibration can adjust the magnitude. Although performance varies from site to site, certain parameter sets, such as VIC set 1, show an opportunity for reasonable baseflow simulation for all three gauges. The RMSE in VIC set 1 from 1984 to 1989 is relatively consistent in all three gauges with 0.49, 0.57, and 0.58 mm/day at Cannonsville, Pepacton, and Lehigh, respectively. However, spatial heterogeneity may become increasingly important when all available gauges are combined. Some parameter sets have very different behaviour compared to observations between the gauges. For instance, the VIC set 2 has a higher possibility of overestimating baseflow in Lehigh than Pepacton gauges. Therefore, parameters should be varied by location in future calibrations due to the heterogeneity in streamflow response. In addition, there is an intra-annual difference in performance in different seasons. For example, the RMSE of VIC set 1 at Cannonsville in summer (June, July, August) is 0.3, while in spring is 0.6.

3.5.2.2 Baseflow sensitivity analysis

The impact of individual parameters on baseflow can be quantified through the local sensitivity analysis using the performance indices of mean and standard deviation. Figure 18 shows the result of six parameters (θ_j), and *ws* is plotted separately due to the design of the parameter runs (see Section 3.3.1). Each parameter in Figure 18 is run for three values. The blue bar shows the sensitivity between the low value and middle, and the orange bar between the middle and high values. The standard deviation is calculated from the daily baseflow and the difference between the two intervals in color indicates the nonlinear impact of the parameter on baseflow simulation.

The *exp*, *infil*, and *depth2* parameters have a larger impact on mean baseflow (left plot), with an inverse relationship with increasing parameter values leading to lower mean baseflow. The *dsmax*, *depth3*, and *ds* parameters have a large influence on the standard deviation of daily baseflow. The increased *infil* leads to a decreased infiltration capacity, where a smaller amount of infiltration is available for vertical drainage and to become baseflow. Similarly, an increased *exp* would result in a lower hydraulic conductivity and less baseflow. The *dsmax* is the largest baseflow quantity that can be generated from soil layer 3, and *ds* is a fraction of *dsmax*. Therefore, both are expected to have a positive relationship with mean baseflow, but the contribution is small based on the sensitivity results. The parameters in the baseflow generation equation, *dsmax*, *ds*, and *depth3*, have a larger impact on changing the variability of the curve rather than the average. When soil layer 2 is thicker, more water goes to evapotranspiration and results in a lower baseflow on average. On the other hand, a thinner layer would not have enough moisture stored in the soil to meet the vegetation and atmosphere and can result in an overestimated streamflow (Demaria et al., 2007).

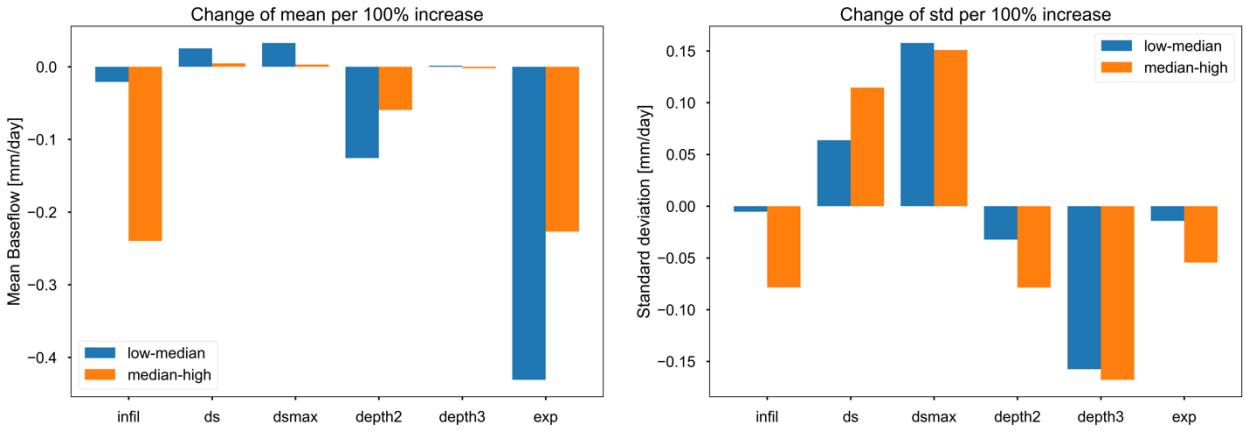

Figure 18: Change in baseflow mean and standard deviation per 100% increase in the parameter value. Other parameters are held at the median value (l is constant). The blue bar is the change between the low and median values of the parameters, and orange is the change between median and high values.

Because the parameters impact interrelated processes, it is also important to understand the impact of one parameter on another's sensitivity. Tables 3 and 4 show the effects of other parameters on the sensitivities of the target parameters (θ_j) per 100% increase in parameter value.

Each row focuses on the impact of adjusting one additional parameter to its higher value (*l*, refer to eq. 3-6), with the rest set to the median. Each column indicates a target parameter under different second parameters that set at high, while others are held in median. The diagonal cells show the value, as in Figure 18, representing the change in the performance index with all others held at the median. Other cells would show how much the second parameter in rows could vary the change of the performance index in the target parameter in the columns. The more it varies from the diagonal value, the more sensitive it can be to other parameters in baseflow simulation. The comparison within a column can help to identify the most influential parameter to the target parameter in that column. Table 4 repeats this analysis for the standard deviation.

Table 3: Second parameter impact on mean daily baseflow. The values along the diagonal are the changes in mean baseflow between the median and high value of that parameter, with all other parameter values held to the median. The other values along the column indicate the change in mean baseflow both varying the original parameter (column) and a second parameter (row). For example, the bottom value in the first column (-0.2737) is the change in mean baseflow from median value to high value of infil under a high value of exp (others held to median).

ψ = Mean baseflow	Infil	ds	dsmax	depth2	depth3	exp
infil (high)	-0.2398	0.0002	0.0003	-0.1158	-0.0029	-0.2748
ds (high)	-0.2423	0.0046	0.0016	-0.0607	-0.0024	-0.2287
dsmax (high)	-0.2438	0.0011	0.0030	-0.0595	-0.0022	-0.2293
depth2 (high)	-0.2652	0.0036	0.0030	-0.0594	-0.0127	-0.2449
depth3 (high)	-0.2401	0.0044	0.0030	-0.0699	-0.0022	-0.2307
exp (high)	-0.2737	0.0022	0.0017	-0.0896	-0.0086	-0.2268

Table 4: As in Table 3 but for the impact on standard deviation of daily baseflow.

ψ = STD baseflow	infil	ds	dsmax	depth2	depth3	exp
infil (high)	-0.0784	0.0730	0.0998	-0.1082	-0.1195	-0.1198
ds (high)	-0.1018	0.1146	0.1435	-0.1031	-0.1968	-0.0693
dsmax (high)	-0.1552	0.0948	0.1509	-0.1584	-0.2116	-0.0943
depth2 (high)	-0.0918	0.0950	0.1270	-0.0786	-0.1479	-0.0490
depth3 (high)	-0.0567	0.0913	0.1378	-0.0587	-0.1678	-0.0443
exp (high)	-0.1274	0.0948	0.1311	-0.0695	-0.1509	-0.0545

According to the local sensitivity analysis with the performance index, the mean and standard deviation per 100% increase of the target parameter, the *infil*, *exp,* and *dsmax* can largely vary the performance of target parameters. Specifically, *infil* and *exp* largely interact with each other and are the most influential environmental parameter mutually (see Appendix B). In addition, *infil* also has a significant influence on *ds* and *dsmax* for both simulating the mean and standard deviation of baseflow, and *depth2* for only mean baseflow. The *exp* also has a large influence on *depth2* and *depth3* for mean baseflow. In addition, *dsmax* can vary standard deviation change on *infil*, *depth2,* and *exp*. Therefore, based on Figure 18 and Tables 3 and 4, baseflow simulation is most sensitive to the *infil, dsmax,* and *exp* parameters in the study area.

The three important parameters of *infil, dsmax,* and *exp* were identified by the sensitivity test, which emphasized that the processes of infiltration, baseflow generation, and vertical drainage between soil layers are all significant in baseflow simulation. The *infil* parameter can vary baseflow performance and impacts the performance of other parameters the most. This is because it determines the first hydrologic process of partitioning precipitation into infiltration, thereby affecting the soil moisture available in the soil column. The smaller the *infil*, the more precipitation is partitioned to infiltration and affects every other parameter in different levels. The interaction between *infil* and *exp* is also highly related to this process because of the relationship between infiltration and soil moisture. The *dsmax* is the only sensitive parameter that directly controls the baseflow generation equation, which may indicate that the baseflow generation curve could be simplified. The non-linear curve plays a more significant role in the baseflow generation, and the linear part might not be that important to point out. The *dsmax* has a large impact on baseflow variability but not the average. In addition, the other baseflow generation parameters including *ds* and *depth3* are likely to have a variation to baseflow by themselves but no big interaction with others. The *exp* might be the key to get the right soil moisture states, and it impacts the magnitude

of mean baseflow. Figure 19 plots the time series of baseflow and soil moisture change with different values of *exp* in the second and third soil layers.

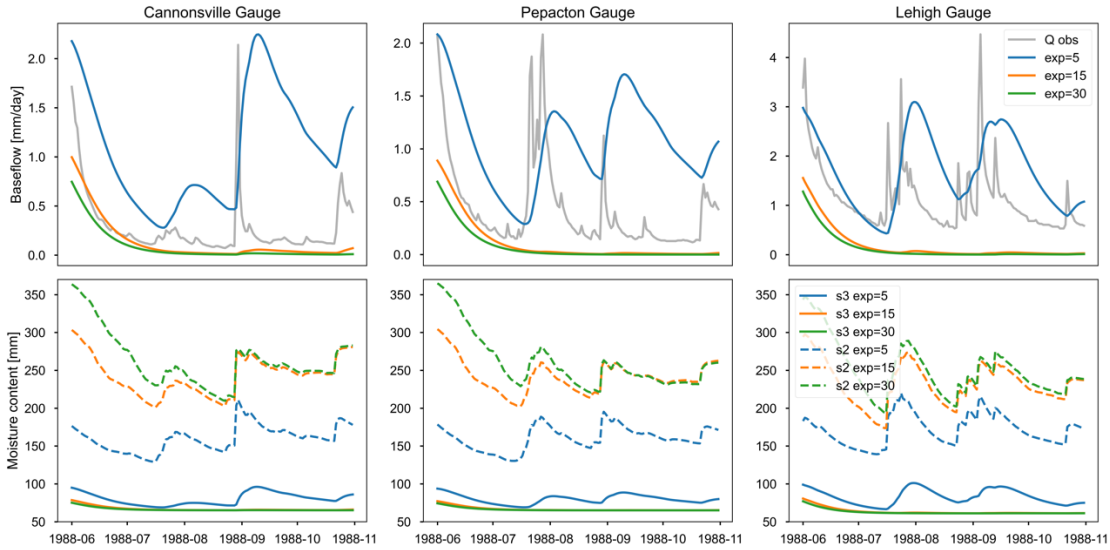

Figure 19: Time series of baseflow and soil moisture content in soil layer 2 and layer 3 with different exp values in color. The dashed line is in soil layer 2 and the dotted line is in soil layer 3.

A smaller *exp* would lead to more drainage and result in lower soil moisture in layer 2 and higher soil moisture in layer 3, and more baseflow is generated. The baseflow curve is likely to follow the soil moisture in layer 3 with a small lag, indicating the importance of the soil characteristics, where baseflow can be affected by the initial conditions at the start of the season. As the *exp* parameter increases, soil moisture in layer 3 will have a smaller change due to the slower vertical drainage, and it will release consistently low baseflow, possibly drying out the bottom soil layer. For example, the *exp* in the median and large value model runs merge together at the Pepacton gauge beginning in September, resulting in a drought period. This slower vertical drainage may allow vegetation to use the soil moisture in layer 2 before it can reach layer 3.

In addition to the six parameters, the *ws* parameter has little effect on other parameters due to the small variation of curves with different *ws* (see Appendix B). The impact of *ws* on baseflow is also fairly small, which indicates the insensitivity of *ws*. There is an embedded relationship between *ws* and *ds* which makes the sensitivity test more difficult. Analytically, the more *ws* differs from *ds*,

the flatter the baseflow generated. Therefore, *ws* need to be rebuilt for future runs although it has a small impact on the baseflow simulation.

3.5.2.3 Surface runoff sensitivity

Runoff and baseflow together determine streamflow, and a similar sensitivity analysis for runoff is executed (see Appendix B). The linear relationship of different value in other parameters reveal that runoff is insensitive to varying subsurface parameters, except for *depth2* which have a small and nearly linear response in magnitude. Surface runoff is likely to depend only on *infil* and *exp* among the seven soil parameters, which again emphasizes the importance of *infil* and *exp* for baseflow. The *infil* between 0.01 and 0.3 has a significant change in surface runoff, where almost all the water infiltrates when the *infil* is 0.01. In addition to the direct partitioning from precipitation, the drainage process of the soil layer is also important for surface runoff simulation.

3.6 Discussion and conclusions

Although the initial VIC implementation could not simulate well the baseflow and naturalized hydrologic signatures, the sensitivity runs show that VIC has the potential to simulate the correct baseflow. This indicates that model calibration can allow for VIC to be implemented in this basin to provide naturalized estimates of hydrologic signatures, at least those dependent on accurate baseflow simulation. However, the calibration should not be done using monthly mean streamflow due to the poor recession curve and baseflow proportion. Instead, objective functions should be used that prioritize the full range of hydrologic behaviour. The results show that optimal parameters are not easily transferrable across stations, and spatial heterogeneity must be considered in any future calibration.

Successful calibration requires understanding the sensitivity of the model to various parameters. This chapter's local sensitivity analysis identifies the most important parameters in baseflow: *infil*, *exp,* and *dsmax*. For the individual parameter impacts on mean baseflow, the model

is most sensitive to the *exp* has the largest change in baseflow mean. *dsmax* has a significant effect on the change in standard deviation both individually and on other parameters. For the interactions between parameters, the *infil* has the largest impact on other parameters in both magnitude and variability. The *infil* and *exp* might have a correlation for selecting the optimal parameter set where the smaller *infil* is likely to match a larger *exp*, and they are the most sensitive additional parameters on each other. On the other hand, the influence of *depth2*, *ds*, and *ws* are relatively limited to baseflow simulation.

The *infil* and *exp* also have a large impact on simulating surface runoff, which emphasizes the importance of both partitioning the precipitation at the surface and the vertical drainage process through the soil column. For calibration, *infil* and *exp* are recommended with the same or higher priority as the parameters for the baseflow generation curve. The hydroclimatic parameters were found to be more dominant than soil characteristics in the streamflow simulation (Demaria et al., 2007), which matches our finding in baseflow. Snow processes are not studied but they may affect runoff from winter to spring and varies the optimal *infil* and *exp* during different seasons. The optimal *infil* is likely to change with climate while VIC is not available for intra-annual settings. The hydroclimatic features might be associated with parameter sensitivity; for instance, mean precipitation might strongly correlate to the sensitivity of baseflow generation parameters (Sepúlveda et al., 2022). Therefore, integrity checks in different hydroclimatic areas might be crucial in a region with a large range of precipitation. The climate type also strongly varies the parameter sensitivity, and Sepúlveda et al. (2002) found that *ds*, *dsmax*, *ws*, and *depth3* are more sensitive to streamflow in the humid area. This differing result might be due to the different metrics of evaluation and also the focus on a lateral comparison between arid and wet regions. Similar to Demaria et al. (2007), we found the baseflow generation parameters might be simplified with a nonlinear curve and *ws* could be eliminated.

The optimal parameter set can vary largely for different regions, basic VIC inputs, and methods of evaluation objective. The calibration parameters may lose their identifiability because different subsets of them may produce a similar result, often called equifinality in the literature (Beven & Freer, 2001). Since no calibration parameter is directly related to ET, there might be a systematic error. Sensitivity analysis has limitations on parameter "heterogeneity". Parameters can have different impacts based on both the form of the equations they are associated with and the specific hydrologic processes they control. Parameters may appear in equations as exponents, such as *infil* and *exp*. These parameters may tend to have a more pronounced effect on the overall system response than others. In addition, parameters governing critical hydrologic processes have an important impact on the output. For example, the *infil* and *exp* are sensitive to runoff. For future studies on parameter sensitivity, the Distributed Evaluation of the Local Sensitivity Analysis method (DELSA) (Rakovec et al., 2014) can help with a functional selection with the respective multiple functions. Formal sensitivity runs and analyses are required to quantify the impact of different parameters with multiple metrics. The RMSE will emphasize high flow by squaring, and low flow may not be detected by this method. A Box-Cox transformation RMSE can help to complement the low flow view (Misirli et al., 2003). In addition, a combination of bias (e.g., absolute bias) and flashiness (e.g., flow duration curve) calculations may also need to be added to the comparison between sets. ET can also be a critical component of runoff, but its evaluation can be complex.

Future work is required to fulfill the original goal of using the model-based approach to evaluate hydrologic alteration in the Delaware River Basin. Finer intervals are required to determine the parameters' sensitivity, and *ws* needs to be tested with independent values that are not dependent on other parameter values. After analysis with DELSA using multiple metrics, a calibration based on daily streamflow could be applied and the hydrologic signatures can be checked on a monthly scale. This can take multiple versions of runs and a final validation is needed

to show the ability of the VIC model to correctly capture all select hydrologic signatures. Local sensitivity analysis may not be able to capture all parameter effects and may miss the potential interactions and dependencies between parameters. In addition, the non-linear response such as the exponent change of a parameter may result in a disproportionate change and are not able to be inspected by local sensitivity analysis. This limits the ranking of parameter importance and may lead to a misleading result. Therefore, global sensitivity analysis, such as the method of Morris (1991), can also be useful for qualitative assessment of parameter influence from a global perspective in combination with local sensitivity analysis. The method for quantifying the downstream impact of dams can be duplicated in different river systems, but the soil parameter in the VIC model needs to be reanalyzed, and hydrologic signatures from modeled streamflow always need to be validated before being used. Additionally, the comparison of the downstream impact from Chapter 2 would provide isolated dam impact.

Chapter 4: Conclusions

The objectives of this thesis are to quantify the downstream effects of the dam through observations and to explore the capability of a hydrologic model to calculate hydrologic signatures in an unregulated river. The research found the following results to answer the posed research questions. First, the study found that downstream propagation of dam impacts can be quantified using observations. Second, the study found that the NYC reservoirs significantly affect hydrologic signatures immediately downstream of the dams, and the length scale for hydrologic signatures to return to their natural state in the Delaware River Basin is approximately 35 km. Finally, the study examined the ability of the VIC model to simulate hydrologic signatures and provide estimates of the naturalized hydrologic regime. The study found that the performance of the VIC model can be improved through parameter calibration and identification of important parameters, where certain combinations of parameters have the ability to correctly simulate streamflow and baseflow characteristics, and *infil*, *dsmax*, *exp*, are more sensitive among the parameters studied.

Overall, this research contributes to the understanding of the downstream propagation of dam impacts on the flow response along a river. The results can inform dam operation and management and provide a basis for further research on this topic. This study provides a simple method that can be replicated in other basins with sufficient streamflow gauges by demonstrating that downstream effects can be quantified using only observations. In addition, this research contributes to our understanding of how the VIC model performs in simulating streamflow, especially baseflow, and how calibration parameters affect the process and how sensitive they are to each other. This can be a guide for future calibration methods to effectively modify the simulation by varying soil parameters.

The limitation of using hydrologic signatures will include the potential loss of information due to the difficulty of proving the sufficiency of capturing all hydrologic characteristics (Fenicia et

al., 2018). Although "informative" statistics have been used to mitigate the missing of strict guidelines (Kavetski et al., 2018), the subjective signature selection might lead to different results. For example, with the same objective of constraining the rate of change, Addor et al. (2018) suggest the use of the FDC slope, while the FDC and rising limb density were recommended by Euser et al. (2013). The choice of thresholds can also contribute to variability in results from a subjective perspective, such as the rising limb calculation; different time steps used for FDC; and variations in BFI calculation equations. In addition, the naturalized hydrologic signatures assume that the hydrologic system is in steady state equilibrium, which may not be true where climate change is significant. Melsen and Guse (2021) have a study across the continental U.S. using Distributed Evaluation of Local Sensitivity Analysis and highlight the importance of climate change in parameter sensitivity in long-term projections of mean streamflow and annual half flow time. Therefore, the climate parameters may also be considered in the future VIC model analysis. Uncertainties of hydrologic signatures may also be crucial and point to the importance of high-quality streamflow and precipitation data, but this uncertainty was not included in this thesis. The quick response of a catchment might not be captured by gauges in a short time, affecting the variability result, while lower uncertainty can be found with signatures using averages in spatial or time (Westerberg & McMillan, 2015). As a result, the headwater of Neversink in Chapter 2 would have a different performance in specific signatures compared with others because of the different hydrological dynamics. Therefore, the hydrologic signatures are difficult to compare in a consistent manner and need to be re-evaluated if being used in another basin.

In addition to the inherent concern with the hydrologic signatures, the identification of human intervention from the observational method in Chapter 2 may be limited where climate change impacts cannot be excluded. The requirement for pre-dam data may also be limited in some basins due to lack of observations and may cause difficulties in generalizability for comparing results to other basins. Geographic differences and the timing of dam construction could also affect

the use of the observational method, where climate may have a greater contribution to recent dam construction. In addition, dense gauging along the river and headwater stations are needed to use the same approach here to study other basins. For future work based on Chapter 2, the impact of the dam on river ecosystems could be evaluated by combining the result of flow alteration and ecological scales such as flow-dependent biodiversity. Stream temperature may also be another interesting avenue to pursue for thermal disturbance and its downstream propagation.

The main limitation of Chapter 3 would be the model run time for the sensitivity analysis and daily streamflow calibration. Some of the hydrologic signatures could be difficult to interpolate when associated with the hydrologic process, such as BFI in the VIC model. Future work for Chapter 3 would include further investigation of the performance of the VIC model through sensitivity analysis: a new *ws* parameter format for execution and a formal distributed evaluation of local sensitivity analysis. In addition, the model simulation should be evaluated with more than one objective or error function to obtain a comprehensive result in both peak and low flow, such as a combination of RMSE and Absolute Error with daily streamflow. Calibration and validation are also recommended on a daily scale. VIC should be validated for both streamflow and hydrologic signatures for the minimally impacted watersheds within the larger river basin so that the hydrologic signatures derived from the model can be expected as a proxy for the unregulated state of naturalized streamflow to further compare the hydrologic signatures tracing from headwater to Trenton, New Jersey combined with Chapter 2. The result of the model approach is expected to overcome the lack of data available in the pre-dam period and isolate the dam effect from climate variability and change. In addition, an open research topic of climate change on hydrologic alteration can be quantified by comparing the pre-dam period with the modeled result and can be coupled with the dam effect.

This approach is also expected to be transferable to other watersheds, improving dam operations, water management strategies, and environmental evaluation. The downstream propagation study can inform decisions about water releases and how downstream would respond. It helps to optimize the management of water resources in different areas. The vulnerable areas can be protected by increasing water release in the dry season, and the protection of tributaries could also be critical where it can mitigate the dam impact on the main stem. Monitoring of hydrological signatures can assess the impact of flow regimes and potential impacts on downstream habitats. The regional scale is recommended for this method because of the complexity and variability in large areas, like the Mississippi River basin, and the uniqueness of dam operations and management. Applying this work to a new watershed requires addressing several issues, such as the adequacy of available streamflow data. The pre-dam and post-dam periods must be separated so that human intervention is not confounded with climate change. Thus, the observation-only method is not appropriate for recently constructed dams. Careful calibration and validation of hydrologic models is essential for the model-based method, and sensitivity analysis is required for the target basin to understand how parameters affect streamflow and hydrologic signatures.

Hydrologic signatures vary from basin to basin, and selection should be based on a study's objective, considering historical streamflow and hydroclimate. The specific hydroclimatic conditions associated with the basin, such as aridity or snow-dominated characteristics, must be considered prior to calibration and validation. For example, snow parameters may be included in the sensitivity analysis. The potential impact of climate change on hydrologic processes is important and may affect the impact of dams, especially in a snow-dominated basin. Earlier snowmelt and reduced snowpack can greatly alter hydrologic signatures where snowmelt runoff is a large component of streamflow. This may also challenge dam operations to adapt to climate-induced changes and prepare for these uncertainties. The consideration of climate change increases the transferability of this research. The hydrologic response to dam impacts with potential impacts

of climate change provide a more robust review to help examine the complexity of hydrologic behavior across basins, such as the snow-dominant basin.

Bibliography

Adams, E., & Aggarwala, R. T. (2021). *New York City drinking water supply and quality report*. 20.

Addor, N., Nearing, G., Prieto, C., Newman, A. J., Le Vine, N., & Clark, M. P. (2018). A Ranking of Hydrological Signatures Based on Their Predictability in Space. *Water Resources Research*, *54*(11), 8792–8812. https://doi.org/10.1029/2018WR022606

Ali, G., Oswald, C. J., Spence, C., Cammeraat, E. L. H., McGuire, K. J., Meixner, T., & Reaney, S. M. (2013). Towards a unified threshold-based hydrological theory: Necessary components and recurring challenges. *Hydrological Processes*, *27*(2), 313–318. https://doi.org/10.1002/hyp.9560

Allen, B., Anderson, M. G., & Creveling, E. (2011). *DELAWARE RIVER BASIN priority conservation areas and recommended conservation strategies*. 116.

Andreadis, K. M., & Lettenmaier, D. P. (2006). Assimilating remotely sensed snow observations into a macroscale hydrology model. *Advances in Water Resources*, *29*(6), 872–886. https://doi.org/10.1016/j.advwatres.2005.08.004

Anghileri, D., Voisin, N., Castelletti, A., Pianosi, F., Nijssen, B., & Lettenmaier, D. P. (2016). Value of long-term streamflow forecasts to reservoir operations for water supply in snow-dominated river catchments. *Water Resources Research*, *52*(6), 4209–4225. https://doi.org/10.1002/2015WR017864

Archer, D., & Newson, M. (2002). The use of indices of flow variability in assessing the hydrological and instream habitat impacts of upland afforestation and drainage. *Journal of Hydrology*, *268*(1–4), 244–258. https://doi.org/10.1016/S0022-1694(02)00171-3

Arnold, J. G., & Allen, P. M. (1999). Automated Methods for Estimating Baseflow and Ground Water Recharge from Streamflow Records1. *JAWRA Journal of the American Water Resources Association*, *35*(2), 411–424. https://doi.org/10.1111/j.1752-1688.1999.tb03599.x

Arthington, A. H. (2016). Environmental Flows: Ecological Limits of Hydrologic Alteration (ELOHA). In C. M. Finlayson, M. Everard, K. Irvine, R. J. McInnes, B. A. Middleton, A. A. van Dam, & N. C. Davidson (Eds.), *The Wetland Book: I: Structure and Function, Management and Methods* (pp. 1–5). Springer Netherlands. https://doi.org/10.1007/978-94-007-6172-8_348-1

Bai, P., Liu, X., Yang, T., Liang, K., & Liu, C. (2016). Evaluation of streamflow simulation results of land surface models in GLDAS on the Tibetan plateau: GLDAS Runoff Simulations on the TP. *Journal of Geophysical Research: Atmospheres*, *121*(20), 12,180-12,197. https://doi.org/10.1002/2016JD025501

Bastola, S., Seong, Y., Lee, D., Youn, I., Oh, S., Jung, Y., Choi, G., & Jang, D. (2018). Contribution of Baseflow to River Streamflow: Study on Nepal's Bagmati and Koshi Basins. *KSCE Journal of Civil Engineering*, *22*(11), 4710–4718. https://doi.org/10.1007/s12205-018-0149-9

Batalla, R. J., Gómez, C. M., & Kondolf, G. M. (2004). Reservoir-induced hydrological changes in the Ebro River basin (NE Spain). *Journal of Hydrology*, *290*(1–2), 117–136. https://doi.org/10.1016/j.jhydrol.2003.12.002

Benedini, M., & Tsakiris, G. (2013). *Water Quality Modelling for Rivers and Streams* (Vol. 70). Springer Netherlands. https://doi.org/10.1007/978-94-007-5509-3

Berga, L., Buil, J. M., Bofill, E., Cea, J. C. D., Perez, J. A. G., Mañueco, G., Polimon, J., Soriano, A., & Yagüe, J. (Eds.). (2006). *Dams and Reservoirs, Societies and Environment in the 21st Century, Two Volume Set: Proceedings of the International Symposium on Dams in the Societies of the 21st Century, 22nd International Congress on Large Dams (ICOLD), Barcelona, Spain, 18 June 2006*. CRC Press. https://doi.org/10.1201/b16818

Beven, K., & Freer, J. (2001). Equifinality, data assimilation, and uncertainty estimation in mechanistic modelling of complex environmental systems using the GLUE methodology. *Journal of Hydrology*, *249*(1), 11–29. https://doi.org/10.1016/S0022-1694(01)00421-8

Botter, G., Basso, S., Porporato, A., Rodriguez-Iturbe, I., & Rinaldo, A. (2010). Natural streamflow regime alterations: Damming of the Piave river basin (Italy): ANTHROPOGENIC STREAMFLOW DISTRIBUTIONS. *Water Resources Research*, *46*(6). https://doi.org/10.1029/2009WR008523

Botter, G., Porporato, A., Daly, E., Rodriguez-Iturbe, I., & Rinaldo, A. (2007). Probabilistic characterization of base flows in river basins: Roles of soil, vegetation, and geomorphology: STOCHASTIC BASE FLOWS. *Water Resources Research*, *43*(6). https://doi.org/10.1029/2006WR005397

Bulygina, N., McIntyre, N., & Wheater, H. (2009). Conditioning rainfall-runoff model parameters for ungauged catchments and land management impacts analysis. *Hydrol. Earth Syst. Sci.*, 12.

Bunn, S. E., & Arthington, A. H. (2002). Basic Principles and Ecological Consequences of Altered Flow Regimes for Aquatic Biodiversity. *Environmental Management*, *30*(4), 492–507. https://doi.org/10.1007/s00267-002-2737-0

Chong, X. Y., Vericat, D., Batalla, R. J., Teo, F. Y., Lee, K. S. P., & Gibbins, C. N. (2021). A review of the impacts of dams on the hydromorphology of tropical rivers. *Science of The Total Environment*, *794*, 148686. https://doi.org/10.1016/j.scitotenv.2021.148686

Clark, M. P., Kavetski, D., & Fenicia, F. (2011). Pursuing the method of multiple working hypotheses for hydrological modeling: HYPOTHESIS TESTING IN HYDROLOGY. *Water Resources Research*, *47*(9). https://doi.org/10.1029/2010WR009827

Collischonn, W., & Fan, F. M. (2013). Defining parameters for Eckhardt's digital baseflow filter: DEFINING PARAMETERS FOR ECKHARDT'S DIGITAL BASEFLOW FILTER. *Hydrological Processes*, *27*(18), 2614–2622. https://doi.org/10.1002/hyp.9391

Cosgrove, B. A., Lohmann, D., Mitchell, K. E., Houser, P. R., Wood, E. F., Schaake, J. C., Robock, A., Marshall, C., Sheffield, J., Duan, Q., Luo, L., Higgins, R. W., Pinker, R. T., Tarpley, J. D., & Meng, J. (2003). Real-time and retrospective forcing in the North American Land Data Assimilation

System (NLDAS) project. *Journal of Geophysical Research: Atmospheres*, *108*(D22), 2002JD003118. https://doi.org/10.1029/2002JD003118

Cottrell, M. T., Waidner, L. A., Yu, L., & Kirchman, D. L. (2005). Bacterial diversity of metagenomic and PCR libraries from the Delaware River. *Environmental Microbiology*, *7*(12), 1883–1895. https://doi.org/10.1111/j.1462-2920.2005.00762.x

Daniels, M. E., & Danner, E. M. (2020). The Drivers of River Temperatures Below a Large Dam. *Water Resources Research*, *56*(5). https://doi.org/10.1029/2019WR026751

DeChant, C. M., & Moradkhani, H. (2014). Toward a reliable prediction of seasonal forecast uncertainty: Addressing model and initial condition uncertainty with ensemble data assimilation and Sequential Bayesian Combination. *Journal of Hydrology*, *519*, 2967–2977. https://doi.org/10.1016/j.jhydrol.2014.05.045

Demaria, E. M., Nijssen, B., & Wagener, T. (2007). Monte Carlo sensitivity analysis of land surface parameters using the Variable Infiltration Capacity model. *Journal of Geophysical Research*, *112*(D11), D11113. https://doi.org/10.1029/2006JD007534

Dettinger, M., Udall, B., & Georgakakos, A. (2015). Western water and climate change. *Ecological Applications*, *25*(8), 2069–2093. https://doi.org/10.1890/15-0938.1

Diehl, R. M., Wilcox, A. C., & Stella, J. C. (2020). Evaluation of the integrated riparian ecosystem response to future flow regimes on semiarid rivers in Colorado, USA. *Journal of Environmental Management*, *271*, 111037. https://doi.org/10.1016/j.jenvman.2020.111037

Dingman, S. L. (2015). *Physical Hydrology: Third Edition*. Waveland Press. https://books.google.ca/books?id=rUUaBgAAQBAJ

Ducoudré, N. I., Laval, K., & Perrier, A. (1993). SECHIBA, a New Set of Parameterizations of the Hydrologic Exchanges at the Land-Atmosphere Interface within the LMD Atmospheric General Circulation Model. *Journal of Climate*, *6*(2), 248–273. https://doi.org/10.1175/1520-0442(1993)006<0248:SANSOP>2.0.CO;2

Eckhardt, K. (2005). How to construct recursive digital filters for baseflow separation. *Hydrological Processes*, *19*(2), 507–515. https://doi.org/10.1002/hyp.5675

Eckhardt, K. (2008). A comparison of baseflow indices, which were calculated with seven different baseflow separation methods. *Journal of Hydrology*, *352*(1–2), 168–173. https://doi.org/10.1016/j.jhydrol.2008.01.005

Elsner, M. M., Gangopadhyay, S., Pruitt, T., Brekke, L. D., Mizukami, N., & Clark, M. P. (2014). How Does the Choice of Distributed Meteorological Data Affect Hydrologic Model Calibration and Streamflow Simulations? *Journal of Hydrometeorology*, *15*(4), 1384–1403. https://doi.org/10.1175/JHM-D-13-083.1

Euser, T., Winsemius, H. C., Hrachowitz, M., Fenicia, F., Uhlenbrook, S., & Savenije, H. H. G. (2013). A framework to assess the realism of model structures using hydrological signatures. *Hydrology and Earth System Sciences*, *17*(5), 1893–1912. https://doi.org/10.5194/hess-17-1893-2013

Fenicia, F., Kavetski, D., Reichert, P., & Albert, C. (2018). Signature-Domain Calibration of Hydrological Models Using Approximate Bayesian Computation: Empirical Analysis of Fundamental Properties. *Water Resources Research*, *54*(6), 3958–3987. https://doi.org/10.1002/2017WR021616

Ferrazzi, M., & Botter, G. (2019a). Contrasting signatures of distinct human water uses in regulated flow regimes. *Environmental Research Communications*, *1*(7), 071003. https://doi.org/10.1088/2515-7620/ab3324

Ferrazzi, M., & Botter, G. (2019b). Contrasting signatures of distinct human water uses in regulated flow regimes. *Environmental Research Communications*, *1*(7), 071003. https://doi.org/10.1088/2515-7620/ab3324

Ferrazzi, M., Woods, R. A., & Botter, G. (2021). Climatic signatures in regulated flow regimes across the Central and Eastern United States. *Journal of Hydrology: Regional Studies*, *35*, 100809. https://doi.org/10.1016/j.ejrh.2021.100809

FitzHugh, T. W., & Vogel, R. M. (2011). The impact of dams on flood flows in the United States. *River Research and Applications*, *27*(10), 1192–1215. https://doi.org/10.1002/rra.1417

Fleischmann, A. S., Paiva, R. C. D., Collischonn, W., Sorribas, M. V., & Pontes, P. R. M. (2016). On river-floodplain interaction and hydrograph skewness: FLOODPLAINS AND HYDROGRAPH SKEWNESS. *Water Resources Research*, *52*(10), 7615–7630. https://doi.org/10.1002/2016WR019233

Galat, D. L., & Lipkin, R. (2000). Restoring ecological integrity of great rivers: Historical hydrographs aid in defining reference conditions for the Missouri River. In M. Jungwirth, S. Muhar, & S. Schmutz (Eds.), *Assessing the Ecological Integrity of Running Waters* (pp. 29–48). Springer Netherlands. https://doi.org/10.1007/978-94-011-4164-2_3

Gillespie, B. R., Desmet, S., Kay, P., Tillotson, M. R., & Brown, L. E. (2015). A critical analysis of regulated river ecosystem responses to managed environmental flows from reservoirs. *Freshwater Biology*, *60*(2), 410–425. https://doi.org/10.1111/fwb.12506

Graf, W. L. (1999). Dam nation: A geographic census of American dams and their large-scale hydrologic impacts. *Water Resources Research*, *35*(4), 1305–1311. https://doi.org/10.1029/1999WR900016

Graf, W. L. (2006). Downstream hydrologic and geomorphic effects of large dams on American rivers. *Geomorphology*, *79*(3–4), 336–360. https://doi.org/10.1016/j.geomorph.2006.06.022

Grant, G. E., Schmidt, J. C., & Lewis, S. L. (2013). A Geological Framework for Interpreting Downstream Effects of Dams on Rivers. In J. E. O'Connor & G. E. Grant (Eds.), *Water Science*

and Application (pp. 203–219). American Geophysical Union. https://doi.org/10.1029/007WS13

Groot, J. J. (1966). Some observations on pollen grains in suspension in the estuary of the Delaware River. *Marine Geology*, *4*(6), 409–416. https://doi.org/10.1016/0025-3227(66)90009-0

Hammond, J. C., & Fleming, B. J. (2021). Evaluating low flow patterns, drivers and trends in the Delaware River Basin. *Journal of Hydrology*, *598*, 126246. https://doi.org/10.1016/j.jhydrol.2021.126246

Harrell, J., Nijssen, B., & Frans, C. (2022). Where and When Does Streamflow Regulation Significantly Affect Climate Change Outcomes in the Columbia River Basin? *Water Resources Research*, *58*(10). https://doi.org/10.1029/2022WR031950

Hoang, L., Mukundan, R., Moore, K. E. B., Owens, E. M., & Steenhuis, T. S. (2019). Phosphorus reduction in the New York City water supply system: A water-quality success story confirmed with data and modeling. *Ecological Engineering*, *135*, 75–88. https://doi.org/10.1016/j.ecoleng.2019.04.029

Hoover Dam. (2015). Bureau of Reclamation. https://www.usbr.gov/

Jha, M., Pan, Z., Takle, E. S., & Gu, R. (2004). Impacts of climate change on streamflow in the Upper Mississippi River Basin: A regional climate model perspective. *Journal of Geophysical Research: Atmospheres*, *109*(D9). https://doi.org/10.1029/2003JD003686

Jumani, S., Deitch, M. J., Kaplan, D., Anderson, E. P., Krishnaswamy, J., Lecours, V., & Whiles, M. R. (2020). River fragmentation and flow alteration metrics: A review of methods and directions for future research. *Environmental Research Letters*, *15*(12), 123009. https://doi.org/10.1088/1748-9326/abcb37

Kavetski, D., Fenicia, F., Reichert, P., & Albert, C. (2018). Signature-Domain Calibration of Hydrological Models Using Approximate Bayesian Computation: Theory and Comparison to

Existing Applications. *Water Resources Research*, *54*(6), 4059–4083. https://doi.org/10.1002/2017WR020528

Khan, S. I., Hong, Y., Wang, J., Yilmaz, K. K., Gourley, J. J., Adler, R. F., Brakenridge, G. R., Policelli, F., Habib, S., & Irwin, D. (2011). Satellite Remote Sensing and Hydrologic Modeling for Flood Inundation Mapping in Lake Victoria Basin: Implications for Hydrologic Prediction in Ungauged Basins. *IEEE Transactions on Geoscience and Remote Sensing*, *49*(1), 85–95. https://doi.org/10.1109/TGRS.2010.2057513

Kibler, K. M., & Alipour, M. (2017). Flow alteration signatures of diversion hydropower: An analysis of 32 rivers in southwestern China. *Ecohydrology*, *10*(5). https://doi.org/10.1002/eco.1846

Kingsford, R. T. (2000). Ecological impacts of dams, water diversions and river management on floodplain wetlands in Australia: IMPACTS OF DAMS AND DIVERSIONS ON FLOODPLAIN WETLANDS. *Austral Ecology*, *25*(2), 109–127. https://doi.org/10.1046/j.1442-9993.2000.01036.x

Kükrer, S., & Mutlu, E. (2019). Assessment of surface water quality using water quality index and multivariate statistical analyses in Saraydüzü Dam Lake, Turkey. *Environmental Monitoring and Assessment*, *191*(2), 71. https://doi.org/10.1007/s10661-019-7197-6

Kumari, N., Srivastava, A., Sahoo, B., Raghuwanshi, N. S., & Bretreger, D. (2021). Identification of Suitable Hydrological Models for Streamflow Assessment in the Kangsabati River Basin, India, by Using Different Model Selection Scores. *Natural Resources Research*, *30*(6), 4187–4205. https://doi.org/10.1007/s11053-021-09919-0

Leach, J. M., Kornelsen, K. C., Samuel, J., & Coulibaly, P. (2015). Hydrometric network design using streamflow signatures and indicators of hydrologic alteration. *Journal of Hydrology*, *529*, 1350–1359. https://doi.org/10.1016/j.jhydrol.2015.08.048

Leck, M. A. (2003). Seed-bank and vegetation development in a created tidal freshwater wetland on the Delaware River, Trenton, New Jersey, USA. *Wetlands*, *23*(2), 310–343. https://doi.org/10.1672/9-20

Liang, X., & Guo, J. (2003). Intercomparison of land-surface parameterization schemes: Sensitivity of surface energy and water fluxes to model parameters. *Journal of Hydrology*, *279*(1), 182–209. https://doi.org/10.1016/S0022-1694(03)00168-9

Liang, X., Lettenmaier, D. P., Wood, E. F., & Burges, S. J. (1994). A simple hydrologically based model of land surface water and energy fluxes for general circulation models. *Journal of Geophysical Research*, *99*(D7), 14415. https://doi.org/10.1029/94JD00483

Liang, X., Wood, E. F., & Lettenmaier, D. P. (1996). Surface soil moisture parameterization of the VIC-2L model: Evaluation and modification. *Global and Planetary Change*, *13*(1–4), 195–206. https://doi.org/10.1016/0921-8181(95)00046-1

Livneh, B., Rosenberg, E. A., Lin, C., Nijssen, B., Mishra, V., Andreadis, K. M., Maurer, E. P., & Lettenmaier, D. P. (2013). A Long-Term Hydrologically Based Dataset of Land Surface Fluxes and States for the Conterminous United States: Update and Extensions. *Journal of Climate*, *26*(23), 9384–9392. https://doi.org/10.1175/JCLI-D-12-00508.1

Magilligan, F. J., & Nislow, K. H. (2005a). Changes in hydrologic regime by dams. *Geomorphology*, *71*(1–2), 61–78. https://doi.org/10.1016/j.geomorph.2004.08.017

Magilligan, F. J., & Nislow, K. H. (2005b). Changes in hydrologic regime by dams. *Geomorphology*, *71*(1–2), 61–78. https://doi.org/10.1016/j.geomorph.2004.08.017

Magilligan, F. J., Nislow, K. H., & Graber, B. E. (2003). Scale-independent assessment of discharge reduction and riparian disconnectivity following flow regulation by dams. *Geology*, *31*, 569. https://doi.org/10.1130/0091-7613(2003)031<0569:SAODRA>2.0.CO;2

Marcinkowski, P., & Grygoruk, M. (2017). Long-Term Downstream Effects of a Dam on a Lowland River Flow Regime: Case Study of the Upper Narew. *Water*, *9*(10), 783. https://doi.org/10.3390/w9100783

Mathai, J., & Mujumdar, P. (2021). *Streamflow indices to identify catchment drivers of hydrograph* [Preprint]. Catchment hydrology/Theory development. https://doi.org/10.5194/hess-2021-307

Maurer, E. P., Wood, A. W., Adam, J. C., Lettenmaier, D. P., & Nijssen, B. (2002). A Long-Term Hydrologically Based Dataset of Land Surface Fluxes and States for the Conterminous United States*. *Journal of Climate*, *15*(22), 3237–3251. https://doi.org/10.1175/1520-0442(2002)015<3237:ALTHBD>2.0.CO;2

McMillan, H. (2020). Linking hydrologic signatures to hydrologic processes: A review. *Hydrological Processes*, *34*(6), 1393–1409. https://doi.org/10.1002/hyp.13632

McMillan, H. K. (2021). A review of hydrologic signatures and their applications. *WIREs Water*, *8*(1). https://doi.org/10.1002/wat2.1499

Mei, X., Van Gelder, P. H. A. J. M., Dai, Z., & Tang, Z. (2017). Impact of dams on flood occurrence of selected rivers in the United States. *Frontiers of Earth Science*, *11*(2), 268–282. https://doi.org/10.1007/s11707-016-0592-1

Melsen, L. A., & Guse, B. (2021). Climate change impacts model parameter sensitivity – implications for calibration strategy and model diagnostic evaluation. *Hydrology and Earth System Sciences*, *25*(3), 1307–1332. https://doi.org/10.5194/hess-25-1307-2021

Melsen, L., Teuling, A., Torfs, P., Zappa, M., Mizukami, N., Clark, M., & Uijlenhoet, R. (2016). Representation of spatial and temporal variability in large-domain hydrological models: Case study for a mesoscale pre-Alpine basin. *Hydrology and Earth System Sciences*, *20*(6), 2207–2226. https://doi.org/10.5194/hess-20-2207-2016

Merritt, D. M., & Wohl, E. E. (2006). Plant dispersal along rivers fragmented by dams. *River Research and Applications*, *22*(1), 1–26. https://doi.org/10.1002/rra.890

Meyer, E. S., Sheer, D. P., Rush, P. V., Vogel, R. M., & Billian, H. E. (2020). Need for Process Based Empirical Models for Water Quality Management: Salinity Management in the Delaware River Basin. *Journal of Water Resources Planning and Management*, *146*(9), 05020018. https://doi.org/10.1061/(ASCE)WR.1943-5452.0001260

Misirli, F., Gupta, H. V., Sorooshian, S., & Thiemann, M. (2003). Bayesian Recursive Estimation of Parameter and Output Uncertainty for Watershed Models. In *Calibration of Watershed Models* (pp. 113–124). American Geophysical Union (AGU). https://doi.org/10.1029/WS006p0113

Morris, M. D. (1991). Factorial Sampling Plans for Preliminary Computational Experiments. *Technometrics*, *33*(2), 161–174. https://doi.org/10.1080/00401706.1991.10484804

Nijssen, B., Lettenmaier, D. P., Liang, X., Wetzel, S. W., & Wood, E. F. (1997). Streamflow simulation for continental-scale river basins. *Water Resources Research*, *33*(4), 711–724. https://doi.org/10.1029/96WR03517

Olden, J. D., & Poff, N. L. (2003). Redundancy and the choice of hydrologic indices for characterizing streamflow regimes. *River Research and Applications*, *19*(2), 101–121. https://doi.org/10.1002/rra.700

Oo, H. T., Zin, W. W., & Thin Kyi, C. C. (2020). Analysis of Streamflow Response to Changing Climate Conditions Using SWAT Model. *Civil Engineering Journal*, *6*(2), 194–209. https://doi.org/10.28991/cej-2020-03091464

Pan, M., Sheffield, J., Wood, E. F., Mitchell, K. E., Houser, P. R., Schaake, J. C., Robock, A., Lohmann, D., Cosgrove, B., Duan, Q., Luo, L., Higgins, R. W., Pinker, R. T., & Tarpley, J. D. (2003). Snow process modeling in the North American Land Data Assimilation System (NLDAS): 2.

Evaluation of model simulated snow water equivalent. *Journal of Geophysical Research: Atmospheres*, *108*(D22). https://doi.org/10.1029/2003JD003994

Pegg, M. A., Pierce, C. L., & Roy, A. (2003). Hydrological alteration along the Missouri River Basin: A time series approach. *Aquatic Sciences - Research Across Boundaries*, *65*(1), 63–72. https://doi.org/10.1007/s000270300005

Petts, G. E. (1979). Complex response of river channel morphology subsequent to reservoir construction. *Progress in Physical Geography*, *3*(3), Article 3. https://doi.org/10.1177/030913337900300302

Poff, N. L., Allan, J. D., Bain, M. B., Karr, J. R., Prestegaard, K. L., Richter, B. D., Sparks, R. E., & Stromberg, J. C. (1997a). The Natural Flow Regime. *BioScience*, *47*(11), 769–784. https://doi.org/10.2307/1313099

Poff, N. L., Allan, J. D., Bain, M. B., Karr, J. R., Prestegaard, K. L., Richter, B. D., Sparks, R. E., & Stromberg, J. C. (1997b). The Natural Flow Regime. *BioScience*, *47*(11), 769–784. https://doi.org/10.2307/1313099

Poff, N. L., & Hart, D. D. (2002). How Dams Vary and Why It Matters for the Emerging Science of Dam Removal. *BioScience*, *52*(8), 659. https://doi.org/10.1641/0006-3568(2002)052[0659:HDVAWI]2.0.CO;2

Poff, N. L., & Zimmerman, J. K. H. (2010). Ecological responses to altered flow regimes: A literature review to inform the science and management of environmental flows: Review of altered flow regimes. *Freshwater Biology*, *55*(1), 194–205. https://doi.org/10.1111/j.1365-2427.2009.02272.x

Pradhanang, S. M., Mukundan, R., Schneiderman, E. M., Zion, M. S., Anandhi, A., Pierson, D. C., Frei, A., Easton, Z. M., Fuka, D., & Steenhuis, T. S. (2013). Streamflow Responses to Climate Change: Analysis of Hydrologic Indicators in a New York City Water Supply Watershed. *JAWRA*

Journal of the American Water Resources Association, *49*(6), 1308–1326. https://doi.org/10.1111/jawr.12086

Prchalová, M., Kubečka, J., Čech, M., Frouzová, J., Draštík, V., Hohausová, E., Jůza, T., Kratochvíl, M., Matěna, J., Peterka, J., Říha, M., Tušer, M., & Vašek, M. (2009). The effect of depth, distance from dam and habitat on spatial distribution of fish in an artificial reservoir. *Ecology of Freshwater Fish*, *18*(2), 247–260. https://doi.org/10.1111/j.1600-0633.2008.00342.x

Rahman, K., Maringanti, C., Beniston, M., Widmer, F., Abbaspour, K., & Lehmann, A. (2013). Streamflow Modeling in a Highly Managed Mountainous Glacier Watershed Using SWAT: The Upper Rhone River Watershed Case in Switzerland. *Water Resources Management*, *27*(2), 323–339. https://doi.org/10.1007/s11269-012-0188-9

Rakovec, O., Hill, M. C., Clark, M. P., Weerts, A. H., Teuling, A. J., & Uijlenhoet, R. (2014). Distributed Evaluation of Local Sensitivity Analysis (DELSA), with application to hydrologic models. *Water Resources Research*, *50*(1), 409–426. https://doi.org/10.1002/2013WR014063

Ravindranath, A., Devineni, N., & Kolesar, P. (2016). An environmental perspective on the water management policies of the Upper Delaware River Basin. *Water Policy*, *18*(6), 1399–1419. https://doi.org/10.2166/wp.2016.166

Razavi, S., & Gupta, H. V. (2015). What do we mean by sensitivity analysis? The need for comprehensive characterization of "global" sensitivity in Earth and Environmental systems models. *Water Resources Research*, *51*(5), 3070–3092. https://doi.org/10.1002/2014WR016527

Richter, B., Baumgartner, J., Wigington, R., & Braun, D. (1997). How much water does a river need? *Freshwater Biology*, *37*(1), 231–249. https://doi.org/10.1046/j.1365-2427.1997.00153.x

Richter, B. D., Baumgartner, J. V., Powell, J., & Braun, D. P. (1996a). A Method for Assessing Hydrologic Alteration within Ecosystems. *Conservation Biology*, *10*(4), 1163–1174. https://doi.org/10.1046/j.1523-1739.1996.10041163.x

Richter, B. D., Baumgartner, J. V., Powell, J., & Braun, D. P. (1996b). A Method for Assessing Hydrologic Alteration within Ecosystems. *Conservation Biology*, *10*(4), 1163–1174. https://doi.org/10.1046/j.1523-1739.1996.10041163.x

Ruano, M. V., Ribes, J., Seco, A., & Ferrer, J. (2012). An improved sampling strategy based on trajectory design for application of the Morris method to systems with many input factors. *Environmental Modelling & Software*, *37*, 103–109. https://doi.org/10.1016/j.envsoft.2012.03.008

Ruhi, A., Hwang, J., Devineni, N., Mukhopadhyay, S., Kumar, H., Comte, L., Worland, S., & Sankarasubramanian, A. (2022). How Does Flow Alteration Propagate Across a Large, Highly Regulated Basin? Dam Attributes, Network Context, and Implications for Biodiversity. *Earth's Future*, *10*(6). https://doi.org/10.1029/2021EF002490

Sabo, J. L., Bestgen, K., Graf, W., Sinha, T., & Wohl, E. E. (2012). Dams in the Cadillac Desert: Downstream effects in a geomorphic context. *Annals of the New York Academy of Sciences*, *1249*(1), 227–246. https://doi.org/10.1111/j.1749-6632.2011.06411.x

Sabo, J. L., Caron, M., Doucett, R., Dibble, K. L., Ruhi, A., Marks, J. C., Hungate, B. A., & Kennedy, T. A. (2018). Pulsed flows, tributary inputs and food-web structure in a highly regulated river. *Journal of Applied Ecology*, *55*(4), 1884–1895. https://doi.org/10.1111/1365-2664.13109

Sankarasubramanian, A., Vogel, R. M., & Limbrunner, J. F. (2001). Climate elasticity of streamflow in the United States. *Water Resources Research*, *37*(6), 1771–1781. https://doi.org/10.1029/2000WR900330

Sawicz, K. A., Kelleher, C., Wagener, T., Troch, P., Sivapalan, M., & Carrillo, G. (2014). Characterizing hydrologic change through catchment classification. *Hydrology and Earth System Sciences*, *18*(1), 273–285. https://doi.org/10.5194/hess-18-273-2014

Sawicz, K., Wagener, T., Sivapalan, M., Troch, P. A., & Carrillo, G. (2011). Catchment classification: Empirical analysis of hydrologic similarity based on catchment function in the eastern USA.

Hydrology and Earth System Sciences, *15*(9), 2895–2911. https://doi.org/10.5194/hess-15-2895-2011

Schaake, J. C. (1990). From climate to flow. In Waggoner, P. E. (Ed.), *Climate change and US water resources.* John Wiley and Sons Inc.

Schumann, G. J.-P., Neal, J. C., Voisin, N., Andreadis, K. M., Pappenberger, F., Phanthuwongpakdee, N., Hall, A. C., & Bates, P. D. (2013). A first large-scale flood inundation forecasting model. *Water Resources Research*, *49*(10), 6248–6257. https://doi.org/10.1002/wrcr.20521

Sepúlveda, U. M., Mendoza, P. A., Mizukami, N., & Newman, A. J. (2022). Revisiting parameter sensitivities in the variable infiltration capacity model across a hydroclimatic gradient. *Hydrology and Earth System Sciences*, *26*(13), 3419–3445. https://doi.org/10.5194/hess-26-3419-2022

Shamir, E., Imam, B., Gupta, H. V., & Sorooshian, S. (2005). Application of temporal streamflow descriptors in hydrologic model parameter estimation: TEMPORAL STREAMFLOW MODEL CALIBRATION. *Water Resources Research*, *41*(6). https://doi.org/10.1029/2004WR003409

Shamir, E., Imam, B., Morin, E., Gupta, H. V., & Sorooshian, S. (2005). The role of hydrograph indices in parameter estimation of rainfall-runoff models. *Hydrological Processes*, *19*(11), 2187–2207. https://doi.org/10.1002/hyp.5676

Sheffield, J., Pan, M., Wood, E. F., Mitchell, K. E., Houser, P. R., Schaake, J. C., Robock, A., Lohmann, D., Cosgrove, B., Duan, Q., Luo, L., Higgins, R. W., Pinker, R. T., Tarpley, J. D., & Ramsay, B. H. (2003). Snow process modeling in the North American Land Data Assimilation System (NLDAS): 1. Evaluation of model-simulated snow cover extent. *Journal of Geophysical Research: Atmospheres*, *108*(D22). https://doi.org/10.1029/2002JD003274

Sheldon, L. S., & Hites, R. A. (1978). Organic compounds in the Delaware River. *Environmental Science & Technology*, *12*(10), 1188–1194. https://doi.org/10.1021/es60146a006

Shoemaker, T., Bista, M., & Brandes, D. (2019). *Streamflow Regime Change in the Delaware River Basin*. https://doi.org/10.26077/W24F-0C17

Singer, M. B. (2007). The influence of major dams on hydrology through the drainage network of the Sacramento River basin, California. *River Research and Applications*, *23*(1), 55–72. https://doi.org/10.1002/rra.968

Singer, M. B., & Dunne, T. (2004). An empirical-stochastic, event-based program for simulating inflow from a tributary network: Framework and application to the Sacramento River basin, California: EMPIRICAL-STOCHASTIC STREAMFLOW SIMULATION. *Water Resources Research*, *40*(7). https://doi.org/10.1029/2003WR002725

Skalak, K. J., Benthem, A. J., Schenk, E. R., Hupp, C. R., Galloway, J. M., Nustad, R. A., & Wiche, G. J. (2013). Large dams and alluvial rivers in the Anthropocene: The impacts of the Garrison and Oahe Dams on the Upper Missouri River. *Anthropocene*, *2*, 51–64. https://doi.org/10.1016/j.ancene.2013.10.002

Smith, J. A., Baeck, M. L., Villarini, G., & Krajewski, W. F. (2010). The Hydrology and Hydrometeorology of Flooding in the Delaware River Basin. *Journal of Hydrometeorology*, *11*(4), 841–859. https://doi.org/10.1175/2010JHM1236.1

State of the Delaware River Basin. (2019). Delaware River Basin Commission.

Stewart, I. T., Cayan, D. R., & Dettinger, M. D. (2005). Changes toward Earlier Streamflow Timing across Western North America. *Journal of Climate*, *18*(8), 1136–1155. https://doi.org/10.1175/JCLI3321.1

Stuefer, S., Yang, D., & Shiklomanov, A. (2011). *Effect of streamflow regulation on mean annual discharge variability of the Yenisei River*. 6.

Su, F., Adam, J. C., Bowling, L. C., & Lettenmaier, D. P. (2005). Streamflow simulations of the terrestrial Arctic domain. *Journal of Geophysical Research: Atmospheres*, *110*(D8). https://doi.org/10.1029/2004JD005518

Thompson, M. Y., & Pindar, C. E. (2021). *Water Withdrawal and Consumptive Use Estimates for the Delaware River Basin (1990-2017) With Projections Through 2060*. 266.

Tracking SDG 7: The Energy Progress Report (2021). (2021). https://www.irena.org/publications/2021/Jun/Tracking-SDG-7-2021

Troy, T. J., Wood, E. F., & Sheffield, J. (2008). An efficient calibration method for continental-scale land surface modeling. *Water Resources Research*, *44*(9). https://doi.org/10.1029/2007WR006513

U.S. Supreme Court. (1954). *New Jersey v. New York. 347 U.S. 995 (1954)*.

Vicente-Serrano, S. M., Zabalza-Martínez, J., Borràs, G., López-Moreno, J. I., Pla, E., Pascual, D., Savé, R., Biel, C., Funes, I., Martín-Hernández, N., Peña-Gallardo, M., Beguería, S., & Tomas-Burguera, M. (2017). Effect of reservoirs on streamflow and river regimes in a heavily regulated river basin of Northeast Spain. *CATENA*, *149*, 727–741. https://doi.org/10.1016/j.catena.2016.03.042

Vörösmarty, C., Lettenmaier, D., Leveque, C., Meybeck, M., Pahl-Wostl, C., Alcamo, J., Cosgrove, W., Grassl, H., Hoff, H., Kabat, P., Lansigan, F., Lawford, R., & Naiman, R. (2004). Humans transforming the global water system. *Eos, Transactions American Geophysical Union*, *85*(48), 509–514. https://doi.org/10.1029/2004EO480001

Wagener, T., Sivapalan, M., Troch, P., & Woods, R. (2007). Catchment Classification and Hydrologic Similarity: Catchment classification and hydrologic similarity. *Geography Compass*, *1*(4), 901–931. https://doi.org/10.1111/j.1749-8198.2007.00039.x

Weisberg, S. B., Himchak, P., Baum, T., Wilson, H. T., & Allen, R. (1996). Temporal Trends in Abundance of Fish in the Tidal Delaware River. *Estuaries*, *19*(3), 723. https://doi.org/10.2307/1352531

Westerberg, I. K., & McMillan, H. K. (2015). Uncertainty in hydrological signatures. *Hydrology and Earth System Sciences*, *19*(9), 3951–3968. https://doi.org/10.5194/hess-19-3951-2015

Wu, H., Adler, R. F., Tian, Y., Huffman, G. J., Li, H., & Wang, J. (2014). Real-time global flood estimation using satellite-based precipitation and a coupled land surface and routing model. *Water Resources Research*, *50*(3), 2693–2717. https://doi.org/10.1002/2013WR014710

Xia, Y., Ek, M., Wei, H., & Meng, J. (2012). Comparative analysis of relationships between NLDAS-2 forcings and model outputs. *Hydrological Processes*, *26*(3), 467–474. https://doi.org/10.1002/hyp.8240

Xie, J., Liu, X., Wang, K., Yang, T., Liang, K., & Liu, C. (2020). Evaluation of typical methods for baseflow separation in the contiguous United States. *Journal of Hydrology*, *583*, 124628. https://doi.org/10.1016/j.jhydrol.2020.124628

Yadav, M., Wagener, T., & Gupta, H. (2007). Regionalization of constraints on expected watershed response behavior for improved predictions in ungauged basins. *Advances in Water Resources*, *30*(8), 1756–1774. https://doi.org/10.1016/j.advwatres.2007.01.005

Yang, Y., Pan, M., Beck, H. E., Fisher, C. K., Beighley, R. E., Kao, S., Hong, Y., & Wood, E. F. (2019). In Quest of Calibration Density and Consistency in Hydrologic Modeling: Distributed Parameter Calibration against Streamflow Characteristics. *Water Resources Research*, *55*(9), 7784–7803. https://doi.org/10.1029/2018WR024178

Yarnell, S. M., Stein, E. D., Webb, J. A., Grantham, T., Lusardi, R. A., Zimmerman, J., Peek, R. A., Lane, B. A., Howard, J., & Sandoval-Solis, S. (2020). A functional flows approach to selecting ecologically relevant flow metrics for environmental flow applications. *River Research and Applications*, *36*(2), 318–324. https://doi.org/10.1002/rra.3575

Yilmaz, K. K., Gupta, H. V., & Wagener, T. (2008). A process-based diagnostic approach to model evaluation: Application to the NWS distributed hydrologic model: PROCESS-BASED DIAGNOSTIC EVALUATION OF HYDROLOGIC MODEL. *Water Resources Research*, *44*(9). https://doi.org/10.1029/2007WR006716

Zhao, Q., Ding, Y., Wang, J., Gao, H., Zhang, S., Zhao, C., Xu, J., Han, H., & Shangguan, D. (2019). Projecting climate change impacts on hydrological processes on the Tibetan Plateau with model calibration against the glacier inventory data and observed streamflow. *Journal of Hydrology*, *573*, 60–81. https://doi.org/10.1016/j.jhydrol.2019.03.043

Zhou, T., Voisin, N., Leng, G., Huang, M., & Kraucunas, I. (2018). Sensitivity of Regulated Flow Regimes to Climate Change in the Western United States. *Journal of Hydrometeorology*, *19*(3), 499–515. https://doi.org/10.1175/JHM-D-17-0095.1

Appendix A – Supplementary Figures for Chapter 2

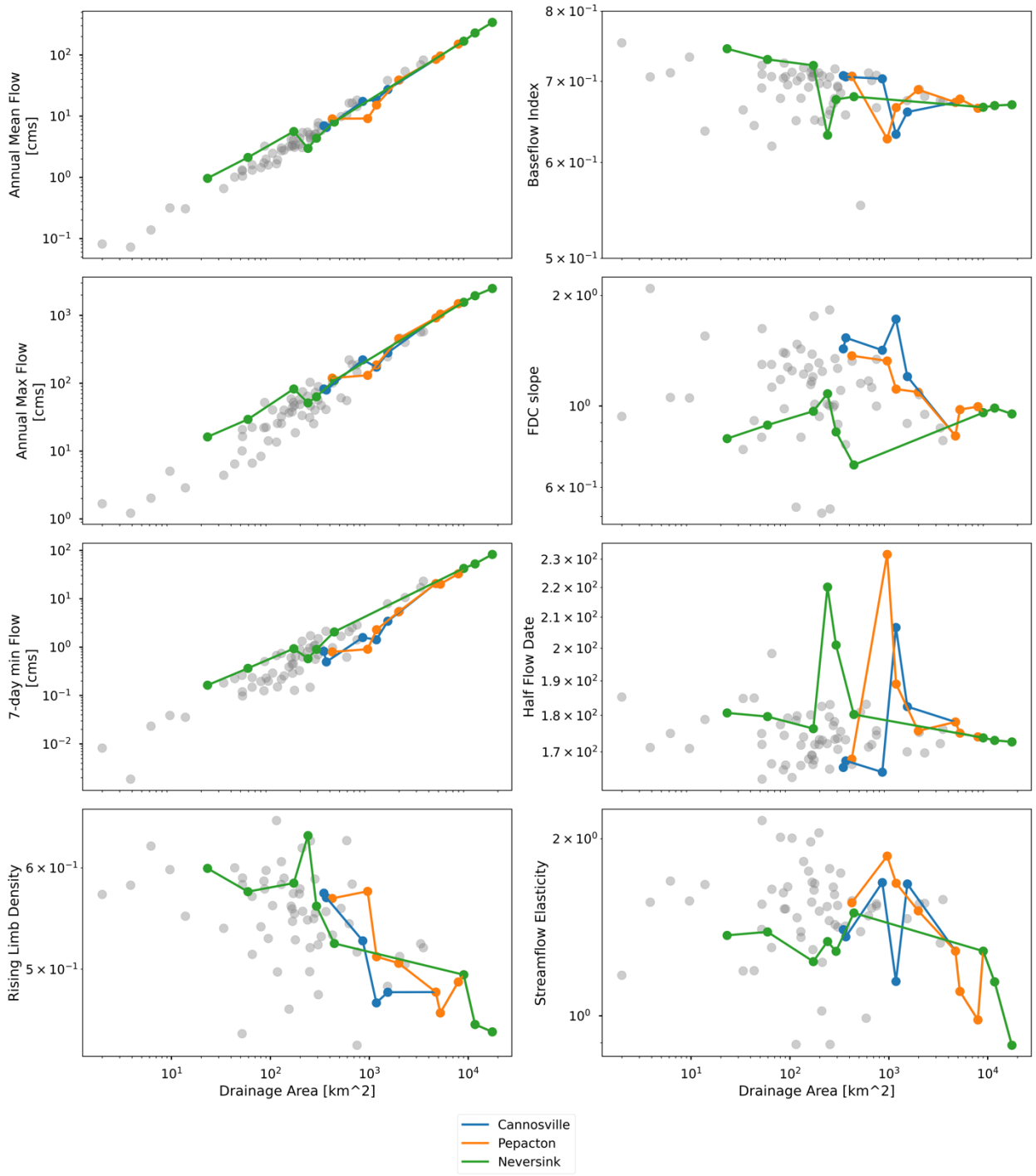

Figure A 1: Relationship of all hydraulic signatures and drainage area. NYC reservoirs are colored dot and tracing downstream in line.

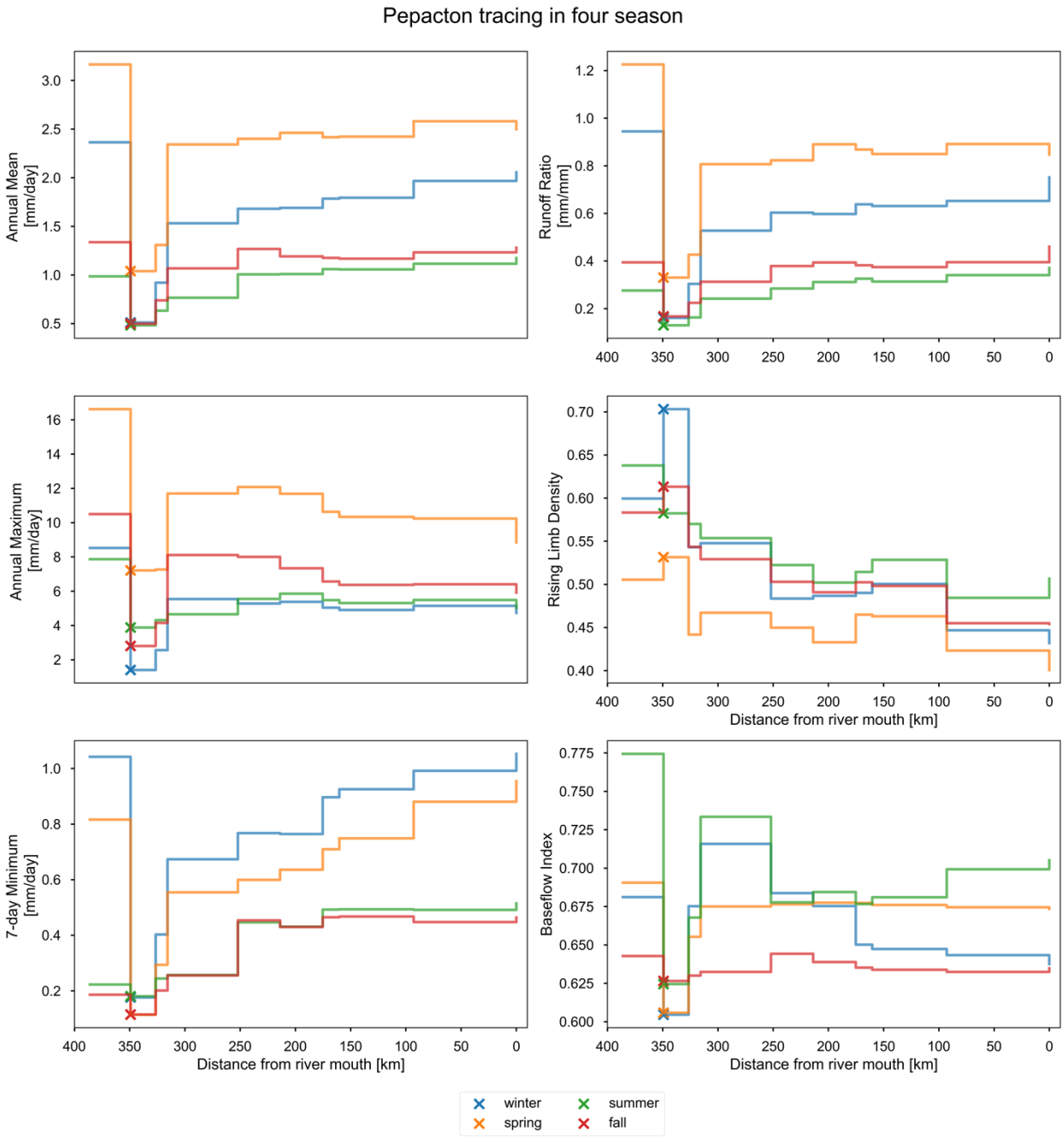

Figure A 2: Tracing passed Pepacton in four seasons.

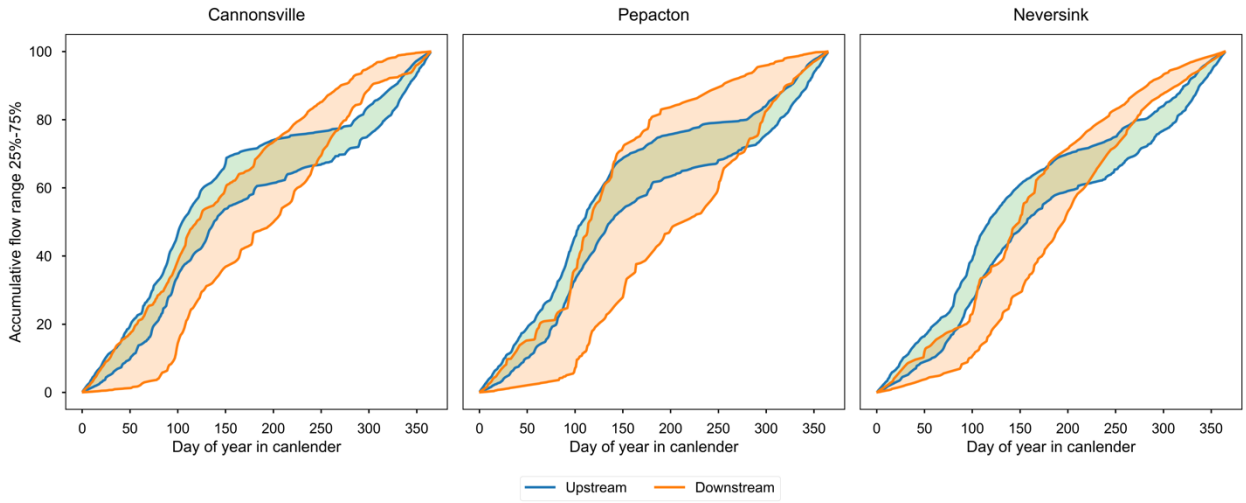

Figure A 3: The cumulative percent of flow in the day of year with 25%-75% quartile for the upstream and downstream local gauge at NYC reservoirs.

Appendix B – Supplementary Figures for Chapter 3

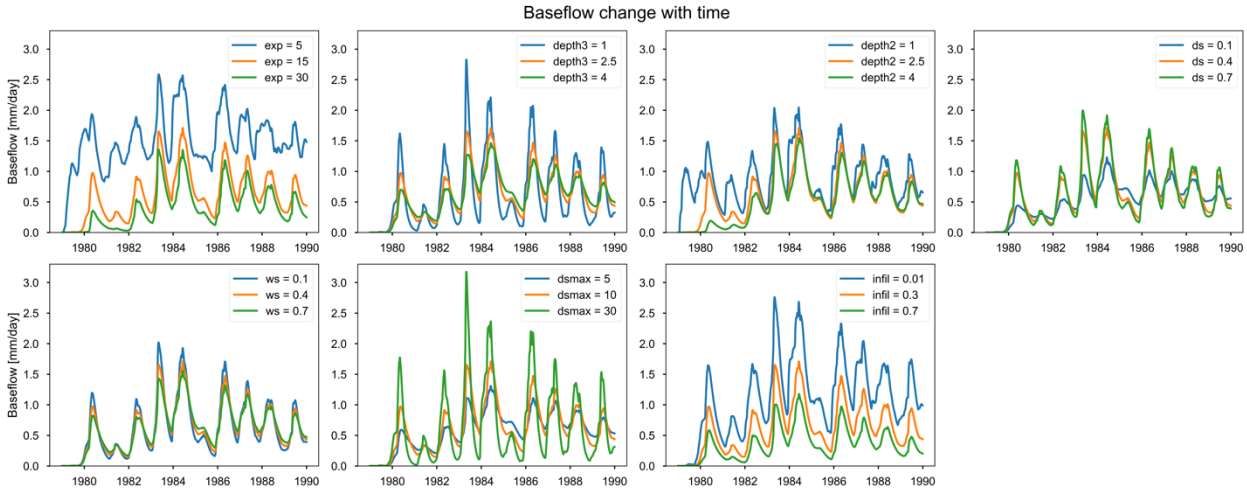

Figure B 1: Baseflow changes in time series that varied individual parameters with a median value fixed to others. Notice ws is ws_{sub} in the varied VIC parameter input.

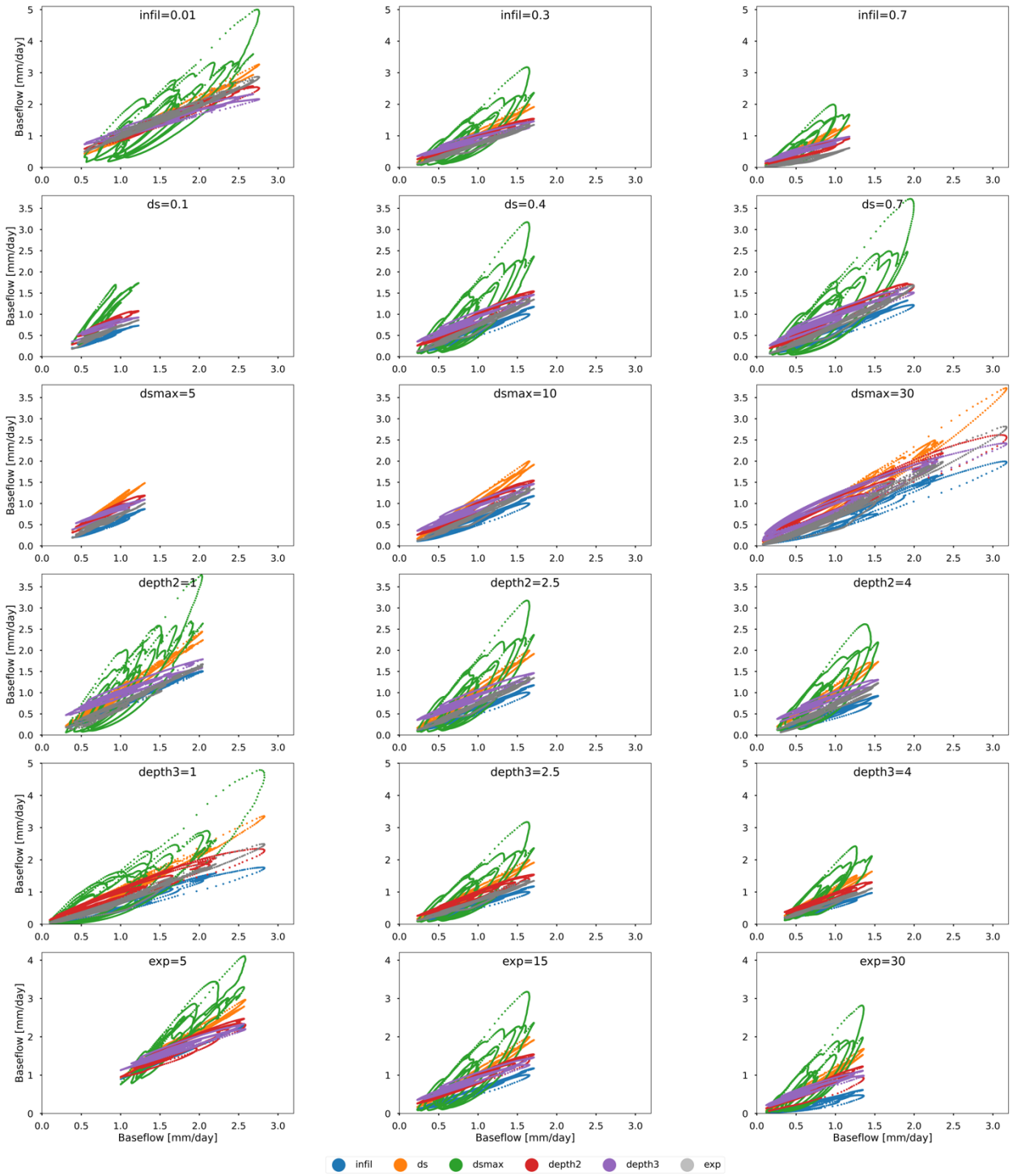

Figure B 2: Sensitivity for variable parameters in VIC baseflow. The target parameter (θ_j) is identified by its color, and the rows and columns are varied by another model parameter (l). The x-axis is the baseflow with the median value of the target parameter and the y-axis is the baseflow with the largest value. The model parameter is the only difference across columns for the x-axis and the rest of the parameters are held in the median. Note that the y-axis scale is not the same throughout the rows.

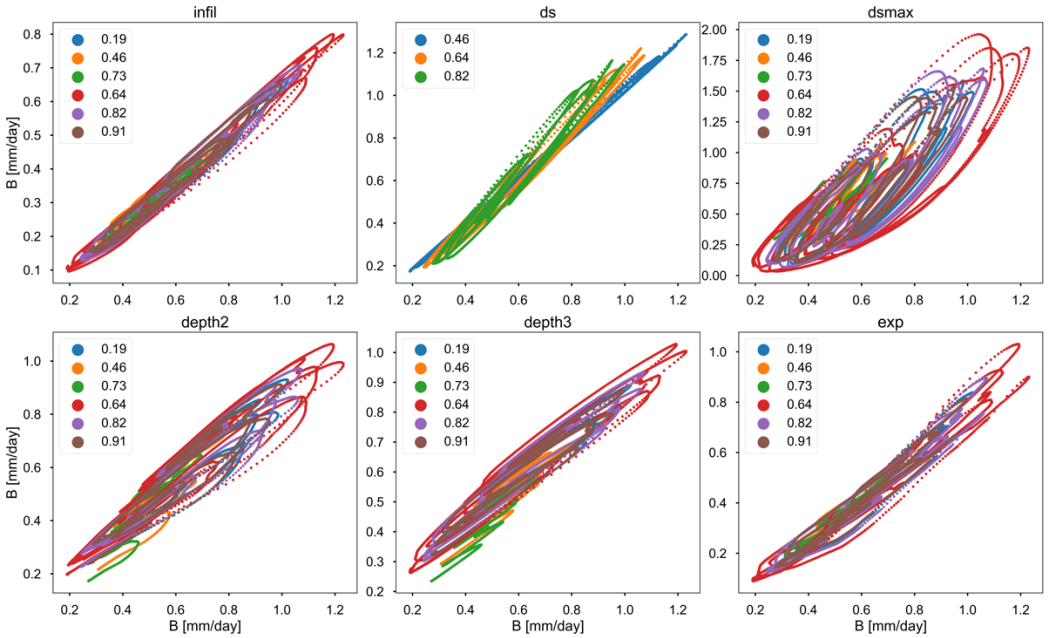

Figure B 3: ws sensitivity to other parameters (similar to Figure B 2). Each value of ws is in color and the y-axis and x-axis are baseflow with high and median values of the target parameter in the title.

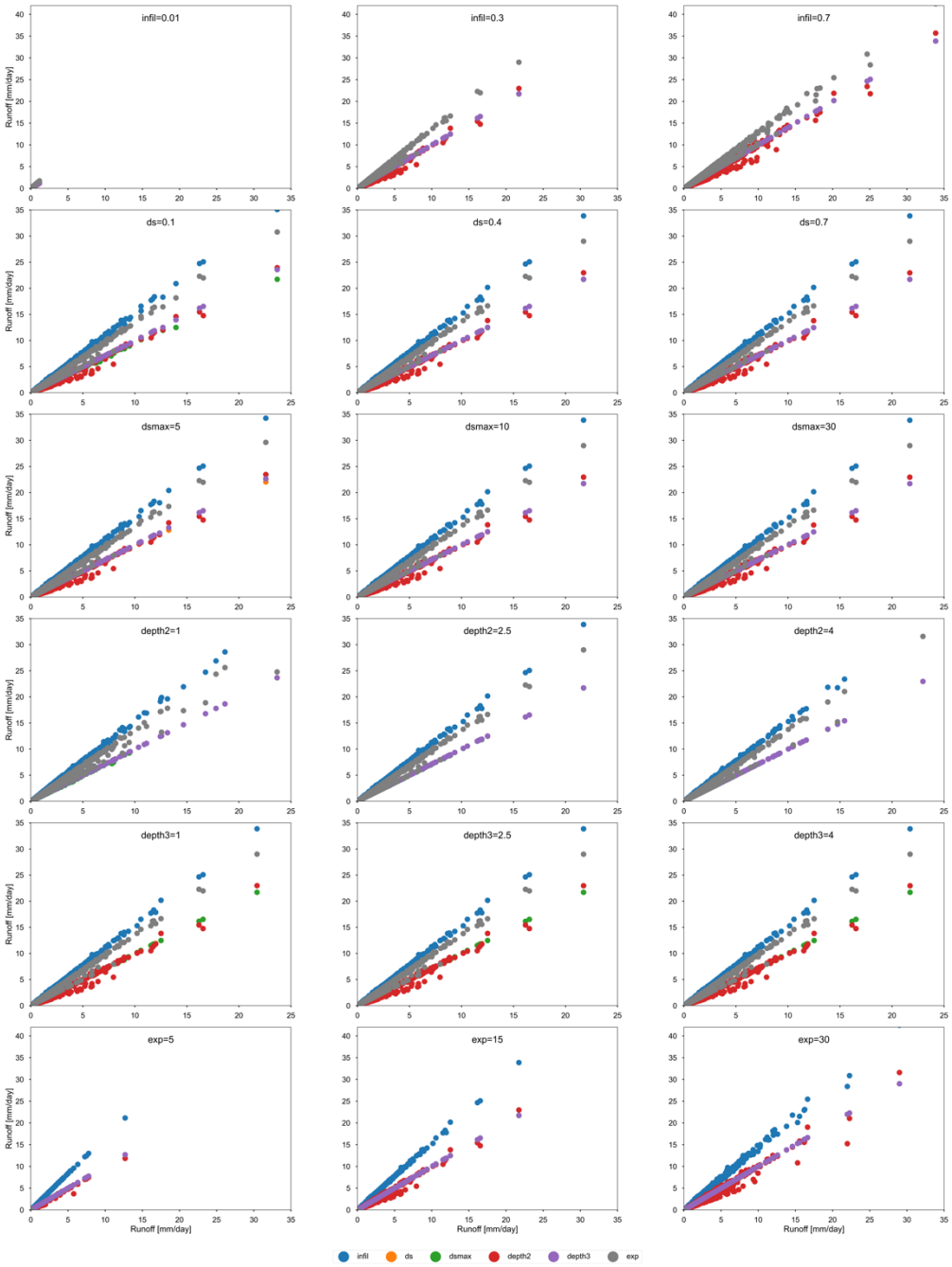

Figure B 4: Sensitivity test of runoff as baseflow in Figure B 2.

Figure B 5: The top 20 performing parameters set for four seasons.

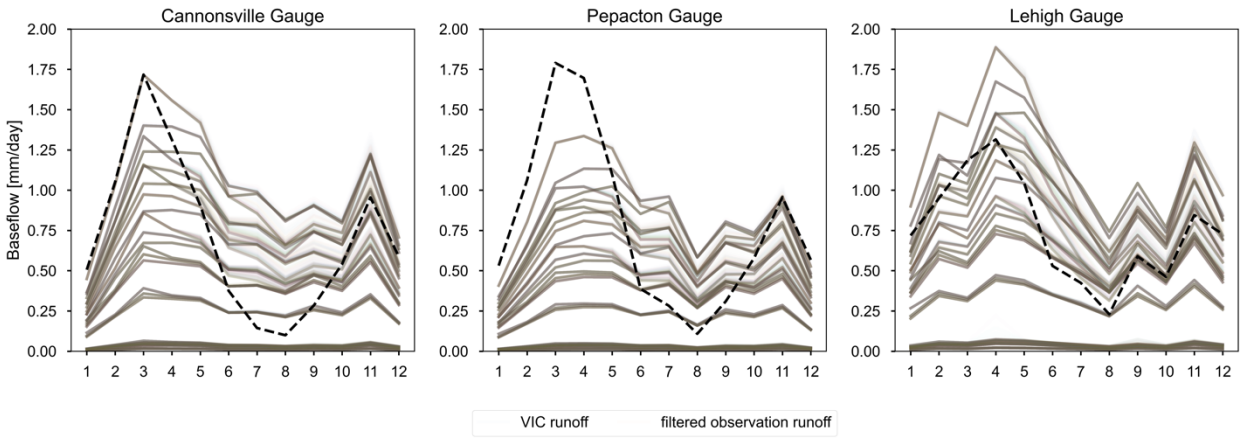

Figure B 6: VIC simulation of surface runoff with different parameter sets is in brown line. The average monthly runoff calculated from the filtered method is in the dotted line.